Calcium decoding in *Marchantia polymorpha*:

the roles of calcineurin B-like proteins (CBLs) and CBL-interacting protein kinases (CIPKs) in abiotic stress responses

Althea Rose

100347046/1

Master of Science by Research: Biomolecular Science

University of East Anglia

February 2023

[25865 words]

Abstract

Plants are sessile organisms, rooted in place. They must respond to stresses as they cannot move away from them. In response to stresses there are localized increases in calcium ion concentration in the cell cytosol or organelles such as the nucleus and chloroplasts. Calcium required for these increases comes from internal stores such as the vacuole, or external sources. Calcium increases encode information which is decoded by calcium binding proteins (CBPs) to distinct, specific downstream signalling pathways. One class of CBPs is Calcineurin-B like proteins (CBLs), sensor relay proteins which bind calcium and interact with CBL-interacting protein kinases (CIPKs). CIPKs phosphorylate downstream targets such as ion channels allowing plant responses to stresses. In *Arabidopsis thaliana* there are 26 CIPKs and 10 CBLs. This is a complex network with much redundancy, meaning that it is difficult to unpick. Therefore, we investigate the CBL-CIPK network in *Marchantia polymorpha*, a basal land plant with only 3 CBLs and 2 CIPKs, making its network easier to unpick. *M. polymorpha* is a good model system because of established molecular genetic techniques and easy propagation and maintenance in the haploid gametophyte generation. This project has demonstrated that the salt sensitivity phenotype of *M. polymorpha cipk-b* knockout mutants previously demonstrated is not due to osmotic stress but is salt-stress specific, identified CBL-A as a candidate gene for osmotic stress response signalling in *M. polymorpha*, and materials have been made to allow future investigation of the calcium dependence of CBL-CIPK interactions in *M. polymorpha*. CBLs and CIPKs are conserved throughout plant species. Knowledge gained from this research can be applied to higher plants including crops, allowing crop improvement to improve plant responses to stress.

Contents

List of Figures

List of tables

List of acronyms

CBP = Calcium binding protein

CCaMK = Calcium and Calmodulin protein kinase

CaM = calmodulin

CML = CaM-like protein

CBL = calcineurin B-like protein

CIPK = CBL-interacting protein kinase

CDPK = Calcium-dependent protein kinase

SOS = salt overly sensitive

ITC = isothermal titration calorimetry

Acknowledgements

Thank you so much to my supervisor Dr Ben Miller for having me in the lab this year for my Master's degree. It has been a privilege and a pleasure to be able to do my own plant calcium signalling research, and you have been an invaluable guiding hand in this who is always pleased to see me (which makes all the difference). Thank you to everyone who has been in the lab this year for making it such a friendly and happy place to work. Thank you to all of the wonderful friends I have made at UEA this year, for making this year the best I have ever had by filling it to the brim with good company and happy times. You are absolute rocks, and the very definition of chosen family.

Roll on the PhD!

1 Introduction

1.1 Plants respond to abiotic stresses via calcium

Plants are sessile organisms which are faced with a huge range of abiotic stress conditions to which they must respond in order to survive. For example, high and low temperatures, wind, drought, flooding, light intensity and ion toxicity (e.g. salinity; He *et al.*, 2018). Plants are rooted in place so cannot move away from these stresses. They have therefore evolved to be able to adapt in a wide range of ways. Cell signalling is key to this. Signalling pathways are activated by stress stimuli and trigger downstream responses by activation of target proteins, for example ion channels and transporters (allowing responses such as ion exclusion), or by regulating gene expression (allowing responses such as transcription of Heat Shock Proteins – molecular chaperones which aid correct protein folding under heat stress; Zhang *et al.*, 2011). Downstream responses vary greatly and this is reflected in the complexity of stress signalling networks.

The enormous variety of responses to stress requires a complex signalling network with many signalling pathways. Many abiotic stress response signalling pathways are integrated by calcium ions as a second messenger. Usually, cytosolic calcium ion concentrations are kept low (~100 nM) against an electrochemical potential difference, to prevent ion toxicity (Tian *et al.*, 2020). In response to abiotic stresses including salt, drought (Knight *et al.*, 1998), reactive oxygen species (ROS; Evans *et al.*, 2005), and cold (Knight *et al.*, 1991; 1996) there are increases in calcium concentration in the cytosol, or organelles such as the nucleus and chloroplasts of plant cells, in the form of spikes, waves and oscillations. These calcium increases trigger activation of distinct, specific downstream signalling pathways (Figure 1.1).

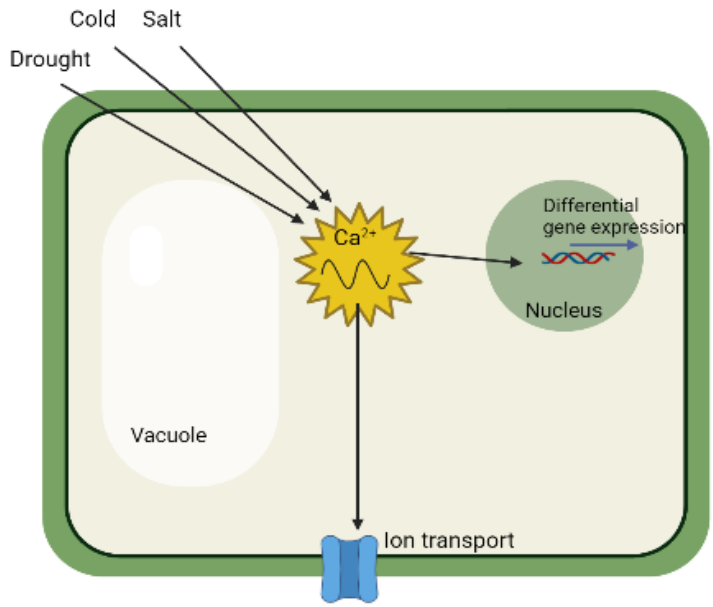

Figure 1.1 Calcium integrates plant stress responses. Calcium increases in the cell cytosol occur in response to a variety of stresses and triggers downstream responses such as activation of ion transporters and alteration of gene expression in the cell.

It is thought that specificity in activation of downstream signalling pathways is allowed by information encoded in the spatial and temporal dynamics of specific calcium increases, controlled by calcium influx and efflux transporters (Figure 1.2; McAinsh and Pittman, 2009).

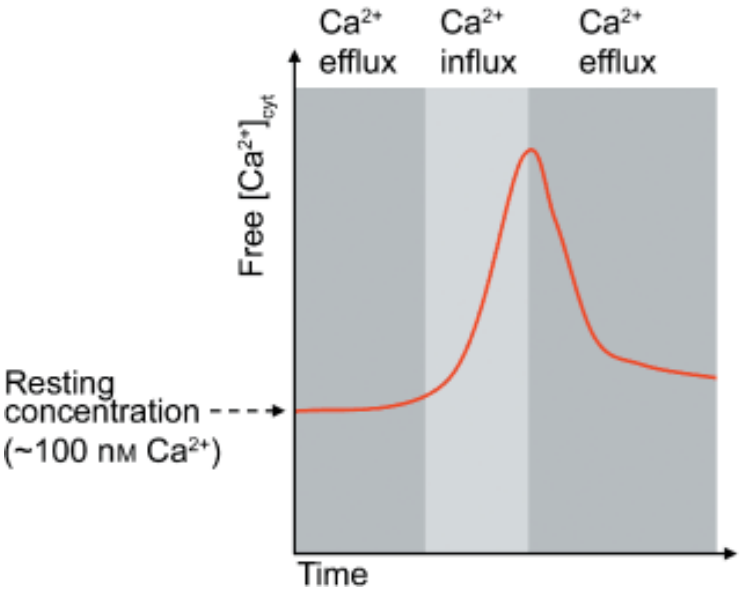

Figure 1.2. Schematic representation of generation and shaping of a calcium signal by coordinated action of calcium influx and efflux transporters (McAinsh and Pittman, 2009).

Calcium influx channels such as cyclic nucleotide gated ion channels and glutamate receptors allow entry of calcium into the cytosol/organelle from internal or external sources, causing a calcium increase. This increase is modulated by calcium efflux transporters, such as P-type

calcium-ATPases and Ca^{2+}/H^{+} exchangers, which pump calcium out of the cytosol/organelle against a concentration gradient, shaping the kinetics of the calcium increase and eventually returning the calcium concentration to basal levels (Dodd *et al.*, 2010). Calcium increases can be single spikes in calcium ions, or repeated increases in the forms of waves or oscillations with amplitude and frequency controlled by calcium influx and efflux transporters. These stimulus-specific calcium increases are termed 'calcium signatures'.

To allow activation of downstream signalling pathways, information encoded in calcium signatures must be decoded. This is done by calcium binding proteins (CBPs), also known as calcium decoding proteins.

1.2 Calcium binding proteins decode calcium signatures to allow plant responses to stress

There are more than 250 calcium binding proteins in the *Arabidopsis thaliana* genome (Day *et al.*, 2002). They can be divided into several families including Calcium/Calmodulin regulated kinases (CCaMKs), Ca^{2+} -dependent protein kinases (CDPKs), Calmodulins (CaMs), CaM-like proteins (CMLs) and Calcineurin B-like proteins (CBLs; Kudla *et al.*, 2018; Figure 1.3).

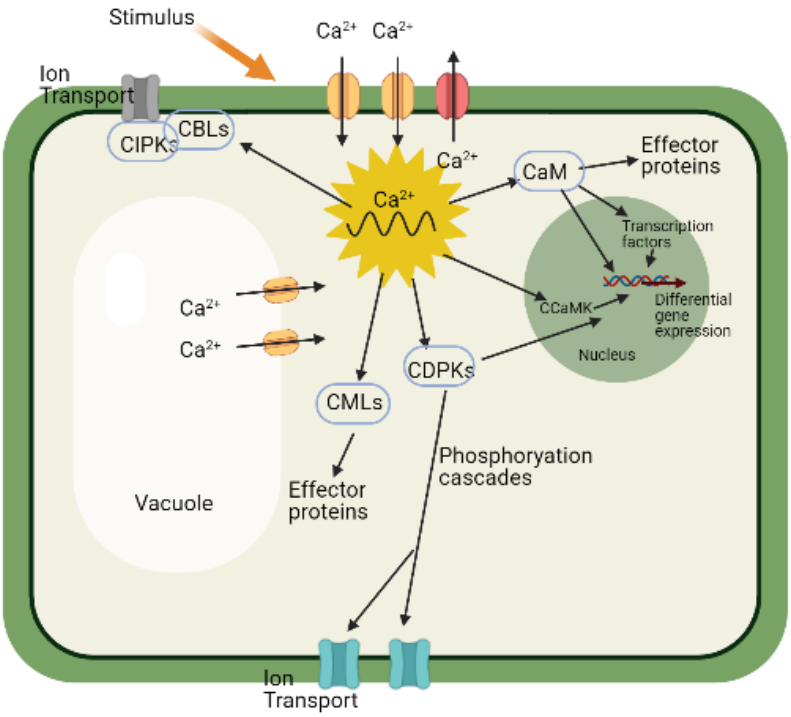

Figure 1.3. Calcium signalling networks in plant cells. Calcium signals occur in response to stress are shaped by calcium influx and efflux transporters and decoded by a variety of calcium binding proteins such as CaM, CDPKs, CMLs, and CBLs to downstream responses such as ion transport and differential gene expression to allow stress tolerance.

It is thought that the variety and number of CBPs provides the ability to decode complex information encoded in calcium signatures to specific downstream responses. Specificity in downstream response is allowed in many, non-mutually exclusive ways. For example, specific CBPs decode specific calcium signatures; calcium signature and CBP localization affects which CBPs are activated by which calcium signatures, and specific interaction of CBPs with downstream proteins allowing activation of specific downstream signalling pathway (Dodd *et al.*, 2010).

CBPs bind calcium via EF-hands: helix-loop-helix domains where the loop region side chain oxygen atoms coordinate calcium ions (Ca^{2+}). The canonical EF-hand has a 12 amino acid long calcium binding loop with the consensus sequence DxDxDGxxDxxE. Calcium ions are coordinated by 7 ligands in a pentagonal bipyramidal arrangement (Figure 1.4a; Gifford *et al.*, 2007). Figure 1.4b shows a schematic of an EF-hand calcium binding loop. Amino acids at positions 1(coordinate X), 3(Y), 5(Z), 7(-Y), 9(-X) and 12(-Z) bind calcium, and their typical amino acid residues are shown (Batistič and Kudla, 2009). The most highly conserved amino acids in the canonical EF-hand calcium binding loop are aspartate at position 1, glycine at position 6 and glutamate at position 12 (Figure 1.4c; Luan *et al.*, 2002; Gifford *et al.*, 2007). Variations can occur at other positions and these affect calcium binding affinity (Sánchez-Barrena *et al.*, 2013). The glycine at position 6 is particularly important as it is essential to maintain the structure of the loop and cannot be substituted with any other amino acid (Luan *et al.*, 2002).

a)

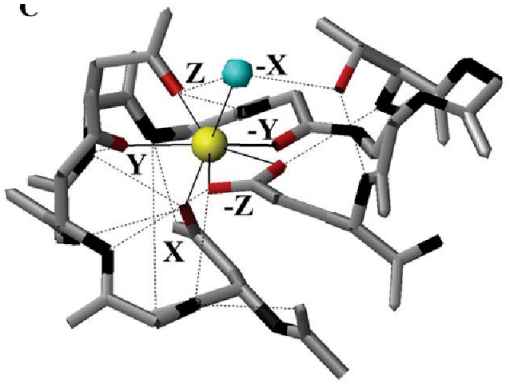

b)

canonical EF hand	Position	1	2	3	4	5	6	7	8	9	10	11	12
	Coordinate	X		Y		Z		-Y		-X			-Z
	Amino acid	D	x	D	x	D	G	x	x	D	x	x	E

c)

EF-loop position	1	2	3	4	5	6	7	8	9	10	11	12
coordinating ligand	X sc		Y sc		Z sc		-Y bb		-X sc*			-Z sc2
most common	Asp 100%	Lys 29%	Asp 76%	Gly 56%	Asp 52%	Gly 96%	Thr 23%	Ile 68%	Asp 32%	Phe 23%	Glu 29%	Glu 92%
also frequently observed		Ala Gln Thr Val Ile Ser Glu Arg	Asn	Lys Arg Asn	Ser Asn		Phe Lys Gln Tyr Glu Arg	Val Leu	Ser Thr Glu Asn Gly Gln	Tyr Ala Thr Leu Glu Lys	Asp Lys Ala Pro Asn	Asp

Figure 1.4. EF-hand structure. A) Calcium ions are coordinated by 7 ligands in a pentagonal bipyramidal arrangement (Gifford *et al.*, 2007). B) Schematic of an EF-hand calcium binding loop. Amino acids at positions 1(coordinate X), 3(Y), 5(Z), 7(-Y), 9(-X) and 12(-Z) bind calcium, and their typical amino acid residues are shown (Batistič and Kudla, 2009). C) The most highly conserved amino acids in the canonical EF-hand calcium binding loop are aspartate at position 1, glycine at position 6 and glutamate at position 12 (Luan *et al.*, 2002; Gifford *et al.*, 2007; figure from Gifford *et al.*, 2007).

There are two types of CBPs: sensor responder proteins, for example CDPKs and CCaMKs, which have both a calcium sensing function and intrinsic kinase activity which activates downstream signalling, and sensor relay proteins, for example CaMs, CMLs and CBLs, which bind calcium but do not have intrinsic kinase activity so must interact with other proteins to allow activation of downstream signalling by phosphorylation (Dodd *et al.*, 2010).

CBLs, named so due to their similarity to the B regulatory subunit of the phosphatase calcineurin (Kudla *et al.*, 1999), are one type of calcium decoding protein of particular interest because of their involvement in plant cell signalling in response to abiotic stresses through ion homeostasis. For example, *A. thaliana* CBL4 is involved in salt tolerance (Liu and Zhu, 1998),

CBL2 is involved in magnesium tolerance (Tang *et al.*, 2015), and CBL1 is involved in low potassium tolerance (Ragel *et al.*, 2015). Therefore, understanding of CBLs has potential applications in crop improvement to withstand stress.

1.3 CBLs are calcium decoding proteins that interact with CIPKs

CBLs consist of 4 EF-hand motifs separated by spacer regions (Figure 1.5). The first EF-hand calcium binding loop is non-canonical: it has 14 amino acids rather than the canonical 12, but still binds calcium (Nagae *et al.*, 2003). This is a distinguishing feature of CBLs from other calcium binding proteins. CBLs are typically localized either to the plasma membrane or tonoplast; localization is allowed by lipid modification at the N-terminus. For example *A. thaliana* CBL2 and CBL3 are targeted to the tonoplast by S-acylation (Batistič *et al.*, 2008), while CBL1 and CBL9 are targeted to the plasma membrane by dual-lipid modification: myristoylation and palmitoylation at an N-terminal MGCXXS/T motif (Batistič *et al.*, 2012).

As CBLs are sensor-relay proteins, they must interact with other proteins to allow activation of downstream signalling by phosphorylation. CBLs interact with CBL-interacting protein kinases (CIPKs) which phosphorylate downstream substrates, allowing signalling (Figure 1.6). CIPKs consist of an N-terminal Ser/Thr protein kinase domain, a junction domain and a C-terminal regulatory domain (Shi *et al.*, 1999; Edel and Kudla, 2015; Figure 1.5: Batistič and Kudla, 2009). The C-terminal regulatory domain contains the autoregulatory NAF domain, named after the three amino acids it is composed of; this is where the interacting CBL binds (Figure 1.5). When CBLs interact with CIPKs, the autoinhibitory NAF domain is released from the CIPK kinase domain and the CIPK is activated (Chaves-Sanjuan *et al.*, 2014). On interaction, CIPKs phosphorylate their cognate CBL at a conserved Ser/Thr residue in the FPSF motif (also named for the amino acids it is composed of) in the C-terminus of most CBLs. This phosphorylation enhances specificity of the CIPK for its interacting CBL and is needed for full activity of the complex (Hashimoto *et al.*, 2012). CIPKs also have a PPI motif where 2C-type protein (PP2C) phosphatases can interact.

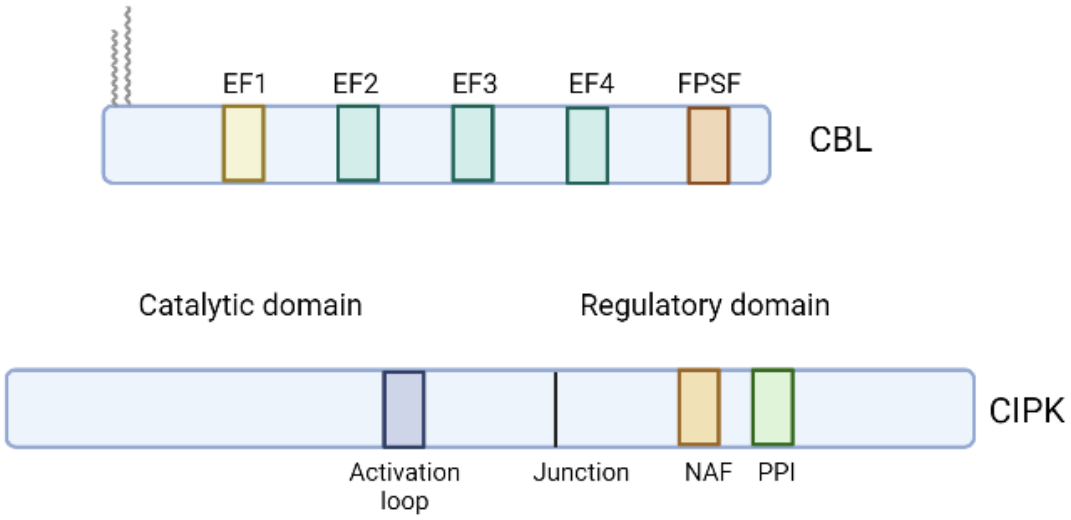

Figure 1.5. Structure of CBLs and CIPKs. CBLs have 4 EF-hands, an FPSF domain and an N-terminal lipid modification. CIPKs have a catalytic domain, a junction domain and a regulatory domain. Adapted from Batistič and Kudla (2009).

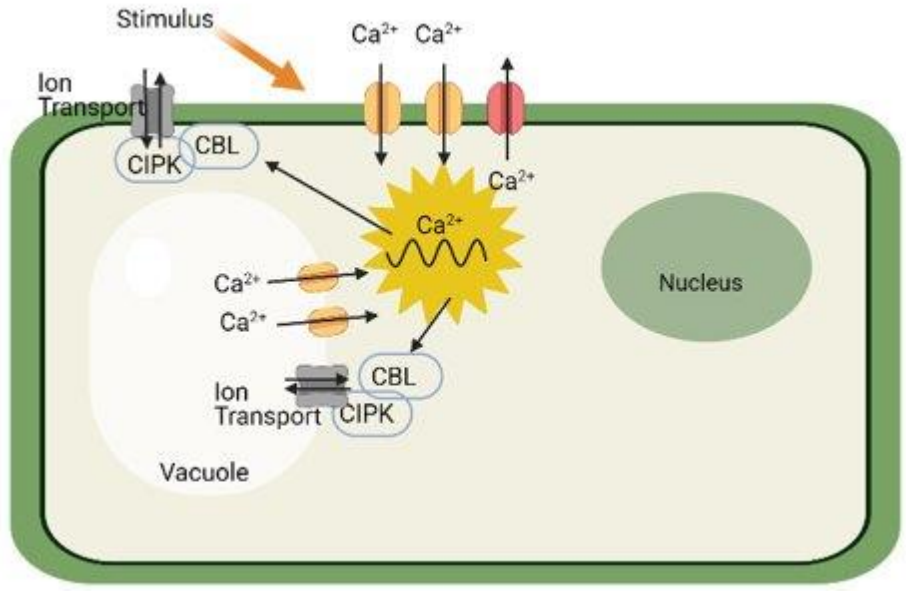

Figure 1.6. CBL-CIPK pairs are activated by calcium increases which occur in response to stress and control ion homeostasis.

CBL-CIPK interaction is specific, but there is some promiscuity: some CBLs can interact with multiple CIPKs, and vice versa, depending on CBL calcium-binding affinities and CBL and CIPK expression patterns. For example, AtCBL1 can interact with AtCIPK26, AtCIPK23 and AtCIPK15 (Ma *et al.*, 2020). This increases the number of possible downstream signalling pathways that can be specifically activated, fine-tuning the response.

CBLs control localization of their interacting CIPKs. When expressed independently of CBLs, CIPKs are localized to the cytosol and nucleus. When they interact with CBLs, they can be seen at membranes (Batistič *et al.*, 2010). This means that the same CIPK can function at different

membranes depending on its interacting CBL. For example, AtCIPK24 is found at the plasma membrane when interacting with plasma membrane-localized CBL4 but at the tonoplast when interacting with tonoplast-localized CBL10 (Halfter, 2000; Ishitani *et al.*, 2000; Kim *et al.*, 2007). This allows one CIPK to have multiple downstream signalling functions depending on where it is localized. CIPKs phosphorylate target proteins such as transcription factors, phosphatases and channels and transporters, affecting downstream signalling and stress responses.

1.4 *Arabidopsis thaliana* case studies

1.4.1 The SOS pathway in *Arabidopsis thaliana* is well researched

CBLs and CIPKs have important roles in salt stress tolerance in *A. thaliana*. High salt causes both osmotic stress and ion toxicity which plants tolerate by ion exclusion, extrusion and compartmentalisation. In response to high salt in *A. thaliana* there are root calcium signals (Knight, 1999) which are decoded by CBL4-CIPK24 to allow a response. Also known as SOS3 and SOS2 respectively, CBL4 and CIPK24 are part of the well-studied salt overly sensitive (SOS) pathway in *A. thaliana*.

When root calcium signals occur in response to high external salt concentrations, plasma membrane-localized, N-myristoylated AtCBL4 (AKA SOS3) binds calcium at EF-hand domains and recruits AtCIPK24 (AKA SOS2) Ser/Thr kinase via its C-terminal regulatory domain (Halfter, 2000). SOS3 interaction with SOS2 is calcium dependent (Ishitani *et al.*, 2000). CBL4 phosphorylation by its CIPK24 partner is needed for full activity of the complex (Hashimoto *et al.*, 2012). The CBL4-CIPK24 complex phosphorylates SOS1 Na^+/H^+ plasma membrane antiporter at Ser1138 (Qiu *et al.*, 2002), activating it to allow more sodium to be pumped out of the cell, allowing salt tolerance via extrusion.

The SOS pathway does not exist in isolation. Salt stress also affects SOS1 via the phospholipase D pathway. Salt stress causes increase in PLDα1 enzyme activity, resulting in accumulation of phosphatidic acid (PA) lipid second messenger. PA activates Mitogen-Activated Protein Kinase 6 (MPK6) which phosphorylates SOS1 (Yu *et al.*, 2010), allowing ion exclusion and homeostasis. Also, CBL10 is an alternative regulator of CIPK24 in the shoots where SOS3 is not very highly expressed (Quan *et al.*, 2007). Existence of these overlapping proteins and pathways complicate experiments.

SOS proteins also contribute to salt tolerance in other ways. SOS proteins regulate auxin gradients under mild salt, affecting lateral root development and helping plants to grow away from high salt (Wang, Li and Li, 2009; Zhao *et al.*, 2011). SOS proteins also affect cytoskeleton

dynamics. SOS1 interacts with the root cortical cytoskeleton and SOS3 is needed for calcium-dependent actin reorganisation in response to salt stress which is needed for salt tolerance (Wang *et al.*, 2007).

The SOS pathway is further complicated by the existence of targets outside of salt stress response. For example, CIPK24 (SOS2) interacts with tonoplast proteins like CAX1 Ca^{2+}/H^{+} antiporter and vacuolar H^{+}-ATPase (Cheng *et al.*, 2004; Batelli *et al.*, 2007), affecting vacuolar transport of ions other than sodium. This complicates interpretation of transcriptomic data for example, as upregulation of SOS2 as happens in response to salt stress (Liu *et al.*, 2000) is not necessarily indicative of a salt stress response. Figure 1.7 shows a summary of the SOS pathway in *A. thaliana* and its interacting proteins.

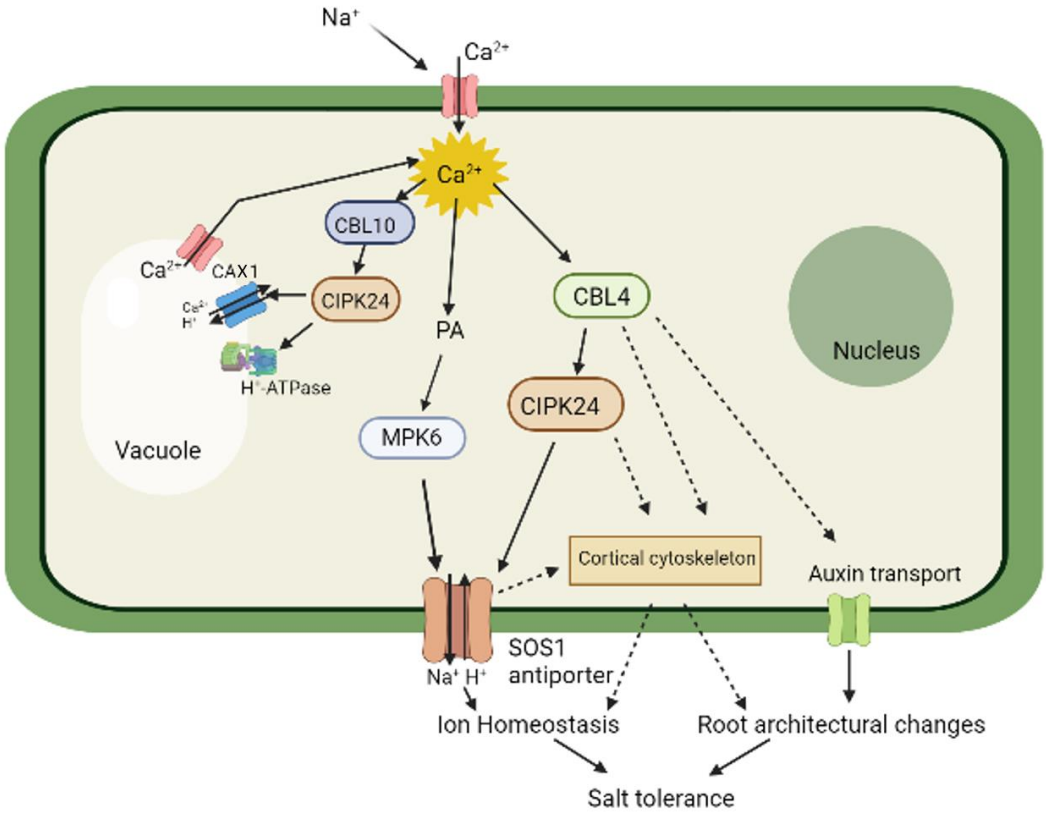

Figure 1.7. The SOS pathway and its interacting proteins. High salt causes a calcium increase which activates signalling through CBL4 and CIPK24 to activate Na^{+}/H^{+} SOS1 antiporters to allow salt tolerance by extrusion. The root cortical cytoskeleton, auxin transport, and vacuolar transport is also affected to allow salt tolerance. Adapted from Ji *et al.* (2013).

Overall, the Salt Overly Sensitive pathway is an important stress response pathway in *A. thaliana* that has been well studied but is more complicated than it first appears. It is a good example of the importance of CBLs and CIPKs in plant stress tolerance.

1.4.2 *A. thaliana* CIPK23 is a multifunctional CIPK

A. thaliana CIPK23 is a central regulator of ion homeostasis, controlling a range of ion channels and transporters for ions including potassium, nitrate, ammonium, manganese, magnesium, zinc and iron (Li *et al.*, 2006, Xu *et al.*, 2006, Ho *et al.*, 2009, Maierhofer *et al.*, 2014, Ragel *et al.*, 2015, Tang *et al.*, 2015, Tian *et al.*, 2016, Straub *et al.*, 2017, Dubeaux *et al.*, 2018,Tang *et al.*, 2020; Figure 1.8). This is an interesting example of a multi-functional CIPK and a good case study to demonstrate the ways that specificity of action are defined. Multi-functional CIPKs and CBLs exist in both higher land plants and are very likely to exist in basal land plants where (a smaller network of proteins must allow response to just as many stresses, so they are important to understand.

One of the roles of CIPK23 is in potassium homeostasis. Interactions with CBL1 or CBL9 allow phosphorylation of *A. THALIANA* K^+ TRANSPORTER 1 (AKT1) in roots, resulting in K^+ uptake (Li *et al.*, 2006; Xu *et al.*, 2006). CBL1-CIPK23 also activates HIGH AFFINITY K^+ TRANPORTER 5 (HKT5; Ragel *et al.*, 2015), and at low potassium, CIPK23 activates K^+ UPTAKE TRANSPORTER 4 (Wang *et al.*, 2020) which is needed for *A. thaliana* root hair tip growth, allowing root surface area to increase, increasing foraging for sufficient K^+ from the soil. CIPK23 also activates *A. thaliana* Two Pore K^+ (TPK) channels in the tonoplast in response to low potassium, allowing K^+ flux from the vacuole to the cytosol. This role is shared with CIPK9 and CIPK26 (Tang *et al.*, 2020), raising the question of under which circumstances each is used and how this is defined. Clearly, there are multiple plant responses to low K^+ controlled by CIPK23. This requires further definition of specificity than simply identifying the stress; this will be an interesting topic for future investigation.

CIPK23 is also involved in nitrate homeostasis via control of NITRATE TRANSPORTER 1.1 (NRT1.1), also known as CHLORATE RESISTANT 1 (CHL1) and NRT1/PTR FAMILY 6.3 (NPF6.3). CIPK23 phosphorylation of NRT1.1 at Thr101 (Liu and Tsay, 2003; Léran *et al.*, 2015) happens under low nitrate conditions and depends on calcium (Ho *et al.*, 2009) and CBL1/9 (Léran *et al.*, 2015). Phosphorylation allows the NRT1.1 homodimer to dissociate to a stable monomer which has higher nitrate affinity (Sun *et al.*, 2014). Nitrate binds to this high-affinity monomer at concentrations where it does not bind to the lower affinity dimer and more nitrate is transported into the cell. Through this mechanism, nitrate uptake can be closely regulated.

As well as improving uptake of important ions, CIPK23 helps prevent accumulation of toxic ion levels. At high ammonium concentrations, CBL1-CIPK23 inactivates AMMONIUM TRANSPORTER 1;1 and 2;2 (AMT1;1 and 1;2), decreasing ammonium transport into the cell (Straub *et al.*, 2017). Similarly, CBL2/3-CIPK23/3/9/26 allows sequestration of magnesium to

the vacuole by regulating a vacuolar magnesium transporter, possibly TPC1 (Ródenas and Vert, 2021). These roles are also important in maintaining plant health.

CIPK23 is also involved in iron homeostasis as well as homeostasis of the non-iron metals zinc, manganese, cobalt and cadmium through the control of IRON-REGULATED TRANSPORTER 1 (IRT1). These non-iron metals are essential in small amounts but toxic when accumulated too highly. When iron availability in the soil is low, non-iron metals such as manganese are disproportionately transported resulting in accumulation to toxic levels (Vert *et al.*, 2002). CIPK23 is involved in prevention of this. CIPK23-IRT1 interaction occurs when non-iron metals load onto IRT1 (Dubeaux *et al.*, 2018). Phosphorylation of IRT1 by CIPK23 facilitates recruitment of an E3 ubiquitin ligase, facilitating IRT1 degradation. Degradation of IRT1 under low iron conditions may therefore prevent plants from accumulating highly reactive metals such as manganese from the soil, preventing toxicity (Tang *et al.*, 2020).

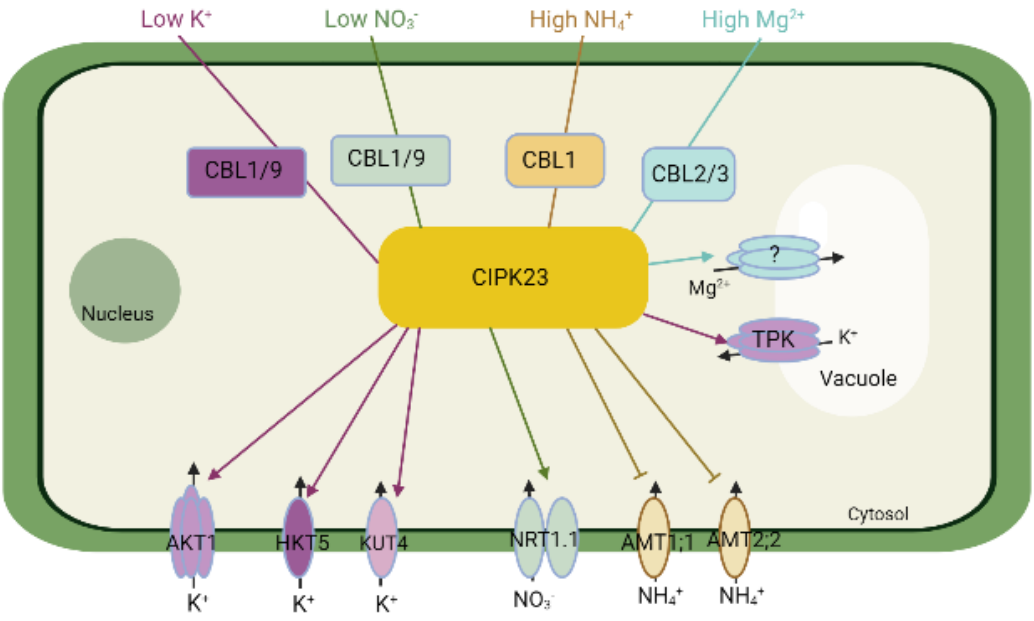

Figure 1.8. Control of ion homeostasis through multifunctional CIPK23. CIPK23 is activated by a range of CBLs in response to a range of ion stresses and modulates ion transporters to allow homeostasis. Adapted from (Ródenas and Vert, 2021).

The multiple roles of one single kinase, CIPK23, raises the important question of how specificity of downstream action is defined. There are many ways this can be done; these are summarised in Figure 1.9 below. First, the calcium signature hypothesis states that different stresses trigger different calcium signals. Information about the nature of the stimulus is encoded in the dynamics of these increases and is decoded by calcium binding proteins like

CBLs (McAinsh and Pittman, 2009). Specific calcium signatures formed in response to stresses, for example different ion stresses, can activate specific CBLs in specific ways, for example by varying calcium binding dynamics or calcium binding to specific EF-hands (calcium-binding domains), allowing them to recruit the appropriate CIPK. Specific CBL-CIPK complexes activate different downstream targets, perhaps due to differing conformation affecting ability to physically interact with their target, resulting in the appropriate response. However, as previously discussed, CBLs have the potential to interact with more than one CIPK, and in the case of multi-functional CIPK23, even once the CIPK activated has been defined there can be multiple different downstream signalling responses. Therefore, further levels of specificity are required.

Specificity can be further defined by modulation of CIPK activity level by upstream phosphatases. For example, ABI2, a PP2C phosphatase binds the CIPK24 PPI domain (Ohta *et al.*, 2003), reducing phosphorylation by CIPK24. It is possible that different ion channels require phosphorylation at different residues in order to be activated, and modulation of CIPK activity is a way in which this could be allowed, introducing more specificity in ion channel activation.

Specificity can be defined spatially. Specific localization of calcium signatures to specific tissues or cell types affects which CBLs are activated. Specific localization of the proteins that make up CBL-CIPK complexes to nanodomains close to the ion channel target also allows specificity. For example, CBL2 and CBL3 are localized to the tonoplast, close to the specific magnesium ion transporters they activate (Tang *et al.*, 2015).

Specificity can also be achieved by specific temporal expression of the protein complex binding partners so that the proteins needed to form the CBL-CIPK complex that defines the downstream response are only expressed in response to the specific stress. This may be achieved due to specific transcriptional reprogramming allowed by calcium signatures caused by specific stresses. For example, CIPK23 expression increases in response to ammonium shock and low K^+ (Straub *et al.*, 2017; Cheong *et al.*, 2007; Lara *et al.*, 2020).

These different mechanisms of defining specificity are not mutually exclusive. Rather, they work together to allow intricate signalling using calcium as a central second messenger, and to define function of multi-functional CIPKs like CIPK23. There are probably other mechanisms that contribute to specificity too, for example the requirement of other signalling events, or calcium sensitivity priming (Young *et al.*, 2006): modulation of calcium sensors by physiological stimuli, affecting their competence to respond to calcium signals.

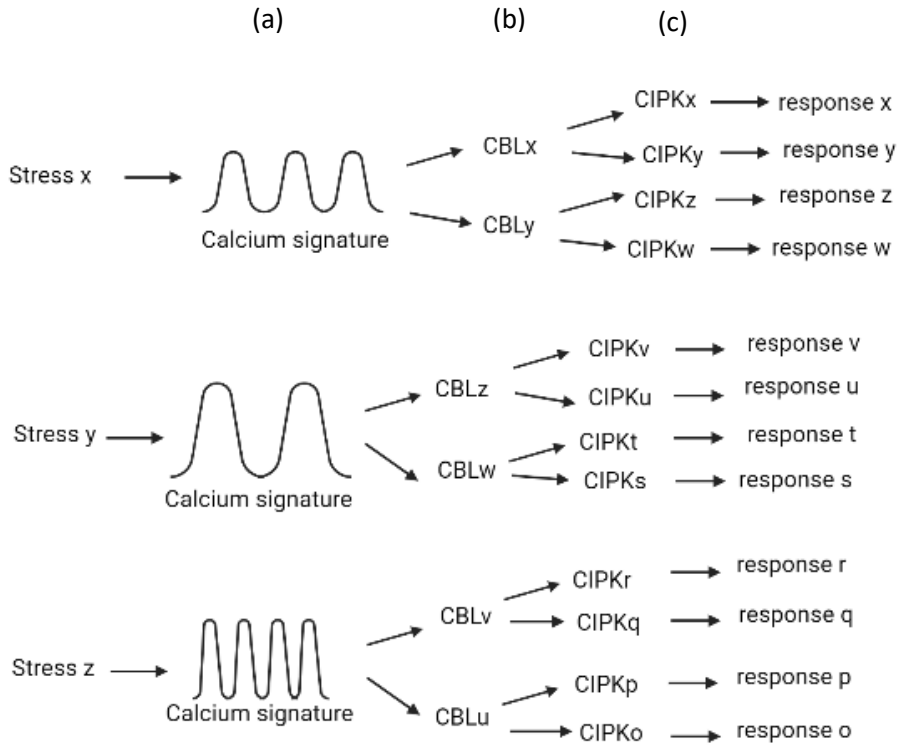

Figure 1.9. Factors contributing to specificity in calcium signalling. A) different stresses trigger distinct, specific calcium signatures. B) Calcium signatures activate and affect expression of specific CBLs. C) Specific CBLs interact with specific CIPKs with some promiscuity. Together these factors allow distinct, specific downstream responses to stresses. Other factors which contribute to specificity include localization of calcium increases and calcium signalling machinery, and temporal expression of calcium signalling machinery.

Overall, CIPK23 is an interesting example of a multi-functional CIPK. How exactly specificity of downstream signalling is defined requires further investigation but there are several proposed ways in which this may happen.

1.5 *Marchantia polymorpha* is a good model system

Marchantia polymorpha (common liverwort) is part of the Marchantiophyta (liverwort) division of the bryophytes: avascular land plants. Its simple morphology, for example lacking stomata, points towards its early divergence compared to other land plants. *M. polymorpha* has a leafy thalloid form. Photosynthetic leaf-like structures, each with two or more lobes, radiate out from the centre of the plant. Each lobe has an apical notch where the meristem is

located and from which the plant grows (Shimamura, 2016; Figure 1.10).

Figure 1.10. *M. polymorpha* morphology. Thallus tissue is lobed and mature tissue develops gemma cups which produce clonal progeny called gemmae.

M. polymorpha has a short lifecycle (Figure 1.11). It undergoes the alternation of generations, alternating between a diploid sporophyte and a haploid gametophyte stage. It spends most of its lifecycle in the haploid gametophyte stage.

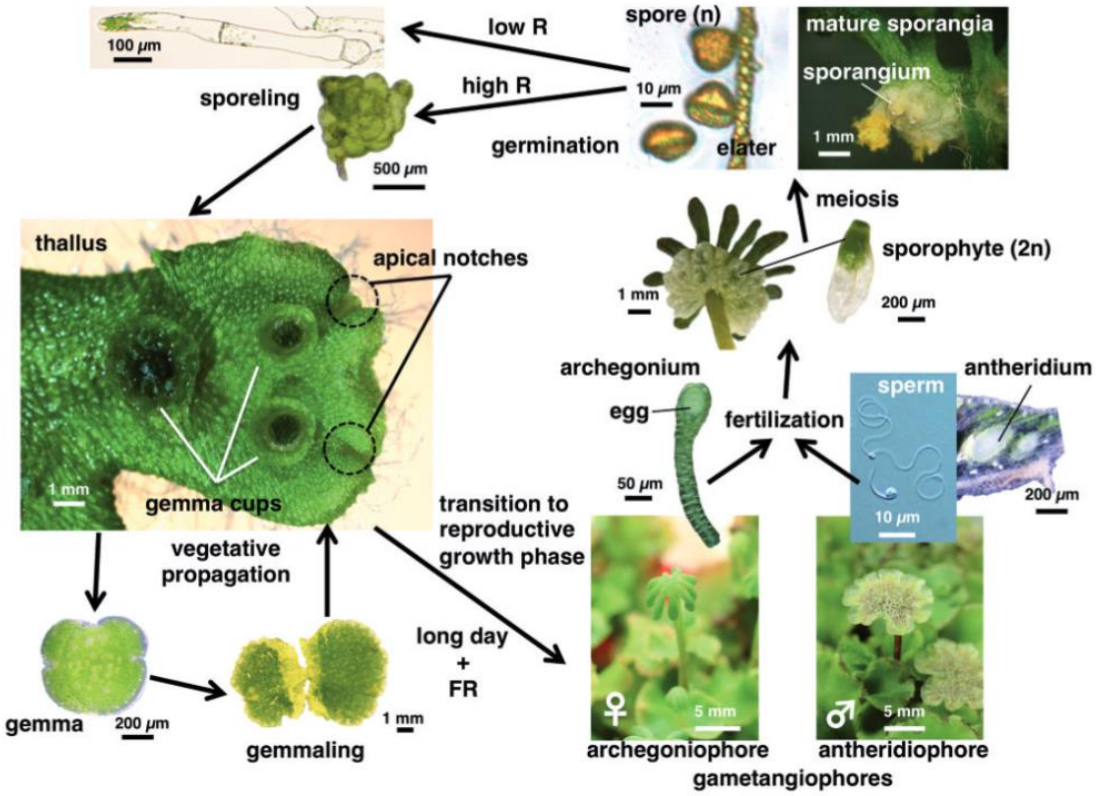

Figure 1.11. Lifecycle of *M. polymorpha*.
Diploid sporophyte produces haploid spores. Spores germinate to form a protonema with rhizoids (mitosis). Protonema apical cell division forms a haploid gametophyte which is the thallus. Asexual reproduction occurs by production of multicellular gemmae from gemma cups which form on the thallus. In sexual reproduction, male or female gametangia are produced on umbrella-like branches (gametangiophores) of thalli. Each antheridium makes spermatogonia (sperm cells) which fertilize the egg formed in the venter of an archegonium of a female plant. Zygote develops into a diploid sporophyte inside the archegonium. The venter grows to a calyptra. The diploid sporophyte hangs upside down under the archegoniophore. Meiosis in the capsule produces haploid spores which are released. (Shimamura, 2016) (Image from Ishizaki *et al.*, 2016).

M. polymorpha can undergo both sexual and asexual reproduction. In vegetative growth, gemma cups form on mature thallus tissue which produce dozens of gemmae (clonal progeny) that each develop into new plants. In reproductive growth, gametangiophores (umbrella-like branches) develop on the thallus, upon which male and female gametangia (sex organs) are produced. Sexual reproduction produces genetically distinct haploid spores which are released and develop into individual plants.

Many of the characteristics of *M. polymorpha* make it a good model system for study. It has a short lifecycle, and is easily propagated by growing excised thallus fragments, meaning that clonal experimental material can be produced quickly and easily. The sexual reproduction

lifecycle takes about 3 months in total, but asexual reproduction will generate mature thallus tissue from gemmae in just 2 to 3 weeks (Ishizaki *et al.*, 2016). Asexual reproduction allows production of clonal progeny which is useful to allow controlling for genetic background in comparative experiments.

M. polymorpha spends most of its lifecycle in the haploid gametophyte stage where heterozygosity does not occur. This accelerates genetic analysis as only one allele per gene needs to be targeted when generating mutants, allowing phenotypes to be seen more rapidly.

There are established techniques for gene editing in *M. polymorpha*. Sugano *et al.* (2014) demonstrated that the CRISPR-Cas9 system for gene editing is effective in *M. polymorpha*. There are also established methods for *Agrobacterium*-mediated transformation of *M. polymorpha*. Sporelings (Ishizaki *et al.*, 2013), gemmalings (Tsuboyama-Tanaka and Kodama, 2015) or thallus tissue (Kubota *et al.*, 2013) can be transformed. Production of sporelings for transformation requires the induction of reproductive growth, making it more time consuming than gemmaling and thallus tissue transformation. Sporelings produced will be genetically different, so transformants from different sporelings will have different genetic backgrounds. However, due to the large number of spores produced by a plant, sporeling transformation can be high throughput and this can increase transformation success. Gemmaling and thallus tissue transformation, both based on asexual reproduction, are more readily performed and allow generation of transformants with the same genetic background, improving consistency between resulting transformants. This makes *M. polymorpha* a useful model system.

1.6 Investigating stress response signalling in *M. polymorpha*

M. polymorpha is a good model system in which to investigate abiotic stress response signalling via the CBL-CIPK network. CBL-CIPK networks have become more complex as plants have evolved. Early diverging single cell Chlorophyta have only one CBL-CIPK pair while the late diverging higher plant *A. thaliana* has 10 CBLs and 26 CIPKs (Kolukisaoglu *et al.*, 2004), giving a possible 260 distinct complexes. *M. polymorpha* has 3 CBLs and 2 CIPKs (Edel and Kudla, 2015; figure 1.12), giving a simpler network with less redundancy than *A. thaliana* (Bowman *et al.*, 2017), making it easier to unpick, but one still large enough to have potential for specificity. This makes *M. polymorpha* an attractive model system in which to investigate the CBL-CIPK network, including the roles of CBLs and CIPKs and CBL-CIPK complexes in *M. polymorpha* responses to environmental stimuli.

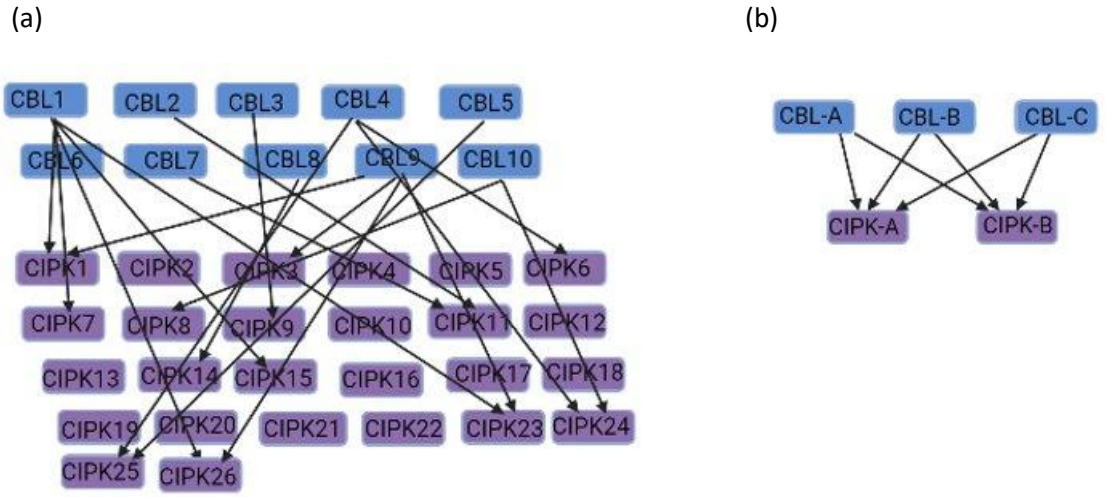

Figure 1.12. A) *A. thaliana* has 10 CBLs and 26 CIPKs forming a complicated network. B) *M. polymorpha* has 3 CBLs and 2 CIPKs, forming a simpler network. Arrows show known CBL-CIPK interactions.

Little work investigating the CBL-CIPK network has been done in *M. polymorpha* before. It will be interesting to investigate, based on phylogenies between *M. polymorpha* and *A. thaliana* CBLs and CIPKs, whether there are *M. polymorpha* CBLs and CIPKs with equivalent roles to *A. thaliana* ones, for example *A. thaliana* SOS protein homologs. This would give some indication of how transferable knowledge gained in *M. polymorpha* is to higher plants, an important factor when applying research results to crop improvement.

It will also be interesting to find out if the simpler CBL-CIPK network in *M. polymorpha* also lacks the complicating factors such as other targets and interacting proteins featured in *A. thaliana* CBL/CIPK signalling pathways such as the SOS pathway. If so, this would make

experimental results in *M. polymorpha* easier to interpret, another advantage of this model system over higher plants.

To allow *M. polymorpha* to respond to a wide range of stresses through a small CBL-CIPK network, it is likely that multi-functional CBLs and CIPKs are used, like *A. thaliana* CIPK23. It will be interesting to investigate whether this is the case and how specificity of downstream signalling is defined.

One stress which plants commonly face and must respond to is salinity stress. Moderate soil salinity can result in yield losses of 55% in maize (Satir and Berberoglu, 2016). Salinity stress is composed of two stresses: osmotic stress, because high extracellular ion concentrations cause a water potential gradient that causes water to leave plant cells into the surrounding soil by osmosis, and ion toxicity, because sodium ions interfere with cellular processes such as ion transport. Salinity stress is becoming more prevalent with climate change due to increased need for irrigation as drought becomes more prevalent, and responses are mediated by CBL-CIPK networks.

The salt and osmotic-stress responsive calcium signals have been characterized in *M. polymorpha*. Previous work in the Miller lab transformed the Tak1 accession of *M. polymorpha* with constructs containing R-GECO: a fluorescent calcium reporter which allows detection of calcium signals at single cell resolution. Application of 100 mM NaCl gave a biphasic calcium peak over 40 minutes which was blocked by lanthanum chloride calcium ion channel blocker. Application of 200 mM sorbitol (induces osmotic stress) gave a single calcium peak over 40 minutes (Miller, unpublished; Figure 1.13). Compared to established stress response signals in *A. thaliana*, calcium peak shapes were similar, but signals in *M. polymorpha* lasted over a much longer time frame, with *A. thaliana* calcium signals lasting approximately 3 minutes (Schmockel *et al.*, 2015).

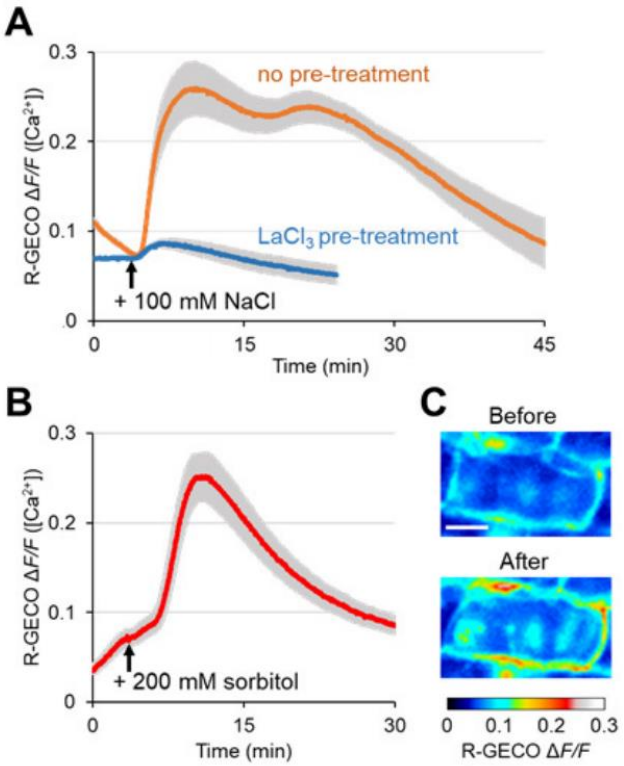

Figure 1.13. *M. polymorpha* calcium signals. A) R-GECO Tak1 *M. polymorpha* detected a biphasic signal in response to salt (100 mM NaCl) over 40 minutes that could not be detected with lanthanum chloride pre-treatment. B) R-GECO Tak1 *M. polymorpha* detected a monophasic signal in response to osmotic stress (200 mM sorbitol) over 30 minutes. C) Fluorescence images of the salt induced signal before and after salt treatment. White bar represents 50 µm. (Image provided by Miller, unpublished; Figure and legend taken from Tansley, 2021).

In *A. thaliana*, plants respond to salinity via the salt overly sensitive (SOS) pathway, involving CBL4 (SOS3) and CIPK24 (SOS2). In order to find the CIPK24 homolog in *M. polymorpha*, Connor Tansley, a previous PhD student in the Miller group, created phylogenetic trees comparing *A. thaliana* and *M. polymorpha* CBLs and CIPKs based on amino acid sequence similarity (Figure 1.14; Tansley *et al.*, 2023). The CIPK phylogenetic tree shows that *MpCIPK-B* is closely related to *AtCIPK24,* suggesting it may be involved in salt stress signalling.

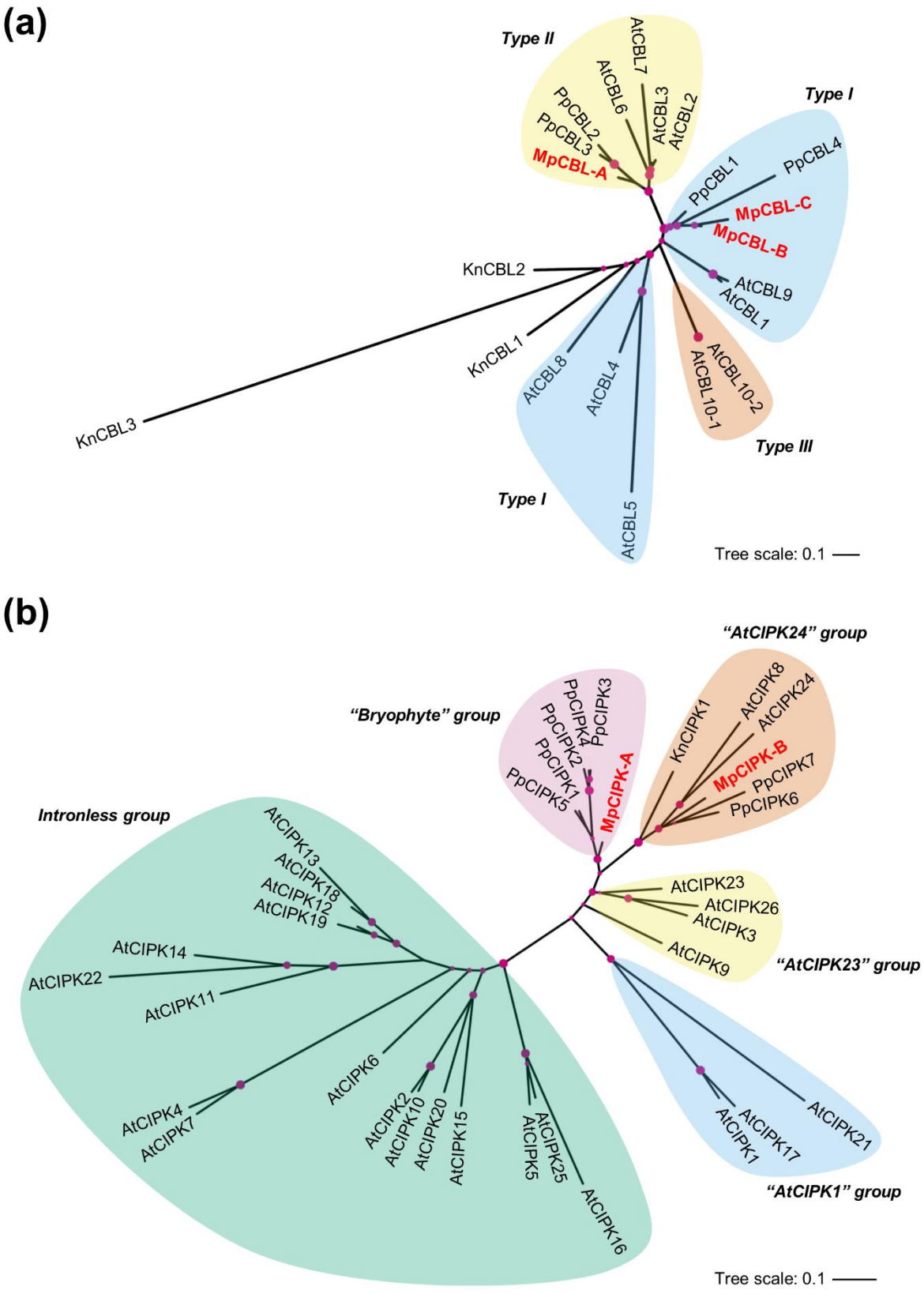

Figure 1.14. Phylogenetic tree of *M. polymorpha* and *A. thaliana* thaliana CBLs (a) and CIPKs (b) (Tansley *et al.,* 2023).

Tansley created *cipk-b* knockout lines of *M. polymorpha* and investigated the effect of salinity stress on wildtype and *cipk-b* knockout mutant growth by supplementing media with NaCl. Results showed that *cipk-b* mutants grew significantly less than wildtype *M. polymorpha* at 50 mM salt (Figures 1.15, Tansley *et al.,* 2023) which suggests that *CIPK-B* is involved in salt tolerance in *M. polymorpha.* This was supported by qRT-PCR data which found that CIPK-B expression reduces in response to salt stress after one week of treatment (Figure 1.16), matching the expected result for genes involved in salt stress signalling, based on data for the *A. thaliana* SOS pathway which shows that SOS2 and SOS3 are upregulated at 24 hours post treatment, but downregulated after 6 days (Ji *et al.*, 2013; Rolly *et al.*, 2020).

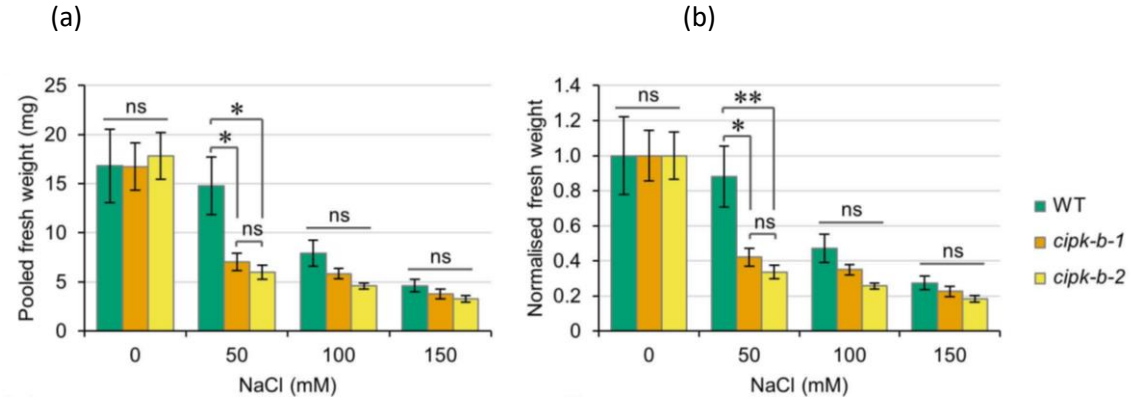

Figure 1.15. Salt phenotyping data. (a) Mean pooled mass of 5 pieces of thallus tissue of wildtype and *cipk-b* mutant lines grown at varying salt concentrations for 1 week. (b) normalization of data in (a). Error bars represent one standard error above and below the mean. * = P < 0.05, ** =P < 0.001 (Tansley *et al.,* 2023).

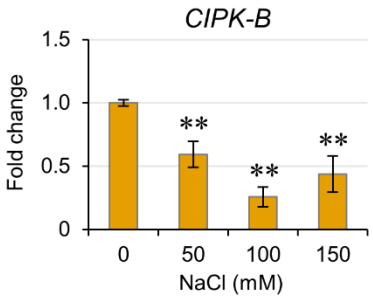

Figure 1.16. qRT-PCR data for gene expression of CIPK-B in *M. polymorpha*. RNA used in qRT-PCR extracted from thallus tissue grown on 1/2MS media supplemented with differing concentrations of NaCl. ** significance level p < 0.01 (Tansley *et al.*, 2023).

Because salinity stress is composed of ion toxicity and osmotic stress, it is important to investigate whether the salt sensitivity phenotype of the *cipk-b* mutant is in fact due to osmotic stress. This was one aim of this project.

MpCIPK-B is also closely related to AtCIPK23 (see Figure 1.14), a multifunctional CIPK with roles in homeostasis of a range of ions including manganese and magnesium. Another aim of this project was therefore to investigate whether CIPK-B is a multifunctional CIPK with roles in Mg^{2+} or Mn^{2+} tolerance as well as salt tolerance, and if CIPK-B is an AtCIPK23 homolog.

1.7 *M. polymorpha* CBL-CIPK interactions

In *A. thaliana,* most CBL-CIPK interactions are calcium dependent. For example, CBL4-CIPK24 interactions (Ishitani *et al.*, 2000). However, there are some cases of CBL-CIPK interactions occurring in the absence of calcium. For example, formation of the AtCBL2-CIPK14 complex is calcium independent (Akaboshi *et al.*, 2008).

It is assumed that CBL-CIPK interactions in *M. polymorpha* occur after calcium binding to CBL EF-hands, but this has not been shown. It may be the case that some or all CBL-CIPK interactions in *M. polymorpha* are calcium independent. Making the materials to allow investigation of this was therefore the third objective of this project.

1.8 Aims and Objectives of this project

This project had three main aims. First, to determine whether the *cipk-b* salt sensitivity phenotype previously observed in the Miller group is due to osmotic stress. Second, to investigate potential multifunctionality of CIPK-B by finding out whether CIPK-B has roles in manganese or magnesium tolerance, and third, to determine whether MpCBL-MpCIPK interactions are calcium dependent.

Understanding the calcium-decoding network in *M. polymorpha* at the genetic level gives useful insight into how CBL-CIPK calcium decoding networks work across plant species. This may have downstream applications in crop improvement to improve stress tolerance, a task increasing in importance with climate change.

Objective 1: Determine if the Mp*cipk-b* salt sensitivity phenotype is due to osmotic stress by observing the phenotype of Mp*cipk-b* mutants grown on media supplemented with sorbitol.

Wildtype (CAM2E), *cipk-b-1 and cipk-b-2* lines were grown on media supplemented with sorbitol and the effect of this on fresh weight measured. If CIPK-B contributes to osmotic stress tolerance, not just salt tolerance, *cipk-b* lines would grow significantly less than wildtype CAM2E.

To identify genes involved in the osmotic stress tolerance pathway in *M. polymorpha*, gene expression was investigated in sorbitol-treated wildtype (CAM2E) plants by qRT-PCR. Genes involved in the osmotic stress tolerance pathway would be differentially regulated in response to increasing stress.

Objective 2: Determine if MpCIPK-B is involved in manganese or magnesium tolerance by observing the phenotype of Mp*cipk-b* mutants grown on media supplemented with manganese or magnesium.

Wildtype, *cipk-b-1* and *cipk-b-2* lines were grown on media supplemented with varying concentrations of $MnSO_4$ or $MgSO_4$ and the effect of this on fresh weight measured. If CIPK-B contributes to manganese or magnesium tolerance, *cipk-b* lines would grow significantly less on media supplemented with these ions than wildtype CAM2E.

Objective 3: Determine whether MpCBL-CIPK interactions are calcium dependent by generating constructs containing CBL EF-hand quadruple mutants (cannot bind calcium) fused to the luciferase LgBiT and wildtype CIPKs fused to the luciferase SmBiT and performing a luciferase assay for interactions in transiently transformed tobacco leaves.

Point mutations in MpCBL EF-hand binding loops were made by overlap extension PCR. EF-hand point mutants are unable to bind calcium. These were incorporated into Golden Gate constructs containing a mutant CBL fused to part of the enzyme luciferase and a wildtype CIPK fused to another part of the enzyme luciferase. These Golden Gate constructs can be used in future experiments to investigate the calcium dependence of MpCBL-CIPK interactions by a split luciferase assay for interactions in transiently transformed *Nicotiana benthamiana* (Figure 1.17). If proteins interact, the two parts of the luciferase will be brought together, assembling the luciferase holoenzyme which biolumineses; bioluminescence can be measured using a plate reader. All possible CBL-CIPK pairs will be tested as previous work by PhD student Connor Tansley used biomolecular fluorescence complementation (BiFC) of *M. polymorpha* CBLs and CIPKs in transiently transformed *Nicotiana benthamiana* to show that all 3 MpCBLs interact with both MpCIPKs (Tansley *et al.,* 2023).

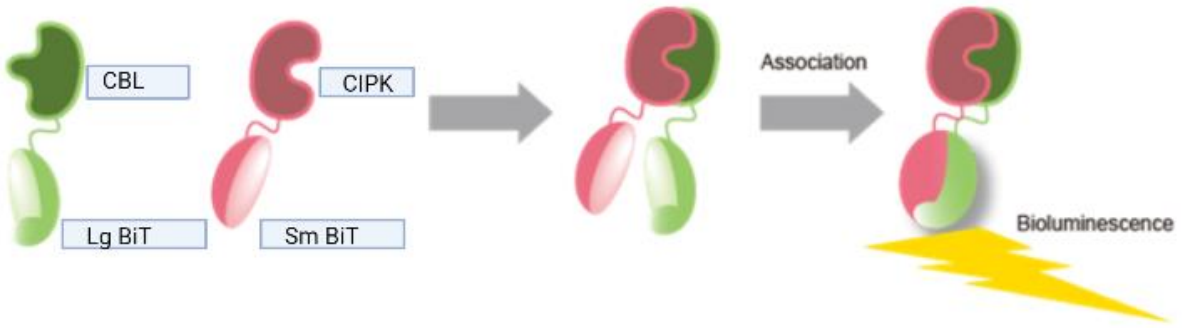

Figure 1.17 Split luciferase assay for CIPK-mutant CBL interactions. Formation of a CBL-CIPK complex will cause luciferase holoenzyme formation and result in bioluminescence which can be quantified.

2 Background to Key Methods

2.1 Overlap extension PCR

Overlap extension PCR (Bryksin and Matsumura, 2010) is a method by which mutations can be introduced to a region internal to a DNA sequence. Figure 2.1 shows the principals of overlap extension PCR. Template DNA is primed in the 5'- 3' direction at the location of the mutation to be introduced. This primer is not completely complementary to the template DNA, but contains one or two mismatches which will be introduced into DNA fragments which are synthesized by PCR using this primer. This primer is paired with a primer at the 3' end of the DNA. These are used in an end-point PCR reaction to generate a fragment with an introduced mutation at the desired location; spanning from here to the 3' end of the template sequence.

A primer at the 5' end of the DNA is paired with a primer at the location of the mutation to be introduced is paired with the reverse complement of the 5' – 3' primer used in the earlier PCR reaction, for priming on the complementary strand of the first PCR, and these are used in another end-point PCR reaction to generate a fragment with an introduced mutation at the desired location; spanning from here to the 5' end of the template sequence.

Products from these two end-point PCR reactions are then used in an overlap extension PCR reaction using primers for the 5' and 3' end of the DNA template sequence to generate a DNA strand spanning the entire length of the template sequence and including the introduced mutation desired.

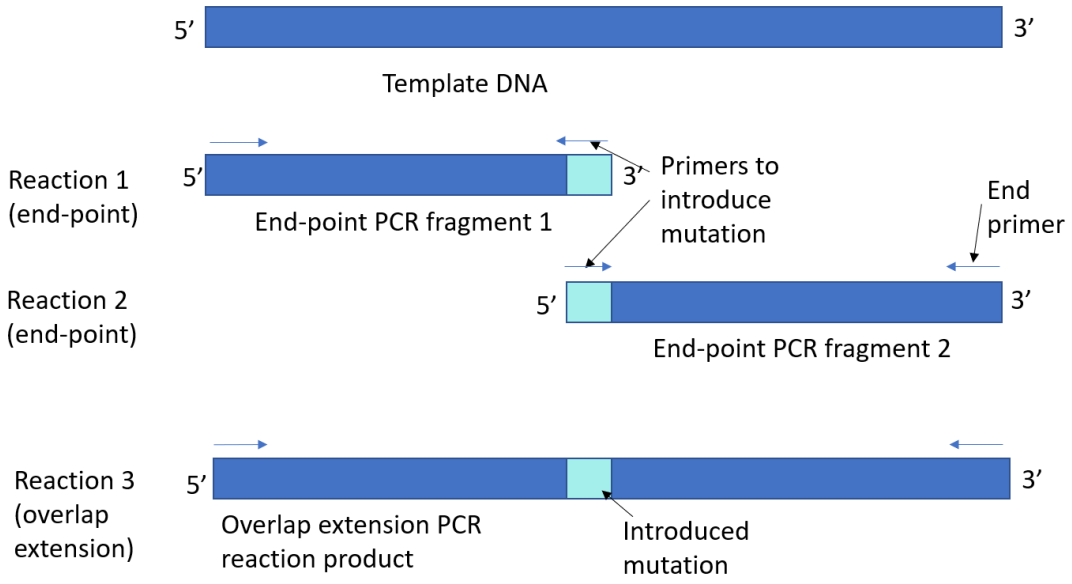

Figure 2.1. Overlap extension PCR methodology. Two truncated DNA fragments are made by end-point PCR; containing the mutation of interest. These are used to generate a full length fragment in an overlap extension PCR reaction.

2.2 Golden Gate Cloning

Golden Gate cloning is a modular cloning system that uses type IIS restriction enzymes which cleave at a known distance from their recognition site (Engler *et al.*, 2008). In level 0, modules with specific overhangs are made and these are cloned into plasmids. It is the overhangs which define the position and order of modules when they are joined together in level 1 of cloning (Lebedenko *et al.*, 1991). Level 0 modules include promoters (P), 5’ untranslated regions (U), signal peptides (S), coding sequences (C) and terminators (T) which are combined in level 1 to make a ‘PUSCT’ transcriptional unit which is cloned into a plasmid (Weber *et al.*, 2011; Figure 2.2).

Dependent on the case, not all types of level 0 modules may be necessary. In these cases, modules can be combined using the 5’ overhang for the 5’ module and the 3’ overhang for the 3’ module. In this way, P and U can be combined to form a PU construct and S and C can be combined to make an SC construct. The addition of a second C position allows tag proteins to be added to the C-terminus of the protein in the first C position, or SC1 position if S and C are combined. If both an N and C-terminal tag on the coding sequence are required, the gene of interest can be cloned into the C1 position and a tag in both C2 and S positions (Patron *et al.*, 2015).

In level 2, level 1 constructs are combined to form multi-gene constructs (Figure 2.2). Level 2 plasmids have 7 possible positions for DNA inserts; their order is defined by overhangs made by Type IIS restriction enzymes. If not all 7 positions are filled, the plasmid is closed using end linkers (Weber *et al.*, 2011).

Plasmid backbones used for Golden Gate cloning encode antibiotic resistance. Level 0 plasmids include a spectinomycin resistance gene, level 1 plasmids an ampicillin resistance gene, and level 2 plasmids a kanamycin resistance gene. This allows selection of transformed *Escherichia coli* bacteria at each stage.

Level 0 and level 1 plasmids contain a *lacZ* gene which is cleaved out and replaced with DNA insert(s) during the Golden Gate reaction, allowing blue/white screening. The *lacZ* gene encodes a β-galactosidase which turns X-gal substrate blue. When *E. coli* colonies transformed with Golden Gate products are grown on media supplemented with X-gal, they will be white if the gene of interest has been successfully inserted and *lacZ* disrupted or blue if the *lacZ* gene remains intact. Level 2 plasmids contain a *CRed* operon which encodes biosynthesis of canthaxanthin – a red pigment which can be used for red/white screening (Weber *et al.*, 2011).

Type IIS restriction enzymes cleave outside their recognition site. Level 0 plasmids are cleaved by BpiI type IIS restriction enzyme. Level I plasmids by BsaI, and level 2 plasmids by BpiI. These enzymes are used to create overhangs which are used to assemble modules in a defined order in a single reaction. DNA inserts are ligated to the plasmid using T4 DNA ligase. In Golden Gate cloning, the recognition site is cleaved out of the plasmid along with the *lacZ* gene/*CRed* operon during the reaction. This means that cleavage and ligation can be combined into a single step reaction (Engler *et al.*, 2008) as further cleavage of the plasmid is impossible once the recognition site has been removed.

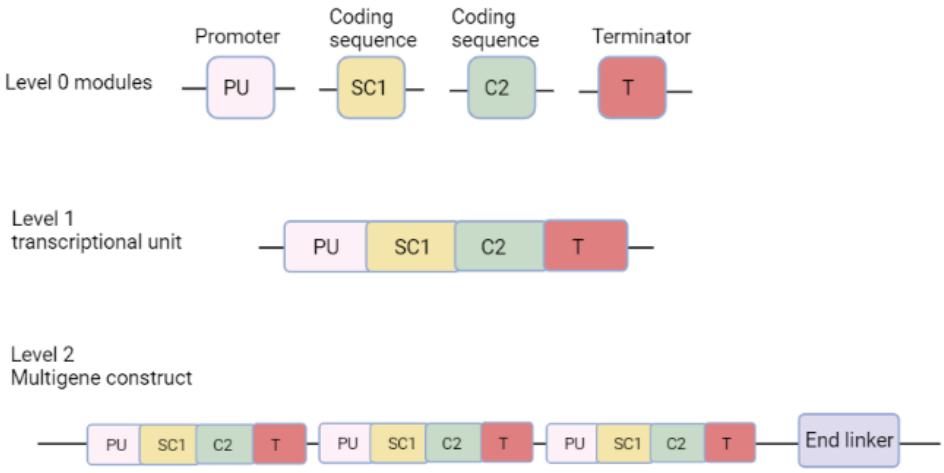

Figure 2.2. Golden Gate Cloning. Level 0 modules including promoters (P), 5' untranslated regions (U), signal peptides (S), coding sequences (C) and terminators (T) are combined in level 1 to make a 'PUSCT' transcriptional unit which is cloned into a plasmid. In level 2, level 1 constructs are combined to form multi-gene constructs. An end linker is used to closer the plasmid.

Objective 3 of this project is to generate level 2 modules which will allow testing of CBL-CIPK interactions when CBLs are unable to bind calcium. Figure 2.3 shows structure of the level 0, level 1 and level 2 constructs to be generated as part of this objective. Tables 2.1, 2.2 and 2.3 show the level 0, 1 and 2 construct names and their components. Level 2 constructs include a GUS reporter which will indicate successful transformation of *Nicotiana benthamiana* by production of a blue pigment when provided with an X-Glc substrate.

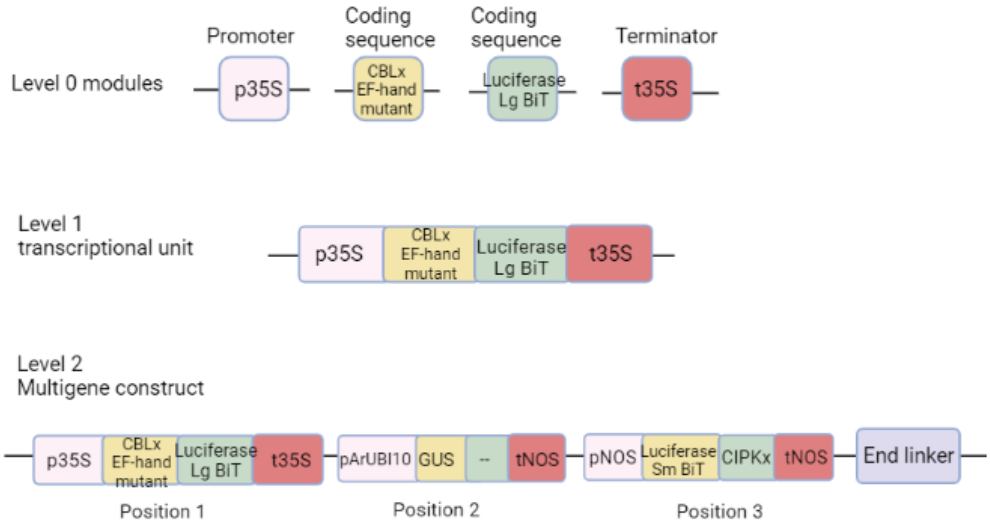

Figure 2.3. Level 0 Golden Gate cloning modules which will be used in objective 2 of this project, and their assembly into corresponding level 1 and level 2 constructs.

Table 2.1. Level 0 constructs

Construct ID	Description
BM01325	CBL-A mutant in EF-hands 1, 2, 3 and 4
BM01327	CBL-B mutant in EF-hands 1, 2, 3 and 4
BM01331	CBL-C mutant in EF-hands 1, 2, 3 and 4

Table 2.2. Level 1 construct designs

ID	Name	Backbone	PU	SC1	C2	T
BM01349	pL1M-R1-p35S-MpCBL-A-EF1234-LgBiT-t35S	EC47802 pL1V-R1	EC15058 p35S(short)	BM01325 pL0M-SC1-MpCBL-A-EF1234	BM00916 pL0M-C2-LgBiT	EC41414 t35S
BM01350	pL1M-R1-p35S-MpCBL-B-EF1234-LgBiT-t35S	EC47802 pL1V-R1	EC15058 p35S(short)	BM01327 pL0M-SC1-MpCBL-B-EF1234	BM00916 pL0M-C2-LgBiT	EC41414 t35S
BM01351	pL1M-R1-p35S-MpCBL-C-EF1234-LgBiT-t35S	EC47802 pL1V-R1	EC15058 p35S(short)	BM01331 pL0M-SC1-MpCBL-C-EF1234	BM00916 pL0M-C2-LgBiT	EC41414 t35S

Table 2.3. Level 2 construct designs (one for each CBL-CIPK pair)

ID	Name	Backbone	Position 1	Position 2	Position 3	End linker
BM01352	pL2B-MpCBL-A-EF1234-GUS-MpCIPK-A	EC50505 pL2V-1	BM01349	BM01178 - GUS	BM01067 - CIPK-A	EC41766
BM01353	pL2B-MpCBL-B-EF1234-GUS-MpCIPK-A	EC50505 pL2V-1	BM01350	BM01178 - GUS	BM01067 - CIPK-A	EC41766
BM01354	pL2B-MpCBL-C-EF1234-GUS-MpCIPK-A	EC50505 pL2V-1	BM01351	BM01178 - GUS	BM01067 - CIPK-A	EC41766
BM01355	pL2B-MpCBL-A-EF1234-GUS-MpCIPK-B	EC50505 pL2V-1	BM01349	BM01178 - GUS	BM01068 - CIPK-B	EC41766
BM01356	pL2B-MpCBL-B-EF1234-GUS-MpCIPK-B	EC50505 pL2V-1	BM01350	BM01178 - GUS	BM01068 - CIPK-B	EC41766
BM01357	pL2B-MpCBL-C-EF1234-GUS-MpCIPK-B	EC50505 pL2V-1	BM01351	BM01178 - GUS	BM01068 - CIPK-B	EC41766

3 Methods

3.1 Cloning methodologies

3.1.1 Overlap extension PCR to generate CBL EF-hand mutants

Initial PCR reactions contained 1X HF Phusion buffer, 0.2 mM dNTPs, 1 µM forward primer, 1 µM reverse primer (see table 3.1 for primers used), 50 ng template DNA, 0.02 U Phusion High Fidelity DNA Polymerase, dH_2O to a total reaction mixture volume of 20 µl.

Overlap extension PCR reactions contained 3.2 µl dNTPs at 10mM concentration, 8 µl of 5X HF Phusion buffer (Thermofisher Scientific), 1 µM forward primer, 1 µM reverse primer, 2.5 µl of DNA product from each initial PCR reaction to be used in the overlap extension, 0.6 U Phusion polymerase, and dH_2O to a total volume of 40 µl.

Overlap extension PCR reactions began with heating to 95°C for 30 seconds, followed by 40 cycles of 95°C for 10 seconds to denature dsDNA, 45°C for 5 minutes to allow primer annealing, and 72°C for 7 minutes to allow extension.

3.1.2 Agarose Gel electrophoresis

PCR products were separated by electrophoresis at 110 V on a 1% agarose in TAE buffer gel. Gels were stained in an ethidium bromide bath and imaged using a transilluminator.

3.1.3 Extract DNA from band on gel

The band of interest was cut out of the gel and DNA was extracted according to the following protocol:

300 µl QIAquick gel extraction solubilization buffer (Qiagen) was added to each sample in an Eppendorf tube. The samples were incubated at 55°C with 700 rpm shaking for approximately 10 minutes until dissolved. 100 µl pure isopropanol was added, followed by 10 µl silicon dioxide suspension made according to the protocol from Li, Li and Sheen, 2010. Samples were left for two minutes to allow DNA binding. Samples were centrifuged for 13 seconds. Supernatant was tipped away. 500 µl Promega miniprep column wash solution was added and the pellet disturbed. Samples were vortexed, then centrifuged for 13 seconds. Supernatant was discarded. 20 µl dH_2O was added and the pellet disturbed by pipetting up and down. Samples were incubated for 2 minutes at 70°C, then centrifuged for 2 mins at full power. The supernatant was harvested as this contained the DNA of interest. 5 µl of DNA extraction product was run on 1% agarose gel for quality control.

3.1.4 Golden Gate Cloning

The reaction mixture contains 0.1 mg/ml Bovine serum albumin (BSA), 1X T4 DNA ligase buffer (NEB), 1.5 µl T4 DNA ligase (NEB), BpiI or BsaI, 100 ng vector backbone, 100 ng of each assembly piece, and dH_2O to bring the reaction mixture to a total volume of 15 µl. The reaction

was performed in a thermocycler, with 25 cycles of 3 minutes at 37°C to allow digestion by the restriction enzyme followed by 4 minutes at 16°C to allow ligation by the T4 DNA ligase. This was followed by one cycle of 5 minutes at 50°C and 5 minutes at 80°C to denature the enzymes.

3.1.5 Transformation of *E. coli*

1µl of Golden Gate cloning reaction mixture was used to transform 20 µl of competent *E. coli* cells (DH5α). Cells were incubated on ice with DNA for 30 minutes, followed by a 30 second heat shock at 42°C, then 1 minute on ice. 500 µl SOC medium (table 3.4) was added to each sample and cells were incubated at 37°C for 1 hour, with shaking at 300 rpm.

200 µl of transformed cell mixture was used to spread LB plates (see table 3.4 for media compositions). Plates for *E. coli* cells transformed with level 0 Golden Gate cloning products contain X-gal and IPTG to allow blue-white screening and spectinomycin to allow antibiotic selection. Level 1 plates contain X-gal and IPTG and ampicillin. Level 2 plates contain kanamycin (table 3.5 shows antibiotic concentrations used). Plates were incubated overnight at 37°C to allow colony formation. Selective media allows colonies to be screened for successful transformation by antibiotic resistance and blue/white or red/white screening.

3.1.6 Colony PCR

Colonies that grow on selective media were screened by colony PCR.

Colony PCR reaction mixture: 5 µl Gotaq polymerase (Promega), 1 µM each primer (gene specific primers; see table 3.1 for primers used), 3 µl water. Bacteria from a colony was picked using a pipette tip and added to the reaction mixture by pipetting up and down.

The reactions began with heating to 98°C for 10 minutes to lyse cells, followed by 30 cycles of 98°C for 10 seconds to denature dsDNA, 53°C for 20 seconds to allow primer annealing, and 72°C for 1 minute to allow extension. This was followed by 5 minutes at 72°C.

Reaction products were separated by agarose gel electrophoresis, stained using ethidium bromide and imaged using a transilluminator. Samples with a positive colony PCR result showed a band of the expected size for the amplified fragment.

3.1.7 Overnight cultures

Colonies with positive colony PCR results were grown in liquid culture overnight. Transformed *E. coli* cells from the colony of interest were transferred using a pipette tip into liquid media consisting of 5 ml LB broth, with appropriate antibiotic for selection (spectinomycin, ampicillin or kanamycin depending on the construct level, see table 3.5 for antibiotic concentrations used). Cultures were grown overnight at 37°C with shaking at 180 rpm.

3.1.8 Miniprep DNA extraction

DNA was extracted from liquid bacterial cultures following the Promega DNA extraction kit protocol. 5 ml samples were centrifuged at 400 rpm for 10 minutes. Supernatant was discarded and 250 µl of cell resuspension solution was added. Samples were vortexed for thorough resuspension and the mixture transferred to 1.5 ml Eppendorf tubes. 250 µl of cell lysis solution was added and tubes inverted four times then left for 5 minutes while cell lysis occurred. 10 µl alkaline protease solution was added and tubes inverted four times before leaving for 5 minutes while protein digestion occurred. 350 µl neutralization solution was added to stop the reaction and tubes invested four times. Samples were centrifuged at 13000 rpm for 10 minutes, then the cell lysate was transferred to a spin column inside a collection tube. Samples were centrifuged for 1 minute, then the flow through discarded. Samples were washed twice using column wash solution, once with 750 µl and centrifuging for 1 minute, and once with 250 µl and centrifuging for 1 minute. Samples were centrifuged for a further two minutes at 13000 rpm, then spin columns transferred to new 1.5 ml Eppendorf tubes. 50 µl of nuclease free water was added and samples centrifuged at 13000 rpm for 1 minute to elute plasmid DNA. Spin columns were discarded.

DNA concentrations in water were checked by using a Nanodrop spectrophotometer, and diluted to 100 ng/µl by addition of further nuclease free water.

3.1.9 Restriction digest

DNA from transformed cells was digested using restriction enzymes as a quality control measure: DNA should give a predicable banding pattern when digested if DNA matches the construct being engineered.

The reaction mixture contained 1 µg DNA, 7 µl water, 2 µl CutSmart buffer and 10 U of restriction enzyme (BsaI for level 0 constructs, BpiI for level 1 constructs and HindIII for level 2 constructs). Mixture was incubated at 37°C for one hour. Loading dye was added and the sample separated by agarose gel electrophoresis at approximately 100 V. The resulting gel was stained using ethidium bromide solution and imaged using a transilluminator to check for the expected banding pattern.

Banding patterns that matched the expected banding pattern for the construct were taken forward. For those that did not, a problem with cloning or transformation must have occurred. Other colony PCR positive colonies were tested instead.

3.1.10 Sanger sequencing

To make certain that the constructs matched the desired sequence completely, level 0 and 1 constructs were sequenced by Sanger sequencing using the Eurofins Genomics overnight

sequencing service. DNA to be sequenced was submitted with a primer to allow sequencing of the correct part (see table 3.2 for primers used). Results were received in the form of a chromatogram and nucleotide sequence. Nucleotide sequences were aligned to the expected sequence of the gene-containing plasmid to ensure no mutations were present in the gene sequence and that relevant start and stop codons were present. Chromatograms were used to identify potential SNPs.

Level 2 constructs could not be sequenced by Sanger sequencing due to their length, so for these, correct restriction digest result was deemed a sufficient indicator of successful assembly.

3.1.11 Glycerol stocks

Positive *E. coli* colonies verified to contain the correct construct insert were used to make glycerol stocks so that the plasmid of interest can be extracted from these bacteria at a later date. Overnight cultures of *E. coli* of interest were grown (5 ml LB with the appropriate antibiotic) and mixed with 40% glycerol to a final storage concentration of 20% glycerol. This mixture was flash frozen using liquid nitrogen and put into long term storage at -80°C.

3.2 Plant Phenotyping and qRT-PCR

3.2.1 Plant accessions and mutants

The CAM2 accession of *M. polymorpha* was used as the wildtype accession in this study. This line was originally collected in Cambridge, UK by the Haseloff Laboratory. The two *cipk-b* mutant lines used in this study were already available in the Miller lab, having been generated in the CAM2 background.

3.2.2 Phenotyping conditions

Pieces of *M. polymorpha* thallus tissue approximately 3mm^2 were cut from a parent plant and grown on ½ MS + agar media (see table 3.4 for media compositions) alone or supplemented with sorbitol, $MgSO_4$ or $MnSO_4$ depending on the experiment. In each replicate, 5 pieces of thallus tissue were grown per plate and masses were measured using a fine balance (measures up to four decimal places) after 1 week of growth in a growth cabinet (23°C 16 hour day, 18°C 8 hour night). Three biological replicates and two technical replicates were done for each genotype and condition; this was supplemented with 3 further replicates of all genotypes for sorbitol phenotyping. For sorbitol phenotyping, sorbitol concentrations of 0, 100, 200 and 300 mM were used. For $MnSO_4$ phenotyping, $MnSO_4$ concentrations of 0, 2, 10, 20 and 50 mM were used. For $MgSO_4$ phenotyping, $MgSO_4$ concentrations of 0, 2, 10, 50 and 80 mM were used.

3.2.3 Plant RNA extraction and cDNA synthesis

qRT-PCR required RNA extraction from wildtype plant material treated with sorbitol, according to the phenotyping conditions set out earlier. This was done using the Qiagen RNA extraction kit. Plant material from 2 technical replicates of the same treatment (10 plantlets) were bulked and flash frozen in Eppendorf tubes using liquid nitrogen to prevent alterations in gene expression. To each sample, 450 µl of RLT buffer containing 2-mercaptoethanol was added and the sample was ground thoroughly on the buffer. Samples were heated to 56°C for 2 minutes. Lysate was transferred to a lilac spin column and this was centrifuged for 2 minutes at 13000 rpm. Supernatant was transferred to a new 2 ml tube. 200 µl ethanol was added to each sample and mixed immediately by pipetting. Mixture was transferred to a pink spin column and centrifuged at 13000 rpm for 15 seconds. Flow through was discarded. 700µl of RW1 buffer was added and the samples centrifuged for 15 seconds at 13000 rpm. Flow through was discarded. 500 µl of RPE buffer was added and the samples centrifuged for 15 seconds at 13000 rpm. Flow through was discarded. Another 500 µl of RPE was added and samples centrifuged at 1300 rpm for 2 minutes. Flow through was discarded. Columns were placed in new collection tubes and centrifuged at 13000 rpm for 1 minute. Columns were then placed in new 1.5 ml Eppendorf tubes and RNA eluted by addition of 30 µl RNase free water and centrifugation at 13000 rpm for 1 minute. Eluted water was then washed through the spin column again to elute as much RNA as possible.

Extracted RNA was then subjected to a DNAse treatment:

0.1 volume 10X DNAse Turbo Buffer and 3 U of Turbo DNAse (Thermofisher Scientific) was added to each sample. Samples were incubated for 30 minutes at 37°C. An additional 3 U of Turbo DNAse was added and samples were incubated for a further 30 minutes at 37°C. 0.1 volume of resuspended DNAse inactivation reagent was added and to samples and mixed. Samples were incubated for 2 minutes at room temperature. Samples were centrifuged for 10 minutes at 10000 rpm and RNA transferred to fresh RNAse free Eppendorf tubes. RNA concentration was quantified using a nanodrop machine to ensure good enough yield.

cDNA was made by reverse transcription using Superscript II.
28 µl of 1 µg RNA + RNAse free water, and 2.5 µl of 50 µM oligo dT17 primer was combined at 65°C for 15 minutes, followed by placement on ice for 2 minutes. 2.5 µl of 10 µM dNTPs, 10 µl of 5X reverse transcriptase buffer, 5 µl of DTT at 0.1M, 40 U RNAsin (inhibits RNases; Promega) and 200 U of Superscript II reverse transcriptase (Invitrogen) were then added to the mixture and incubated at 42°C for 1 hour. cDNA was diluted 1:10 and used in qRT-PCR reactions.

3.2.4 qRT-PCR

qRT-PCR was performed using SYBR Green JumpStart Taq ReadyMix (Sigma-Aldrich) and the Aligent AriaMx Real-time PCR system. The reaction mixture contained 5 µl Sybr Green, 65 µM $MgCl_2$, 4 µM forward primer, 4 µM reverse primer (see table 3.3 for primers used), 2 µl cDNA (1:10 dilution). Samples were heated to 95°C for 4 mins, followed by 40 cycles of 30 seconds at 94°C to denature DNA, 30 seconds at 55°C to allow primer annealing and 30 seconds at 72°C to allow extension. This was followed by cooling and a melt curve. Fluorescent readings were taken after the 55° step and indicate transcript levels.

3 biological and two technical replicates were done for each gene of interest for each sorbitol concentration. Actin and Adenine phosphoribosyl transferase were used as housekeeper genes. Ct values were generated using the AriaMx software. Values from housekeeper genes were used to normalize the data. Ct values were used to calculate fold change in expression compared to the 0mM sorbitol control treatment.

3.2.5 Statistical analysis of data

Data for plant masses and gene expression were analysed using statistical tests. Inter-genotype and inter-concentration differences were analysed using Kruskal-Wallis non-parametric tests (as data were not normally distributed), followed by post-hoc Mann Whitney U tests to determine which differences were statistically significant, using the Dunn-Sidak correction to account for compound error.

3.2.6 Primers used

Table 3.1. Primers for overlap extension PCR and colony PCR

Primer name	Purpose	Sequence
AR001	Mutate CBL-C EF-hand 2 first amino acid to gly	TTTTATCTCTTCGGCACGAAGCAAAAC
AR002	Mutate CBL-C EF-hand 2 first amino acid to gly	GTTTTGCTTCGTGCCGAAGAGATAAAA
AR003	CBL-A EF-hand 1 mutate 1st amino acid ser to gly	TTTAAGAAAATAGGCAGTGCTGTCATA
AR004	CBL-A EF-hand 1 mutate 1st amino acid ser to gly	TATGACAGCACTGCCTATTTTCTTAAA
AR005	CBL-B EF-hand 1 mutate ser to gly	TTTAAGAAACTTGGCTCCACTGTCATC
AR006	CBL-B EF-hand 1 mutate ser to gly	GATGACAGTGGAGCCAAGTTTCTTAAA
AR007	CBL-C EF-hand 1 mutate ser to gly	TTCAAAAAACTTGGCAGCACTGTCGTC
AR008	CBL-C EF-hand 1 mutate ser to gly	GACGACAGTGCTGCCAAGTTTTTTGAA
C29	CBL-A end primer SC1 position	tgtgaagaccaAATGTTGCTGTCTGGGGAG
BM0299	CBL-A end primer SC1 position	CCCGAAGACTCcaccTGACGTATC
C202	CBL-B end primer SC1 position	tgtgaagaccaAAtgggctgcttcagc
BM0300	CBL-B and CBL-C end primer SC1 position	CCCGAAGACTCcaccAGTATT
C33	CBL-C end primer SC1 position	tgtgaagaccaAATGGGCTGCTTCAGCTCG
BM0315	CBL-B end primer SC1 position	CCCGAAGACTCcaccAGTATTTGAATC

Table 3.2. Primers for sequencing

Primer name	Sequence	Purpose
GoldenGate-1	caatacgcaaaccgcctc	FOR sequencing of Level 0 vectors
GoldenGate-2	CCTATAAAAATAGGCGTATCACG	REV sequencing of Level 0 vectors
GoldenGate-3	cccgccaatatatcctgtc	FOR sequencing of Level 1 and 2 vectors
GoldenGate-4	GCGGACGTTTTTAATGTACTG	REV sequencing of Level 1 and 2 vectors

Table 3.3. qRT-PCR primers

Gene	Gene ID (*M. polymorpha*.info)	Forward primer code	Forward primer sequence	Reverse primer code	Reverse primer sequence
CBL-A	Mp2g07750	C180	AGCGGAAAGAGGTGAAACGG	C109	GAGAGGGATGCTGCTGAACC
CBL-B	Mp4g00900	C112	GGGCTGCTTCAGCTCAAAAC	C113	CGCAAGCTGGAACTCTTCCT
CBL-C	Mp5g19810	C116	CAAGTGCTCCACCAGAGGAC	C117	GCCTCCGCAAATGTCTTGTC
CIPK-A	Mp1g05680	C120	AAACACCCTGCGAACGAGAT	C121	ACCTCAAACACCTCTGTGGC
CIPK-B	Mp2g26670	C124	CCTGTACGGATGCACGATGA	C125	AGAACGGAAAGGTTGAGCCC
LEA-like4	Mp1g23200	BM234	GCTAACAGACCCAGGTGAC	BM235	TGTTTCCAACGGCAGAGTG
ACT1	Mp6g10990	BM171	GAGCGCGGTTACTCTTTCAC	BM121	GACCGTCAGGAAGCTCGTAG
APT	Mp3g35140	C170	CGAAAGCCCAAGAAGCTACC	C171	GTACCCCCGGTTGCAATAAG

3.2.7 Media used

Table 3.4. Media used in this project

Media name	Formula per litre
LB	LB Broth Miller 25 g (Formedium LMM0105)
LB + Agar	LB Broth Miller with Agar 40 g (Formedium LMM0202)
SOC	SOC Broth 31.5 g (Formedium SOC0201)
MS + Agar	2.165 g MS with vitamins (Duchefa Biochemie M0222), 8 g Agar (Sigma 05040), 10 g Sucrose (Thermo Scientific J65148.A1)

3.2.8 Antibiotic concentrations used

Table 3.5. Antibiotic concentrations used in this project for colony selection

Antibiotic	Final Concentration (µg/ml)	Solvent
Spectinomycin	200	H_2O
Ampicillin	100	H_2O
Kanamycin	25	H_2O

3.2.9 Bacterial strains used

Escherichia coli strain DH5α (Invitrogen) was used for cloning of plasmids.

4 CIPK-B is not involved in osmotic stress tolerance in *M. polymorpha*

4.1 Introduction

Drought stress causes major crop losses. Data from published studies showed that wheat yields were reduced up to 21% and maize yields up to 30% between 1980 and 2015 due to drought (Daryanto, Wang and Jacinthe, 2016). Salt stress also causes major crop losses. Moderate soil salinity (8 to 10 dS m^{-1}) results in yield losses of 55%, 28% and 15% in maize, wheat and cotton respectively (Zörb, Geilfus and Dietz, 2019).

Climate change is continuing to progress – average global combined land and ocean temperatures are predicted to increase by at least 0.2°C per year going forward (IPCC, 2022) - increasing incidence of drought and salinity stress across the world. Periods of drought cause salts to accumulate in soil as they are not leached out by precipitation, and increased drought is often managed by irrigation which causes secondary salinization. Increased drought and salinity will cause crop losses, while demand for food continues to rise by an expected 35 to 56 percent between 2010 and 2050 (van Dijk *et al.*, 2021) due to population growth and increasing affluence. This poses a serious threat to food security.

It is necessary to produce more food despite increasing abiotic stress. Understanding how salt and osmotic stress tolerance works at the molecular level in plants is invaluable in identifying new avenues towards crop improvement to withstand stresses and boost yields under stress conditions. CBLs and CIPKs in plants are key to abiotic stress responses, in particular salt and osmotic stress responses. Investigating the role of the CBL-CIPK network in *M. polymorpha* in salt and drought stress tolerance will give valuable insight into ways to do this in crop plants.

Previous work in the Miller lab has demonstrated that CIPK-B is involved in salt stress tolerance in *M. polymorpha*, by showing that *cipk-b* knockout mutants have reduced growth under salt stress than wildtype plants at 50 mM salt (Tansley *et al.,* 2023). This data is supported by phylogenetic evidence which shows that CIPK-B is closely related to AtCIPK24, the *A. thaliana* SALT OVERLY SENSITIVE 2 gene (phylogenetic tree: Figure 1.14).

Salt stress causes stress in multiple ways. It causes ion toxicity, where high sodium concentration in a plant cell causes protein denaturation, membrane destabilization, and competes with potassium for uptake into cells via transport proteins, reducing essential K^+ uptake needed for metabolism and growth. Salt stress also causes osmotic stress. Presence of salt lowers the water potential of the media, setting up a water potential gradient and causing

water to leave plant cells into the surrounding media by osmosis, resulting in desiccation stress which limits metabolism and growth (Zhao *et al.*, 2011).

Salt and osmotic stress activate distinct signalling pathways. Signalling pathways affect a range of target proteins including transcription factors which affect gene expression. The salt and osmotic stress signalling pathways regulate distinct sets of genes with some overlap. Investigations by Kreps *et al.* (2002) in *A. thaliana* found 375 salt-regulated genes and 85 osmotic stress-regulated genes, as well as 106 genes regulated by both salt and osmotic stress in roots, measured after 3 hours of stress. In leaves 120 salt-specific genes and 279 osmotic stress-specific genes were found, with 68 overlapping genes. It is expected that there would be some overlap in genes regulated by salt and osmotic stress because salt stress includes osmotic stress so some plant responses to it will be the same. However, it is clear from the data that most of the gene expression changes found are stimulus specific, demonstrating that stresses activate distinct, stimulus-specific signalling pathways in *A. thaliana* and this is likely to be true across species.

It is therefore necessary to investigate whether the *cipk-b* salt sensitivity phenotype is due to osmotic or ionic stress, and therefore determine whether CIPK-B functions as part of the salt or osmotic stress response pathway in *M. polymorpha*. It is useful to understand the role of CIPK-B in salt and osmotic stress as this knowledge can be used to engineer plants which are more stress tolerant, for example by CIPK-B overexpression.

4.2 Results

To investigate whether the *cipk-b* salt sensitivity phenotype previously observed (Tansley *et al.,* 2023) is due to osmotic stress, wildtype and *cipk-b* mutant *M. polymorpha* plantlets were grown on ½ MS media supplemented with either 0, 100, 200 or 300 mM sorbitol, a sugar alcohol which induces osmotic stress, for one week. These concentrations were selected because they caused equivalent osmotic stress (iso-osmotic) to previously tested salt concentrations. Six biological replicates were performed, with two technical replicates for each biological replicate, though some data points were discarded due to contamination. This data was pooled with 3 biological replicates, and two technical replicates for each biological replicate, of already available data collected by a previous student from wildtype CAM2E plants grown in the same way, to increase sample size further.

Growth was visibly reduced in plantlets grown at high sorbitol concentrations (Figure 4.1). Pooled mass of the five plantlets on each plate was measured (Figure 4.2). Data was normalised to 0mM sorbitol allow inter-genotype comparisons and analysed by Kruskal-Wallis non-parametric tests to find differences in median plant mass between within and between

genotypes. Where significant differences were found, post-hoc Mann-Whitney U tests were used to find which differences were significant. The Dunn-Sidak correction was used to account for compound error. This data has since been published in Tansley *et al.,* 2023.

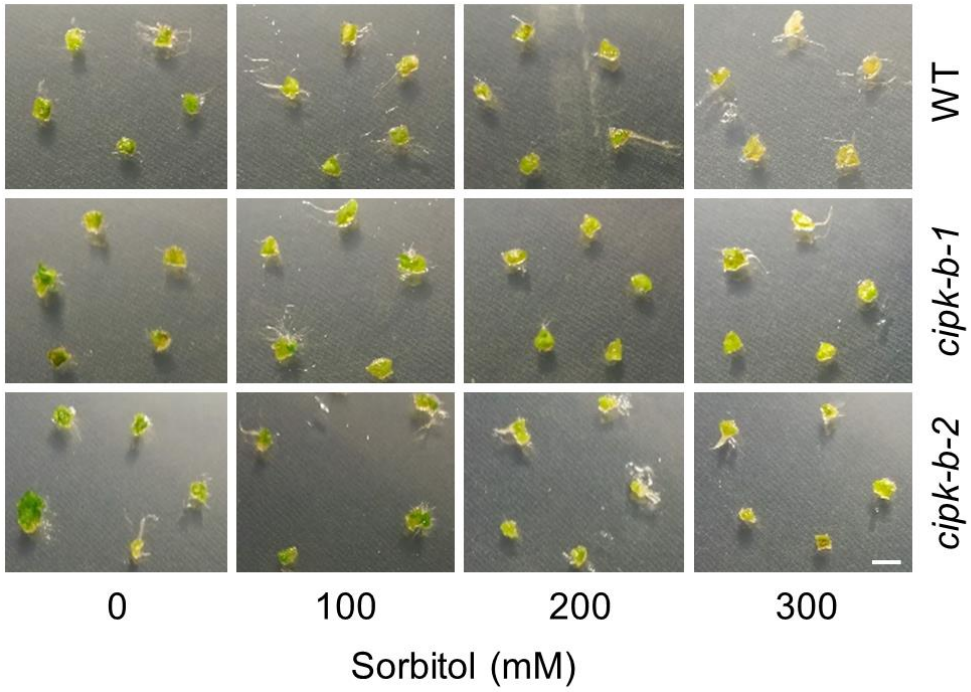

Figure 4.1. Wildtype and *cipk-b* mutant *M. polymorpha* show reduced growth under osmotic stress. Scale bar = 5mm. (Tansley *et al.,* 2023).

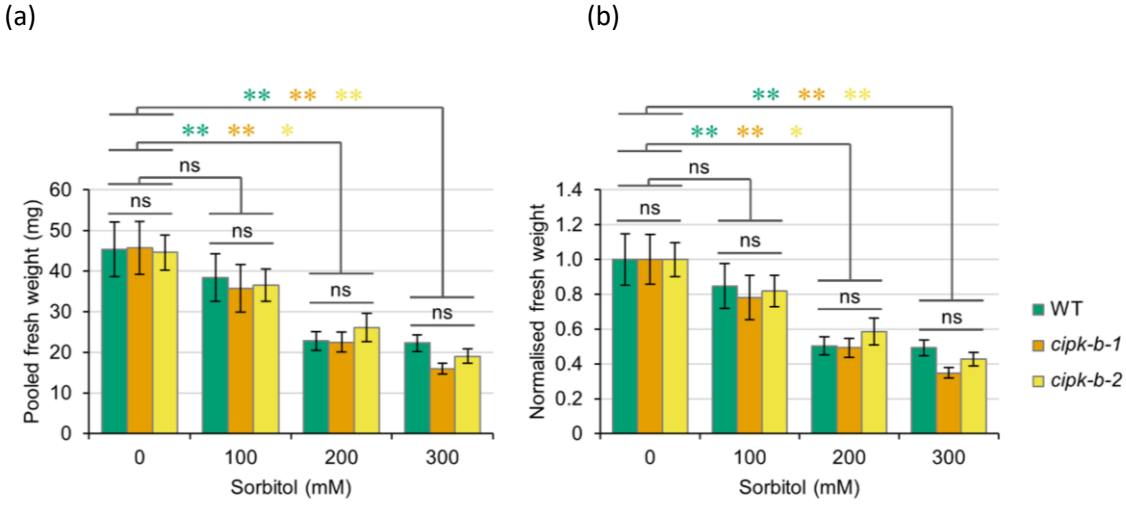

Figure 4.2. Sorbitol phenotyping data. (a) Mean pooled mass of 5 pieces of thallus tissue of wildtype and *cipk-b* mutant lines grown at varying sorbitol concentrations for 1 week. (b) Normalization of data in (a). Error bars represent one standard error above and below the mean. * = $p < 0.05$, ** = $p < 0.01$. (Tansley *et al.* 2023).

Kruskal-Wallis tests found that all three genotypes of *M. polymorpha* grew less under applied sorbitol (CAM2E $p = 0.017$; *cipk-b-1* $p < 0.001$; *cipk-b-2* $p = 0.001$). Mann-Whitney U tests found that differences were between 0 and 200 mM sorbitol, and 0 and 300 mM sorbitol (Figure 4.2). However, there was no significant difference between genotypes at any of the sorbitol concentrations investigated (0 mM sorbitol $p = 0.917$, 100 mM sorbitol $p = 0.895$; 200 mM sorbitol $p = 0.589$; 300 mM sorbitol $p = 0.059$), so knockout of the *CIPK-B* gene did not impact osmotic stress tolerance, suggesting that CIPK-B is not involved in osmotic stress tolerance in *M. polymorpha*.

The involvement of genes from the *M. polymorpha* CBL-CIPK network in osmotic stress response was tested by quantitative real time PCR (qRT-PCR) using material from phenotyping experiments above. Gene expression of *CBL-A, CBL-B, CBL-C, CIPK-A and CIPK-B* was investigated, along with housekeeper genes *ACTIN* and *ADP* as controls for calculating relative expression, and *LEA-like4*, as stress marker gene whose expression increases under stress. Three biological repeats were performed for each gene, with three technical repeats for each biological rep. This data has since been published in Tansley *et al.*, 2023. Changes in gene expression were calculated as fold change and their significance analysed using statistical tests. Results are displayed in Figure 4.3.

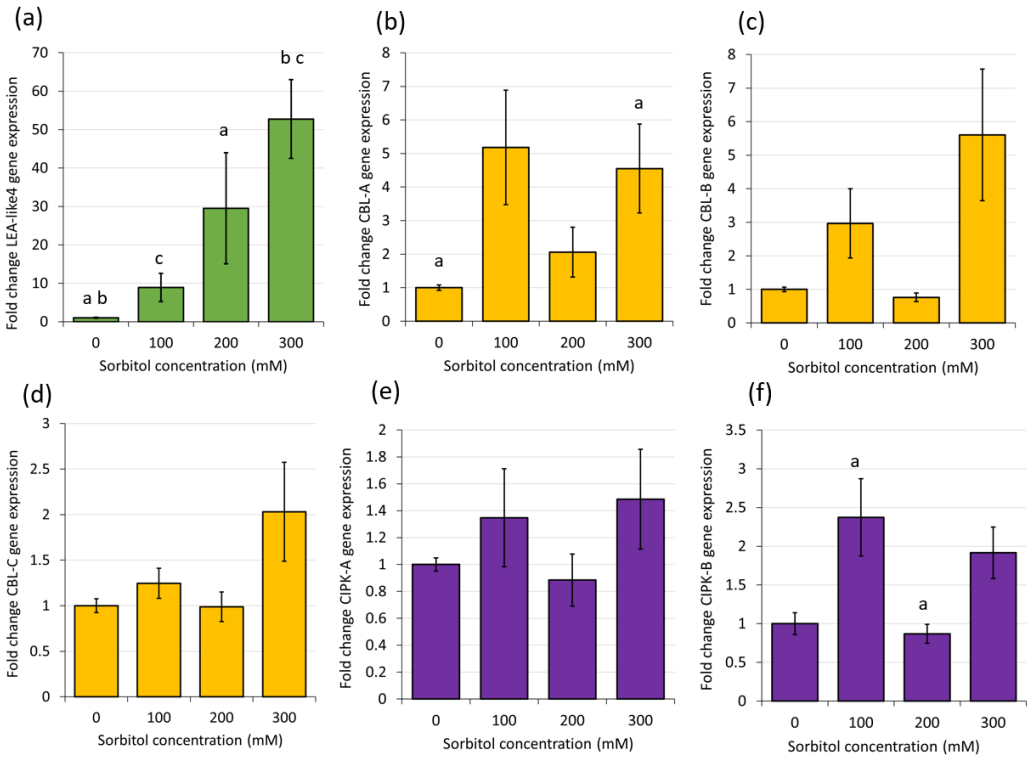

Figure 4.3. Sorbitol qRT-PCR data. a) Fold change *LEA-like4* gene expression in response to sorbitol. B) Fold change *CBL-A* gene expression in response to sorbitol. C) Fold change *CBL-B* gene expression in response to sorbitol. D) Fold change *CBL-C* gene expression in response to sorbitol. E) Fold change *CIPK-A* gene expression in response to sorbitol. F) Fold change *CIPK-B* gene expression in response to sorbitol. Error bars represent one standard error above and below the mean. Letters indicate significant differences in gene expression between two concentrations, for example 'a' in panel (a) indicates a significant difference between 0 and 200 mM sorbitol. All significant differences to $p \leq 0.003$.

For *LEA-like4* (Figure 4.3a), there was significant difference in expression depending on sorbitol concentration (Kruskal-Wallis, $p < 0.001$), between 0 and 200mM sorbitol (Mann-Whitney U, $p = 0.001$), between 0 and 300 mM sorbitol (Mann-Whitney U, $p = 0.001$), and between 100 and 300 mM sorbitol (Mann-Whitney U, $p = 0.003$). This behaviour is as expected for *LEA-like4* which is a stress marker gene so whose expression should increase as stress level increases. This helps demonstrates that the sorbitol treatments used cause transcriptional changes and increase confidence in remaining experimental results.

For *CIPK-B* (Figure 4.3f), sorbitol concentration affected gene expression (Kruskal-Wallis, $p = 0.006$). Plants grown at 200 mM sorbitol showed increased *CIPK-B* gene expression compared to plants grown at 100 mM sorbitol (Mann-Whitney U, $p = 0.003$). This suggests that *CIPK-B* has some kind of role in *M. polymorpha* response to sorbitol. However, there was no significant difference in gene expression between plants grown at 0 mM and any other

concentration, suggesting that *CIPK-B* expression does not change in response to applied sorbitol, and supporting the conclusion from the sorbitol *cipk-b* mutant phenotyping work that CIPK-B is not involved in plant responses to osmotic stress.

For CBL-A (Figure 4.3b), there was a significant difference in expression depending on sorbitol concentration (Kruskal-Wallis, p = 0.003); differences were found between plants grown at 0 and 300 mM sorbitol, suggesting that CBL-A may be involved in osmotic stress tolerance in *M. polymorpha*. There is also a peak in expression at 100 mM sorbitol but, although its value is larger than the peak at 300 mM sorbitol, it is not significantly different from expression at 0 mM sorbitol; this is due to large variance in gene expression between replicates, particularly in biological replicate 3. The absence of a clear trend in change in expression or a single peak in expression at a particular sorbitol concentration raises doubts over the validity of the results of this experiment. More repeats of this experiment should be done to reduce standard error, increase the reliability of the results and confirm if trends shown are actual trends.

For CBL-B, CBL-C and CIPK-A there is no significant difference in gene expression in response to sorbitol (Kruskal-Wallis, p = 0.222; p = 0.442; p = 0.895; Figure 4.3c, d and e respectively), suggesting that these genes are not involved in osmotic stress responses in *M. polymorpha*.

4.3 Discussion

In this objective, phenotyping experiments found that CIPK-B was not involved in osmotic stress tolerance; this was supported by qRT-PCR data. qRT-PCR of other genes identified CBL-A as a possible player in the osmotic stress tolerance pathway in *M. polymorpha*.

Phenotyping experiments proved effective at identifying changes in mass in response to stress. However, contamination was an issue in some cases. Data from contaminated plants could not be used due to potential impacts of presence of microorganisms on cell signalling and gene expression in the plant. Therefore, special attention was paid to aseptic technique to reduce contamination and extra repeats were performed to account for the potential loss of some samples.

Mass was selected as the parameter for measurement in phenotyping experiments due to its ease of observation and because reduction in biomass is a well-established effect of stress on plants. Measurements could be made more accurate by weighing plant material before growth under stress conditions for one week as well as after, to enable collection of exact biomass change data. Attention would have to be paid to sterility of plant material when measuring biomass before application of stress. This could be done by using a designated sterile balance and sterile weigh boats within a laminar flow hood. Other parameters, such as rhizoid length could be measured too to further increase the amount of data for analysis. Rhizoid length

would be useful to investigate as they perform the same function as roots in higher plants: they are the first line of defence against osmotic stress which is sensed in the media. In higher plants like maize and rice, root length can increase in response to mild osmotic stress to allow better scavenging for water, but root growth is inhibited under more severe osmotic stress (Watts *et al.*, 1981; Sharp and Davies, 1989; Kano *et al.*, 2011). A similar pattern to this would be expected to be demonstrated in *M. polymorpha* rhizoids; if CIPK-B is involved in osmotic stress tolerance, *cipk-b* mutants would be expected to show reduce rhizoid growth compared to wildtype under all osmotic stress severities tested.

4.3.1 CIPK-B is salt responsive and may be the SOS2 homolog

Phenotyping data showed no difference in mass between wildtype and *cipk-b* mutant plants grown at any concentration of sorbitol tested. Therefore, CIPK-B is not involved in osmotic stress tolerance. This means that the salt-sensitivity phenotype shown in *cipk-b* mutant plants (Tansley *et al.*, 2023) must be due to ion toxicity. This conclusion is supported by qRT-PCR data which shows that there is no significant difference in *CIPK-B* gene expression between 0mM sorbitol and any other concentration, suggesting that CIPK-B is not involved in osmotic stress tolerance in *M. polymorpha*.

MpCIPK-B is closely related to AtCIPK24, the CIPK involved in the *A. thaliana* Salt Overly Sensitive (SOS) pathway (phylogenetic tree; Figure 1.14). This and the demonstrated role of MpCIPK-B in salt stress tolerance but not osmotic stress tolerance, shown by phenotyping experiments and qRT-PCR data, suggests that MpCIPK-B is the AtCIPK24 homolog. If this is the case, the SOS pathway shows remarkable conservation between *M. polymorpha* and *A. thaliana*, which diverged from each other 450 million years ago (Tena, 2018). If the SOS pathway is conserved between *M. polymorpha* and *A. thaliana*, this suggests that knowledge gained from investigation of the CBL-CIPK network is likely to be transferable to higher land plants such as crops, meaning that useful genes can be identified in *M. polymorpha* for targeting for improvement of crop stress tolerance. For example, CIPK-B is a good target for crop improvement to withstand salinity stress.

To further elucidate the salt stress signalling pathway in *M. polymorpha*, the MpCIPK-B-interacting CBL (the AtCBL4 homolog) should be identified and its role in the salt stress response signalling pathway confirmed. Previous experiments investigating CBL-CIPK interactions have shown that all *M. polymorpha* CBLs and CIPKs are capable of interacting with each other when expressed in *Nicotiana benthamiana* (Tansley *et al.*, 2023). However, it is not known if they interact in *M. polymorpha*. This could be tested by a luciferase assay in *M. polymorpha*. This has not previously been attempted due to difficulties transforming *M.*

polymorpha tissues, however, if this can be optimized, experiments such as this would be informative.

Phylogenetic trees (Figure 1.14) show that AtCBL4 is most closely related to MpCBL-A of all the MpCBLs, suggesting that this may be the AtCBL4 homolog. However, qRT-PCR data shows that MpCBL-C shows the same expression pattern as AtCBL4 in response to salt: upregulation in the first 24 hours of salt regulation (Tansley *et al.,* 2023; Ji *et al.*, 2013), and downregulation after 6-7 days (Tansley *et al.,* 2023; Rolly *et al.*, 2020), whereas CBL-A and CBL-B do not show this expression pattern. This suggests that MpCBL-C is the AtCBL4 homolog. The salt-responsive CBL can be conclusively identified by creating CBL knockout mutants in *M. polymorpha* and phenotyping them in response to applied salt stress. If the CBL tested is needed for the salt stress response, the knockout mutant will show reduced growth under stress conditions when compared to wildtype plants. The salt-responsive CBL identified will be a potential target for crop improvement to withstand salinity stress.

To further confirm that the CBL identified functions in the same signalling pathway as CIPK-B, *cbl-cipk-b* double mutant *M. polymorpha* lines should be generated and used in phenotyping experiments. If double mutants respond in the same way to salt stress as mutants in either the *CBL* in question or *CIPK-B*, in terms of reduction in tissue mass in response to stress, this implies that these genes function in the same pathway, as knocking out one gene inactivates the pathway similarly to knocking out both genes in the pathway. This is a similar approach to what was done by Halfter, Ishitani and Zhu (2000) to demonstrate that *A. thaliana* SOS2 and SOS3 function in the same pathway. Atsos2 and Atsos3 mutants both show hypersensitivity to NaCl stress, with sos2 mutants showing greater sensitivity. sos2-sos3 double mutants behaved the same as sos2 mutants. The non-additive effect on plant tissue mass of knocking out both genes suggests they function in the same signalling pathway.

Though it has been shown that salt and osmotic stress induce calcium signals in *M. polymorpha* (Miller, 2021, unpublished), this in itself does not confirm that the signalling is calcium dependent. That can be investigated by generating EF-hand knockout mutants of the CBL identified to be involved in the salt stress tolerance pathway. EF-hand mutant CBLs will be unable to bind calcium. If *M. polymorpha* lines expressing these mutant CBLs in the place of CBLs with active EF-hands do not activate the salt stress signalling pathway, the conclusion that the salt stress signalling pathway in *M. polymorpha* is calcium dependent can be drawn. Mutating EF-hands in calcium binding proteins has been done before, for example to investigate calcium affinity of recoverin, a neuronal calcium binding protein in humans (Permyakov *et al.*, 2000). We can determine if the salt stress signalling pathway is activated in plants with mutant CBLs by qRT-PCR of genes we know to be upregulated in response to salt

stress in *M. polymorpha*, such as those identified in a recent study by Tan *et al.* (2022) which found 981 differentially expressed genes in response to salt in *M. polymorpha*, with roles in translation elongation, transport, nitrogen assimilation and phenolics. Phenotyping experiments will also reveal if salt stress tolerance is allowed in these circumstances, as plants which are not stress tolerant will display increased chlorosis due to overproduction of reactive oxygen species (Sachdev *et al.*, 2021), and reduced biomass Krishnamurthy *et al.*, 2011).

In *A. thaliana*, there are two CBL-CIPK salt stress response pathways. CIPK24 interacts with CBL4 in the roots to respond to salt stress and with CBL10 in the shoots, where CBL4 is not highly expressed (Quan *et al.*, 2007). This could be the case in *M. polymorpha*, so it is worth investigating tissue-specific expression of CBLs and CIPKs in response to salt stress. However, distinct salt stress response pathways are less likely to exist because the smaller CBL-CIPK network means there is reduced redundancy compared to *A. thaliana*. It would be interesting to test if CIPK-B can interact with AtCBL4 or AtCBL10 as this may indicate whether it functions equivalently to AtCIPK24 in the main SOS pathway in *A. thaliana* roots, or more similarly to the salt response pathway in *A. thaliana* shoots. This could be done by luciferase assays in *Nicotiana benthamiana*.

The CBL and CIPK involved in salt stress tolerance in *M. polymorpha* could be used in crop improvement by overexpression to improve salt stress tolerance. Overexpression of MpCIPK-B in crop plants may result in an increase in salt tolerance. Similar approaches have previously been successful. For example, overexpression of TaCIPK24 in *A. thaliana* improves salt tolerance (Sun *et al.*, 2015). However, this depends on compatibility with existing machinery in these crop plants. It will be important to investigate whether CIPK-B can function as a substitute for the SOS3 equivalent in higher crop plants in their salt response signalling pathways. We are hopeful that this will work as the SOS pathway appears to be a highly conserved stress tolerance pathway between basal land plants, higher model plants and crop species.

If signalling machinery is compatible, overexpression of MpCIPK-B in higher crop plants may increase activation of salt stress tolerance in these crops, increasing salt stress tolerance. This should be tried. However, it is possible that the available interacting CBLs will become the limiting factor in this scenario, and that therefore the interacting CBL will also require overexpression in order to allow formation of more salt-responsive CBL-CIPK complexes and therefore more activation of downstream protein targets and salt stress tolerance.

Similarly, another way to improve salt stress tolerance in crop plants would be to overexpress the SOS1 homologs in these plant species: the ion channel targets if the CBL-CIPK complexes

responsible for salt extrusion. The MpSOS1 homolog can be identified by bioinformatics and validated *in planta* by generating knockout mutant lines of this gene and testing the effect on salt tolerance by phenotyping. Once this is done, this is a viable target for crop improvement.

If new CBL-CIPK salt stress tolerance signalling pathways are identified in *M. polymorpha*, for example involving CBLs, CIPKs and downstream targets which do not have homologs in higher plants, these may point towards similar pathways yet to be identified in crops. Alternatively, they may be unique pathways to *M. polymorpha* which could be engineered into higher crops to create new pathways for stress tolerance.

Previous qRT-PCR data (Tansley *et al.,* 2023; Figure 1.16) shows a decrease in expression of CIPK-B in response to salt stress after one week of treatment. This matches the expected result for genes involved in salt stress signalling, based on data for the *A. thaliana* SOS pathway which shows that SOS2 and SOS3 are upregulated at 24 hours post treatment, but downregulated after 6 days (Ji *et al.*, 2013; Rolly *et al.*, 2020). To further confirm the involvement of CIPK-B in salt stress signalling in *M. polymorpha*, expression of CBLs and CIPKs in response to salt and osmotic stress should be investigated after 24 hours of treatment as well as after one week.

It is possible that tissue-specific expression of the *M. polymorpha* CBLs and CIPKs is masked in both previous salt-responsive qRT-PCR data and osmotic stress-responsive qRT-PCR data from this study, due to use of RNA extracted from a whole thallus *M. polymorpha* tissue sample in the qRT-PCR experiments. Tissue-specific expression of CIPKs has been previously shown in other species. For example, *Triticum aestivum* CIPK22 was found by RT-qRT-PCR to be specifically expressed in roots at plant seedling stage (Sun *et al.*, 2015). This brings into question whether the results of thallus tissue qRT-PCR can be relied upon. For example, MpCIPK-B expression may in fact be affected by osmotic stress even though thallus qRT-PCR does not show this, and other CBLs and CIPKs that are involved in the osmotic stress response may also not have been identified. Therefore, tissue-specific gene expression in response to salt and osmotic stress should be investigated to identify gene expression changes not detectable in thallus qRT-PCR. This will be done by extracting RNA from only tissues of interest for qRT-PCR analysis. For example, expression in rhizoids should be investigated and may show different gene expression to whole thallus tissue because rhizoids are the first line of defence against osmolytes in growth media so are where a response is most likely to occur. If this were the case, this would suggest that salt or osmotic stress responses are local to the root, rather than systemic to the plant, at least at the timepoint after stress at which the gene expression was measured.

Tissue-specific gene expression patterns identified may give insight into tissue-specific signalling pathways in *M. polymorpha*. Tissue-specific signalling pathways are common in higher plants. For example, in the *A. thaliana* Salt Overly Sensitive pathway, CIPK24 is regulated by CBL10 in shoots, as opposed to CBL4 in roots (Quan *et al.*, 2007). Understanding tissue specificity of signalling pathways is useful when deciding how to engineer crop plants to be more stress tolerance. For example, tissue-specific proteins could be engineered to be expressed only in the tissues of interest in modified crop plants, or more widely to test if they would be functional outside of their typical tissue.

Short term salt stress responses such as closing of guard cells and production of compatible solutes are likely to rely on local signalling, and long term salt stress responses such as changes in development (James *et al.*, 2002; Rubinigg *et al.*, 2004) are likely to rely on systemic signalling. Expression of CBLs and CIPKs should be measured by qRT-PCR at different time points and in different tissues to determine whether they are involved in local or systemic signalling, or both, and in short term or long term signalling, or both. If CBLs and CIPKs are found to be involved only in local, short term responses, it is likely that they communicate with other signalling proteins too, to allow systemic responses to salt. Communicating proteins may be identifiable through RNAseq of distal tissues to identify genes involved in the systemic salt stress response, and these may also be useful targets for crop improvement to improve salt stress tolerance.

4.3.2 Elucidating the osmotic stress response pathway in *M. polymorpha*

To identify genes involved in the osmotic stress response in *M. polymorpha*, expression of other CBLs and CIPKs was investigated by qRT-PCR. Results showed increased expression of MpCBL-A in response to osmotic stress, suggesting that CBL-A may be a candidate gene for the osmotic stress tolerance pathway in *M. polymorpha*. However, the effect was not dosage-dependent, nor was there a clear peak in expression, which raises questions about the validity of these results. As there were only 9 data points per gene in the qRT-PCR analysis performed, reliability of results could be improved by performing more repeats of the experiment for every gene tested. This would confirm if trends found are actual trends in the population, and may allow use of parametric tests in data analysis; these are more sensitive to patterns that may not otherwise be detected. Future experiments will create knockout mutants in CBL-A and phenotype responses to osmotic stress to determine whether the difference in genes expression seen is indicative of an osmotic stress response. If CBL-A is involved in osmotic stress tolerance, *cbl-a* mutant plants would be expected to tolerate osmotic stress less well than the wildtype.

Expression of genes CBL-B, CBL-C and CIPK-A was also tested but no significant difference was found under osmotic stress, suggesting that these genes are not involved in osmotic stress responses in *M. polymorpha*. Future experiments will create knockout mutants in these genes and test responses of mutants to different stresses. It would be expected that there will be no osmotic stress sensitivity phenotype in *cbl-b, cbl-c* or *cipk-a* knockout mutants, but stresses they are involved in can be identified this way to improve understanding of roles of CBLs and CIPKs in stress response pathways in *M. polymorpha*.

qRT-PCR experiments did not identify a CIPK involved in osmotic stress tolerance in *M. polymorpha*: CIPK-B phenotyping experiments demonstrate that CIPK-B is not involved in osmotic stress tolerance in *M. polymorpha*, and qRT-PCR of CIPK-A shows no significant difference in expression in response to osmotic stress, suggesting that CIPK-A is not involved in osmotic stress tolerance in *M. polymorpha* either.

It is advisable to further investigate whether CIPK-A is in fact involved in osmotic stress tolerance in *M. polymorpha*. This can be done by more detailed qRT-PCR experiments, investigating gene expression at the tissue-specific level, and at different timepoints after the stress is applied, to unmask tissue and time-specific changes in gene expression that would not be otherwise identified. This can be followed up by phenotyping experiments using CIPK-A knockout mutants in response to osmotic stress to determine if CIPK-A is involved in osmotic stress tolerance in *M. polymorpha*. The same set of experiments can be done for any other genes which may be involved in the *M. polymorpha* osmotic stress tolerance pathway.

If, after further investigation, CIPK-A is not found to be involved in osmotic stress tolerance in *M. polymorpha*, this raises the question of whether *M. polymorpha* responds to osmotic stress, and how this is done. We would assume that *M. polymorpha* responds to osmotic stress, and this is supported by initial data demonstrating that osmotic stress induces a calcium signal in *M. polymorpha* (Miller, 2021, unpublished). However, it is possible that the limited CBL-CIPK network in *M. polymorpha* means that it cannot respond to some stresses: whole genome duplications that have occurred in higher plants have amplified the number of CBLs and CIPKs higher plants have (Tansley, 2021), and it may be that this has allowed development of stress tolerance pathways in higher plants that do not exist in *M. polymorpha* which diverged much earlier.

Whether *M. polymorpha* responds to osmotic stress can be tested by RNAseq to identify osmotic stress-responsive genes in *M. polymorpha*. The promoters for genes which are found to be differentially regulated in response to osmotic stress can be used to help identify transcription factors controlling their expression. CBL/CIPK-transcription factor interactions

could be tested, for example by a luciferase assay in *Nicotiana benthamiana* to find the CBLs and CIPKs involved in osmotic stress signalling pathways in *M. polymorpha*.

It is possible that *M. polymorpha* responds to osmotic stress through other calcium decoders than CBLs and CIPKs. For example, the *M. polymorpha* genome encodes 7 CDPKs (Tansley, 2021). Several *A. thaliana* CDPKs have demonstrated roles in osmotic stress signalling. For example, *Atcpk3* mutants exhibit a salt sensitivity phenotype (Mehlmer *et al.*, 2010), *AtCPK6*-overexpressing plants have enhanced drought stress tolerance (Xu *et al.*, 2010), and AtCPK10 is involved in drought stress tolerance (Zou *et al.*, 2010). Potential involvement of *M. polymorpha* CDPKs in osmotic stress tolerance in *M. polymorpha* could be investigated by looking for changes in gene expression in response to osmotic stress by qRT-PCR, as well as creating knockout mutants in CDPKs and testing for altered osmotic stress tolerance by phenotyping experiments. If CDPKs are shown to be involved in osmotic stress tolerance in *M. polymorpha*, this will give insight into how basal land plants respond to a range of stresses specifically by using different calcium decoding proteins.

4.3.3 Multifunctional CBLs and CIPKs are likely to exist in *M. polymorpha*

Multifunctional CBLs and CIPKs exist in plants. For example, AtCIPK23 is involved in homeostasis of several ions (Ródenas and Vert, 2021). It is likely that most CBLs and CIPKs in *M. polymorpha* are multi-functional, as the small network, with only 6 possible interacting pairs must still respond to the same wide range of stresses as higher plants which have a larger CBL-CIPK network. Future work will test if *M. polymorpha* CBLs and CIPKs are multi-functional by investigating responses of knockout mutants to a variety of abiotic stresses, such as other ions than sodium. Results from these experiments will allow better understanding of the CBL-CIPK network in *M. polymorpha* in terms of which proteins are involved in which signalling pathways, and how they are connected. If multi-functional CBLs and CIPKs are identified, they are potential targets for expression in crop plants to bolster tolerance to multiple stresses at once.

An important question with regards to multifunctional CBLs and CIPKs in *M. polymorpha* is whether there is specificity of activation of downstream signalling and how this is defined if not through the specific CBL/CIPK pair. Whether there is specificity in multifunctional CBLs and CIPKs in *M. polymorpha* can be tested by investigating expression of target genes in response to multiple stresses in plants where only one stress has been applied, but where that stress tolerance signalling pathway is known to go via a multifunctional CBL or CIPK. If target genes of multiple stress response pathways are found to be differentially regulated, this means there is not specificity in downstream signalling pathways activated. In an instance such as this, when

one stress is recognised, multiple stress response pathways are activated simultaneously; these CBLs and CIPKs could therefore be used in crop improvement for broad spectrum stress tolerance.

If there is specificity in activation of downstream signalling in multifunctional CBLs and CIPKs, there are several ways in which this may be achieved. Specificity is likely to be defined by the calcium signal. For example, different calcium signals are likely to result in different calcium binding dynamics to CBLs, and this may encode information that allows specific downstream signalling to affect expression of the appropriate genes. Future experiments will identify multifunctional CBLs and CIPKs and investigate variance in calcium binding dynamics in response to the input stress, and aim to link this to the downstream response. Experiments such as this can be performed by creating CBLs mutant in individual EF-hands and EF-hand combinations investigating whether plants expressing these mutant CBLs are capable of responding to an applied stress the CBLs being tested are ordinarily capable of responding to. This will allow identification of the EF-hands calcium must bind to allow activation of that protein in response to the applied stress. It may be that different EF-hands must be active to allow response to different stresses within a multi-functional CBL; this is a mechanism allowing specificity.

Calcium signals that occur in response to an applied stress vary between species. For example, the calcium signal that occurs in *A. thaliana* in response to salt last approximately 2 minutes (Schmöckel *et al.*, 2015) while the signal in *M. polymorpha* lasts approximately 40 minutes (Miller, 2021, unpublished). The different calcium signals found in higher plants may activate the wrong downstream stress response pathway when multi-functional *M. polymorpha* CBLs and CIPKs which display specificity based on the calcium signal are used in crop improvement. This would be interesting to investigate and would give insight into how easy transferring CBL-CIPK based stress signalling pathways between crops would be.

In conclusion, it is likely that the salt response pathway in *M. polymorpha* involves CBL-C and CIPK-B. Further roles of these proteins, and roles of other proteins in the *M. polymorpha* CBL-CIPK network are yet to be elucidated, with particular questions over the players in the osmotic stress tolerance signalling pathway in *M. polymorpha*. Multi-functional CBLs and CIPKs when identified, could be used in crops to confer tolerance to multiple stresses at once, or multiple stresses specifically and depending on the calcium signal involved.

5 The role of CIPK-B in Mg^{2+} and Mn^{2+} tolerance

5.1 Introduction

Other ions than sodium, such as Mn^{2+} and Mg^{2+}, can cause stress to plants. AtCIPK23 is known to be involved in Mn^{2+} and Mg^{2+} tolerance in *A. thaliana* (Dubeaux *et al.*, 2018; R.-J. Tang *et al.*, 2015). MpCIPK-B is closely related to AtCIPK23 (Figure 1.14), raising the question of whether MpCIPK-B is involved in Mn^{2+} and Mg^{2+} tolerance. This was therefore tested by phenotyping of wildtype and *cipk-b* mutant plants by growing on ½ MS media supplemented with either $MnSO_4$ or $MgSO_4$. Knowledge gained from experiments such as these could be used in crop improvement to withstand Mg^{2+} or Mn^{2+} excess, thereby improving yields of crops exposed to these stresses.

5.2 Results

To investigate whether CIPK-B is involved in magnesium or manganese tolerance, plantlets of wildtype *M. polymorpha* were grown on ½ MS media supplemented with 0, 2, 10, 20 or 50 mM $MnSO_4$, or with 0, 2, 10, 50, or 80 mM $MgSO_4$ (Figure 5.1). These concentrations were selected based on previous experiments investigating $MnSO_4$ and $MgSO_4$ concentrations at which plantlet growth was visibly affected (Houghton, 2021, unpublished). Three biological replicates were performed, with two technical replicates for each biological replicate, though some data points were discarded due to contamination. Pooled mass of the five plantlets on each plate were measured (Figure 5.2) to see the effect of stress on plant biomass. Data was analysed using Kruskal-Wallis non-parametric tests to investigate differences in median plant mass within and between genotypes.

(a)

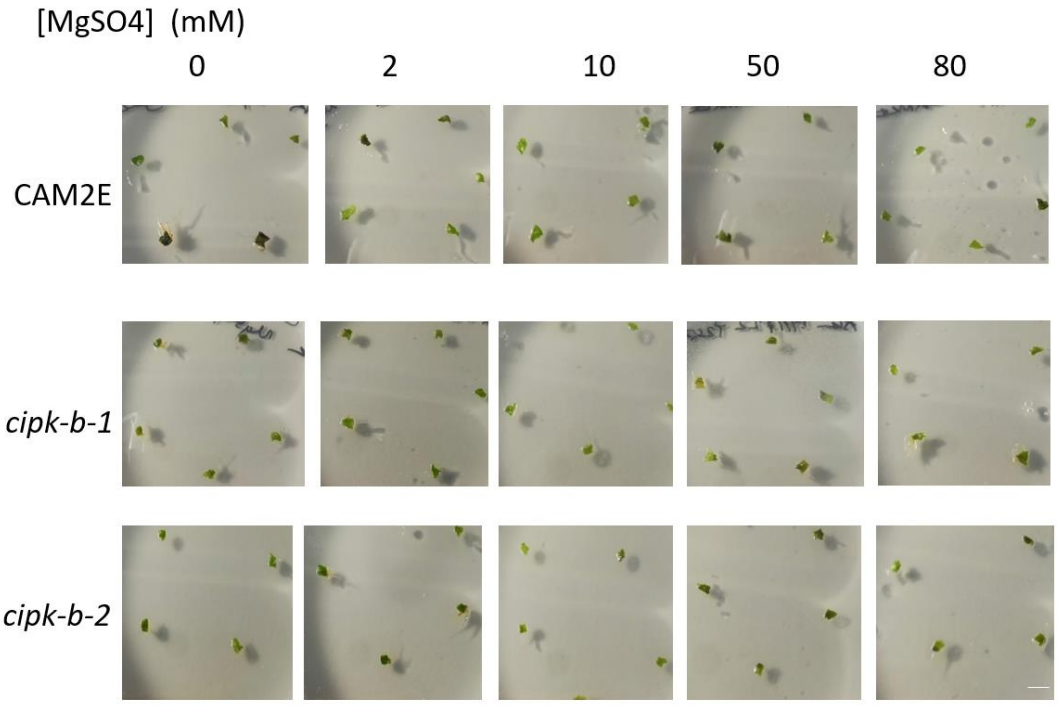

(b)

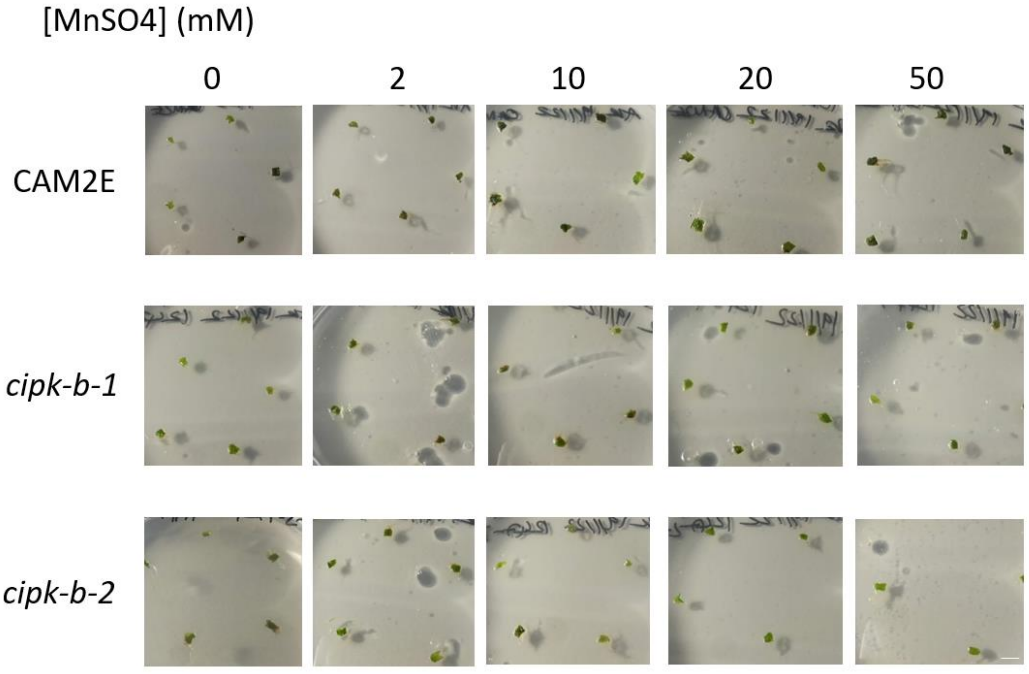

Figure 5.1. Wildtype and *cipk-b* mutant plants grown at increasing concentrations of $MgSO_4$ (a) and $MnSO_4$ (b) for one week. Scale bars = 5mm.

(a)

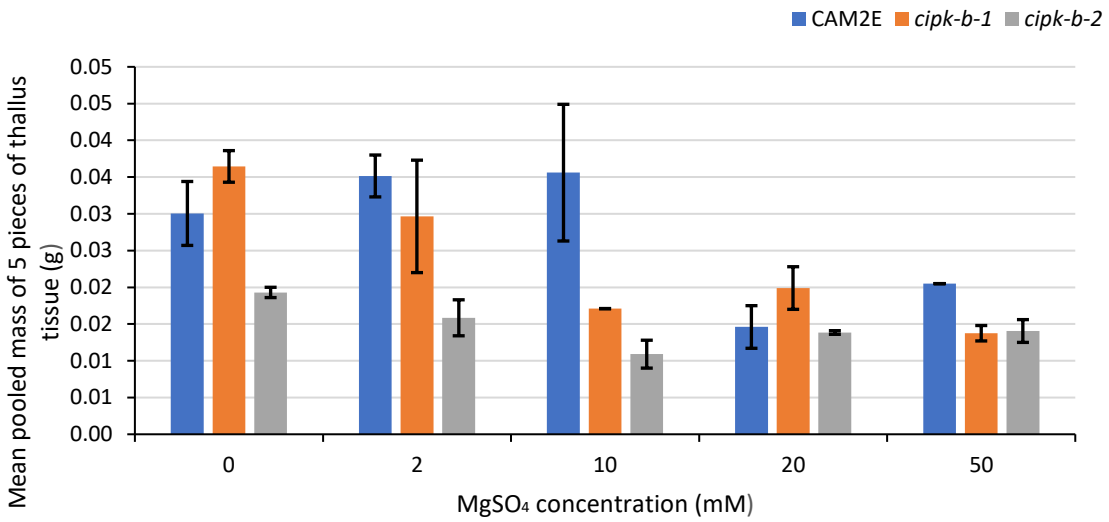

(b)

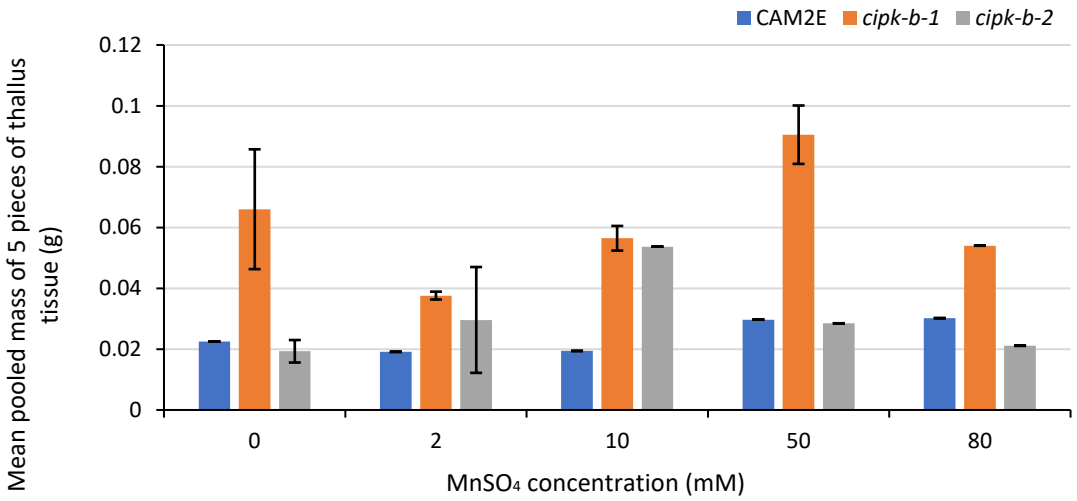

Figure 5.2. Mean pooled mass of 5 pieces of thallus tissue for wildtype (CAM2E), *cipk-b-1* and *cipk-b-2* mutant plants grown on ½ MS media supplemented with varying concentrations of $MgSO_4$ (a) or $MnSO_4$ (b) for one week. Error bars represent one standard error above and below the mean. Kruskal-Wallis tests showed no significant difference in mass between genotypes or concentrations of applied stress.

Kruskal-Wallis tests found no significant difference in mass of any of the genotypes tested in response to applied $MgSO_4$ (CAM2E $p = 0.199$, *cipk-b-1* $p = 0.167$, *cipk-b-2* $p = 0.169$) or $MnSO_4$ (CAM2E $p = 0.406$, *cipk-b-1* $p = 0.220$, *cipk-b-2* $p = 0.576$). Therefore there is no trend of decreased growth in response to applied stress, suggesting that either biomass is not a good

indicator of manganese or magnesium stress levels in *M. polymorpha,* or concentrations of these ions which cause measurable stress effects have not been tested.

Kruskal-Wallis tests also found no significant difference in mass between genotypes at any concentration of applied $MgSO_4$ (0 mM $MgSO_4$ p = 0.156, 2 mM $MgSO_4$ p = 0.180, 10 mM $MgSO_4$ p = 0.165, 20 mM $MgSO_4$ p = 0.368, 50 mM $MgSO_4$ p = 0.368) or $MnSO_4$ (0 mM $MnSO_4$ p = 0.223, 2 mM $MnSO_4$ p = 0.741, 10 mM $MnSO_4$ p = 0.407, 50 mM $MnSO_4$ p = 0.259, 80 mM $MnSO_4$ p = 0.368) tested, suggesting that wildtype and mutant *M. polymorpha* do not respond differently to the applied stresses. However, it is possible that they would at concentrations where the applied stresses have a measurable effect on plant biomass.

5.3 Discussion

Fresh weight of wildtype plantlets showed had high variance and showed no clear trends in mass depending on concentration. The same is true for wildtype plantlets tested. This suggests that the concentrations tested were not optimal for the experiment and means that no conclusions about the involvement of CIPK-B in manganese or magnesium tolerance can be drawn.

Future experiments will optimize the $MnSO_4$ and $MgSO_4$ concentrations used so there is a measurable effect of ion addition on plant growth. Once this has been established, phenotyping can be performed to include *cipk-b* mutant plants to allow comparison between wildtype and mutant lines to investigate whether CIPK-B is involved in tolerance of these ions. Further future experiments could include qRT-PCR to investigate if CIPK-B gene expression is altered under magnesium or manganese stress, and to investigate expression of other genes in the CBL-CIPK network to find the CBLs and CIPKs involved in tolerance to these ion stresses. RNAseq of *M. polymorpha* in response to these ion stresses can also be performed to identify other genes involved in these signalling pathways, and their target proteins.

6 The calcium dependence of CBL-CIPK interactions in *M. polymorpha*

6.1 Introduction

CBL-CIPK interactions are a key component in many stress response pathways in plants, allowing responses to abiotic stresses such as salinity (Ji *et al.*, 2013), drought (Cui *et al.*, 2018) and heavy metals (Jalmi *et al.*, 2018). CBL-CIPK interactions are generally assumed to be calcium-dependent, with calcium binding to CBLs occurring when there is a stimulus-induced calcium signal in a cell and allowing CIPK interaction, and CIPKs continuing the signalling cascade by phosphorylation. However, it is possible that CBL-CIPK interactions occur independently of calcium, though the literature search performed did not reveal any instances of this that have been observed. It may be that calcium binding to CBLs is still required for CBL-CIPK complex activity, or CBL-CIPK complex activity may be possible without calcium. It may be that different CBL-CIPK complexes have different calcium-binding requirements for interaction and activity. Therefore, the calcium dependence of CBL-CIPK interactions should be tested. This was investigated in *M. polymorpha* due to its simple CBL-CIPK network meaning that the calcium dependence of all possible CBL-CIPK interactions could be tested, but knowledge found in *M. polymorpha* of the principles of CBL-CIPK interactions and activity is likely to be translatable to higher plants. Understanding how calcium is involved in CBL-CIPK networks is useful as it may be used to manipulate CBL-CIPK interactions, when they happen, and if CBL-CIPK complexes are active. These manipulations can be used to engineer crop plants which respond more quickly, strongly or constitutively to stresses, improving their stress tolerance.

In order to test the calcium dependence of CBL-CIPK interactions in *M. polymorpha*, CBL mutants can be created by introducing point mutations in EF-hand binding loops, rendering them incapable of binding calcium. These can be used in a split luciferase assay (Kato and Jones, 2010) to test mutant CBL-CIPK interactions. In a split luciferase assay, multi-gene constructs are expressed in *N. benthamiana* which include a mutant CBL fused to one part of the luciferase (LgBiT) and a wildtype CIPK fused to the other part of the luciferase (SmBiT). If CBL EF-hand point mutants interact with wildtype CIPKs, the two parts of the luciferase will be brought together and the holoenzyme will produce light which can be detected from plant protein extract using a plate reader. In this case, the conclusion can be drawn that the CBL-CIPK interaction tested is calcium-independent. If the CBL EF-hand mutants do not interact with wildtype CIPKs, the two parts of the luciferase will remain separate and no light will be produced. In this case, the conclusion can be drawn that the CBL-CIPK interaction tested is

calcium-dependent. Some CBL-CIPK interactions may be calcium-dependent while others may be calcium-independent.

To allow this experiment to be performed, mutant CBLs and mutant CBL-luciferase LgBiT constructs must be made, and these must be assembled with already available CIPK-luciferase SmBiT constructs to multigene constructs. This was done in this objective by Golden Gate cloning. The luciferase assay was not actually performed due to time constraints, but enough materials have been made to test the calcium-dependence of several of the CBL-CIPK interacting pairs in the future.

6.2 Results

Generation of level 2 constructs required generation of CBL mutant genes by overlap extension PCR, followed by level 0, level 1 and level 2 Golden Gate cloning. For simplicity, only results for CBL-A EF-hand mutant constructs will be shown. The same experiments were successfully performed for all other constructs made. During the course of this project, all level 0 and level 1 constructs were successfully generated, while three level 2 constructs were generated (BM01354, BM01355 and BM01356; Table 2.2). The remaining three level 2 constructs (BM01352, BM01353, BM01357; Table 2.2) were not generated within the timescale of this project.

First, existing CBL mutant constructs were used in overlap extension PCR to mutate remaining EF-hands. For CBL-A, the template mutant construct used was mutant in EF-hands 2, 3 and 4, and a point mutation in EF-hand 1 was introduced to generate a construct mutant in all 4 EF-hands. This point mutation mutated the first amino acid of the Ef-hand calcium binding loop from serine to glycine. Overlap extension PCR primary fragments were generated for all three CBLs using primers shown in table 3.2. Figure 6.1 shows electrophoresis images of products of primary PCRs for the CBL-A construct (BM01325; table 2.1).

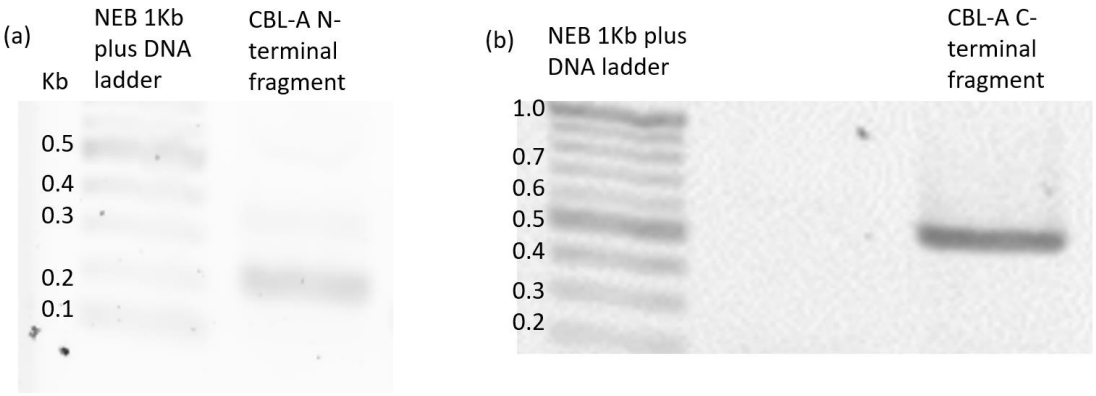

Figure 6.1. Agarose gel electrophoresis of initial fragment PCR products for mutant CBL-A. Fragments were amplified from template DNA for each gene using primers from the point of the mutation to be introduced to the N- or C-terminus of the gene. (a) Lane 1: NEB 1KB plus DNA ladder. Lane 2: CBL-A N-terminal fragment (196 bp). (b) Lane 1: NEB 1KB plus DNA ladder, Lane 2: blank, Lane 3 CBL-A C-terminal fragment (532 bp).

Primary fragments were used in overlap extension PCR to assemble the full length construct with the desired introduced mutations. Figure 6.2 shows the overlap extension product for CBL-A with all EF-hands mutated.

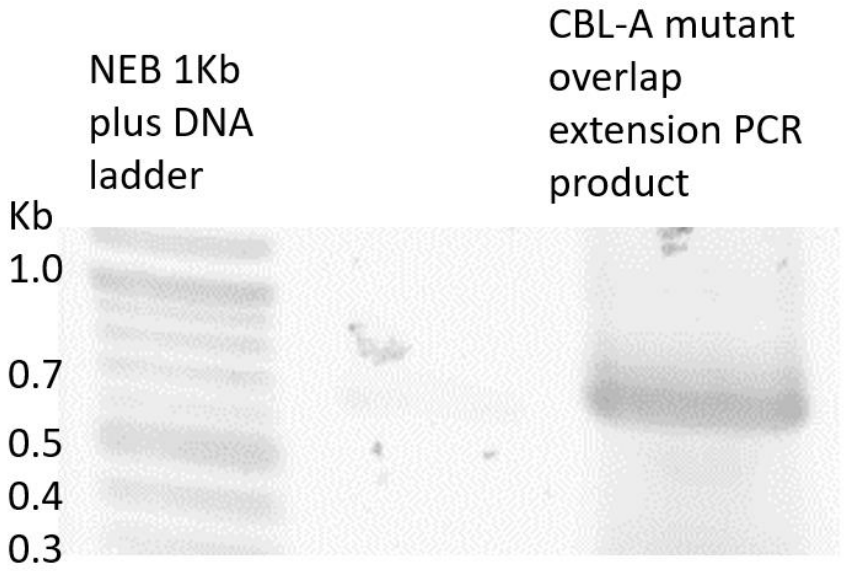

Figure 6.2. Gel electrophoresis of the overlap extension product for CBL-A mutant in all 4 EF-hands. Lane 1: NEB 1KB plus DNA ladder. Lane 2: blank. Lane 3: CBL-A mutant overlap extension product (704 bp).

The overlap extension PCR products were then used in a Golden Gate cloning reaction using BsaI restriction enzyme to generate level 0 modules. Golden Gate cloning products were used to transform *E. coli* (DH5α). Colonies were selected by blue-white screening and spectinomycin

resistance, and confirmed by colony PCR using gene-specific primers. Figure 6.3 shows a positive colony PCR result for the level 0 CBL-A module (module code BM01325).

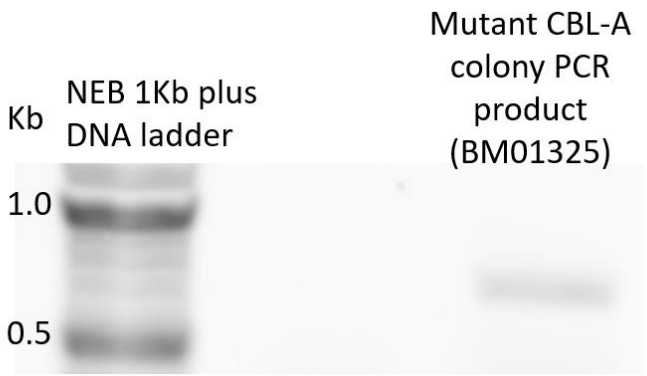

Figure 6.3. Agarose gel electrophoresis of colony PCR products from *E. coli* transformed with mutant CBL-A golden gate products. Mutant CBL-A gene amplified using gene-specific primers. Lane 1: NEB 1KB plus DNA ladder, lane 2: water control, lane 3: mutant CBL-A PCR product (code: BM01325; 712 bp).

Positive colonies were grown up in overnight culture with antibiotic selection and plasmid DNA was extracted. Plasmid DNA was checked by restriction digest using BsaI which should cut at two sites and give a predictable expected banding pattern if the plasmid containing the mutated CBL-A DNA is correctly assembled. Figure 6.4a shows the expected banding pattern for the BM01325 module when digested with BsaI restriction enzyme. Figure 6.4b shows the actual banding pattern generated when the extracted DNA was digested. The banding patterns match, suggesting that the extracted DNA matches the planned sequence of the construct.

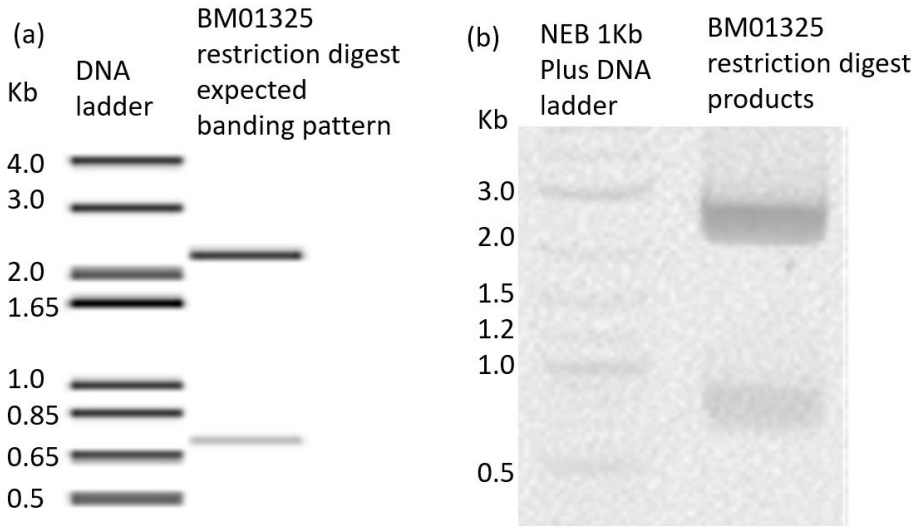

Figure 6.4a) Expected banding pattern of BM01325 when digested by BsaI restriction enzyme. Band sizes of 2235 bp and 708 bp are expected. B) Agarose gel electrophoresis of products of restriction digest of DNA extracted from *E. coli* transformed with products of the BM01325 Golden Gate reaction. Lane 1: NEB 1Kb plus DNA ladder. Lane 2: BM01325 restriction digest products. Bands are present at the expected sizes of approximately 2235 bp and 709 bp.

DNA which had the correct digest banding pattern was sequenced via Sanger sequencing to confirm that no unwanted mutations existed within the gene sequence. Level 0 constructs were sequenced using the GoldenGate1 primer which binds just downstream of the insert in the plasmid vector which the gene was held in. Figure 6.5 shows part of the sequencing alignment for construct BM01325. The sequencing matched the expected sequence. Therefore, this construct was carried forward to the next level of cloning.

Where mutations within the gene sequence were found which altered the amino acid sequence of the protein, a different PCR-positive colony was selected instead until correct DNA was isolated for all three level 0 constructs.

Several other level 0 CBL mutant constructs were made, mutant in different EF-hand combinations, but only mutants in all 4 EF-hands were taken forward and used in the remainder of this project.

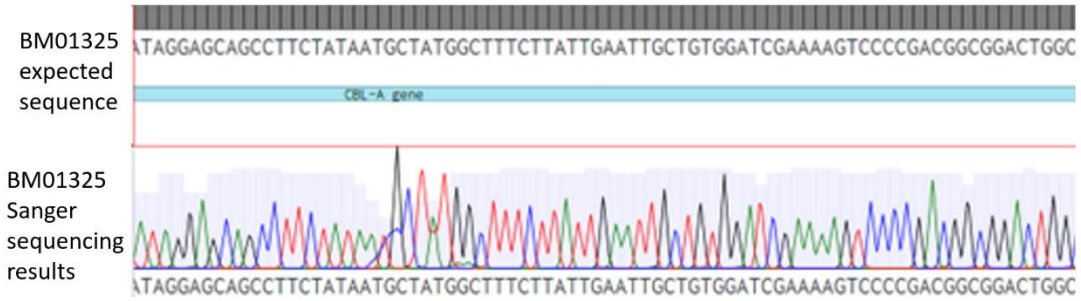

Figure 6.5. Part of the sequencing alignment for the CBL-A EF1234 level 0 construct (BM01325). There was 100% identity between the sequencing results and the construct expected sequence, confirming that this construct is good.

Level 0 constructs generated, as well as pre-existing level 0 modules, were assembled into level 1 Golden Gate constructs (table 2.1 for construct plans) by Golden Gate cloning reactions.

Golden Gate reaction products were used to transform *E. coli* (DH5α) and successfully transformed colonies were selected by blue-white screening and ampicillin resistance, and screened by colony PCR using primers GoldenGate3 and GoldenGate4 which bind either side of the insert in the plasmid vector used. Figure 6.6 shows a positive colony PCR result for the level 1 construct BM01349 (including the components: p35s, CBL-A EF1234, luciferase LgBiT, t35s). Several colonies were screened for all three level 1 constructs.

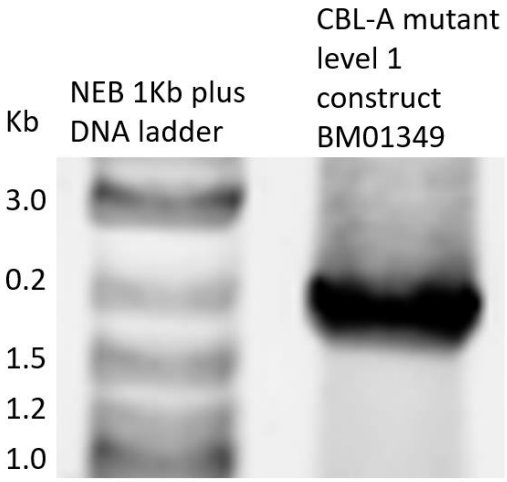

Figure 6.6. Agarose gel electrophoresis of colony PCR products from *E. coli* transformed with the CBL-A-containing level 1 construct BM01349. Lane 1: NEB 1KB plus DNA ladder, lane 2: BM01349 colony PCR product (1955 bp).

DNA was extracted from colonies with positive colony PCR results. DNA was checked by restriction digest using BpiI which should cut at two sites and give a predictable expected banding pattern if the DNA matches the template. Figure 6.7a shows the expected banding pattern for the CBL-A-containing level 1 construct BM01349. Figure 6.7b shows the actual banding pattern generated when the extracted DNA was digested. The digest gave two bands of expected size, suggesting the construct was correctly assembled.

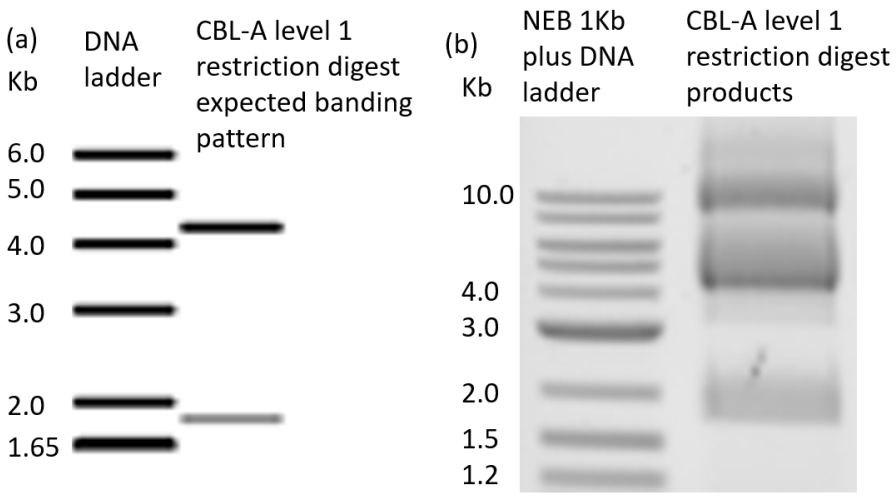

Figure 6.7a) Expected banding pattern of CBL-A-containing level 1 construct when digested by BpiI restriction enzyme. Expected band sizes of 4338 and 1852 bp. B) Agarose gel electrophoresis of products of restriction digest of DNA extracted from *E. coli* transformed with products of the level 1 CBL-A-containing Golden Gate reaction. Lane 1: NEB 1kb plus DNA ladder. Lane 2: digested DNA of the construct. Bands present at ~1852 and ~4338 bp: the expected sizes for the digest.

DNA which had the correct digest banding pattern was sequenced by Sanger sequencing to confirm that no unwanted mutations existed within the gene sequence. Level 1 constructs were sequenced from either end using primers GoldenGate3 and GoldenGate4 which bind either side of the insert in the plasmid vector for the construct. This resulted in sequencing coverage of the full length of the insert. Figure 6.8 shows part of the sequencing alignment for the CBL-A EF1234-containing level 1 construct BM01349. The sequencing matched the expected sequence. Therefore, this construct was carried forward to the next level of cloning. Where mutations within the gene sequence were found which altered the amino acid sequence of the protein, a different colony PCR-positive colony was tested instead until correct DNA was extracted for all three level 1 constructs.

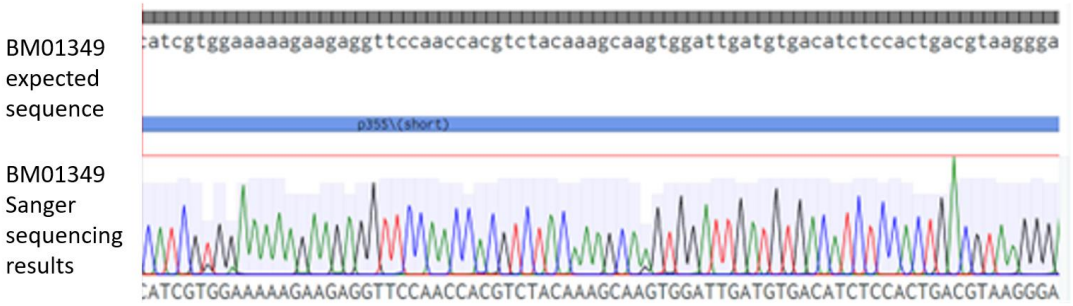

Figure 6.8. Part of the sequencing alignment for the CBL-A EF1234-containing level 1 construct BM01349, sequenced using primer GG3. Sequencing results matched the expected sequence, confirming that this construct is correct.

Level 1 constructs were taken forward to level 2 Golden Gate cloning, for assembly of multi-gene constructs (table 2.2 for level 2 construct plans).

Golden Gate reaction products were used to transform *E. coli* (DH5α) and successfully transformed colonies were selected by red-white screening and kanamycin resistance. Colonies were screened by colony PCR using CBL gene-specific primers (Table 3.2). Figure 6.9 shows positive colony PCR results for the level 2 construct BM01355 (containing the level 1 transcriptional units for CBL-A, GUS and CIPK-B). The third colony screened had the strongest positive band so was taken forward for DNA extraction. Several colonies were screened for all six level 2 constructs.

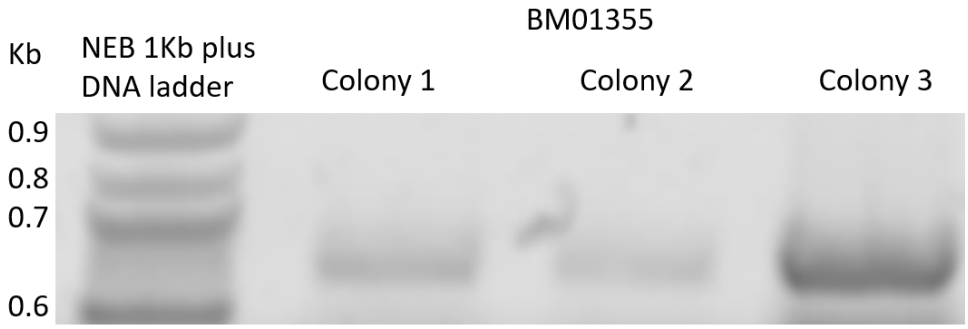

Figure 6.9. Agarose gel electrophoresis of colony PCR products from *E. coli* transformed with golden gate products for level 2 construct BM01355. Lane 1: NEB 1KB plus DNA ladder, lanes 2-4: BM01355 colony PCR products for 3 colonies (~697 bp).

PCR-positive colonies were grown up in overnight culture and DNA extracted. DNA was checked by restriction digest using HindIII which should cut at three sites or four sites depending on the construct and give a predictable expected banding pattern if the DNA

matches the template. Expected digest results were found for three of the level 2 constructs: BM01354 (containing CBL-C and CIPK-A), BM01355 (containing CBL-A and CIPK-B) and BM01356 (containing CBL-B and CIPK-B). Figure 6.10a, b and c show the expected banding pattern for these three constructs, and Figure 6.10d shows the actual banding patterns generated when the extracted DNA for these constructs was digested. The actual banding patterns match the expected banding patterns, suggesting that the extracted DNA matches the planned sequence of the construct. Level 2 constructs are not sequenced by Sanger sequencing as they are too large for this to be useful. These level 2 constructs will be taken forward to split luciferase assay future experiments in *N. benthamiana* to test the calcium dependence of *M. polymorpha* CBL-CIPK interactions.

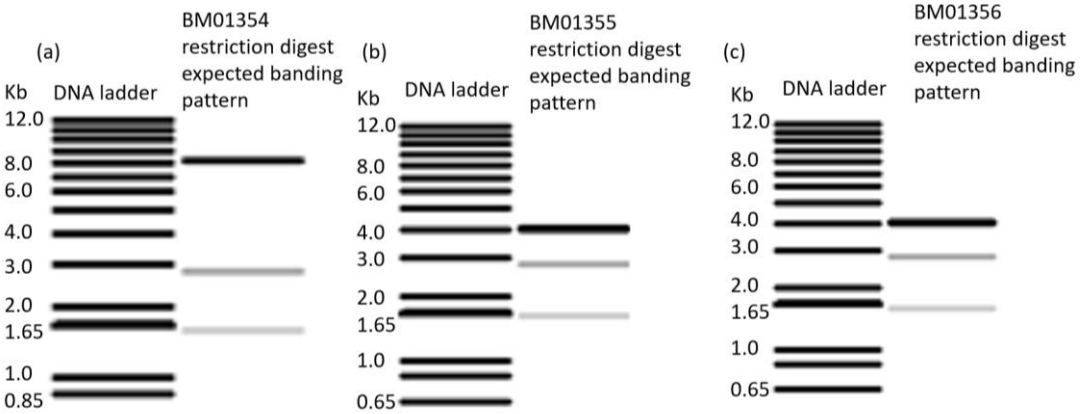

(d)

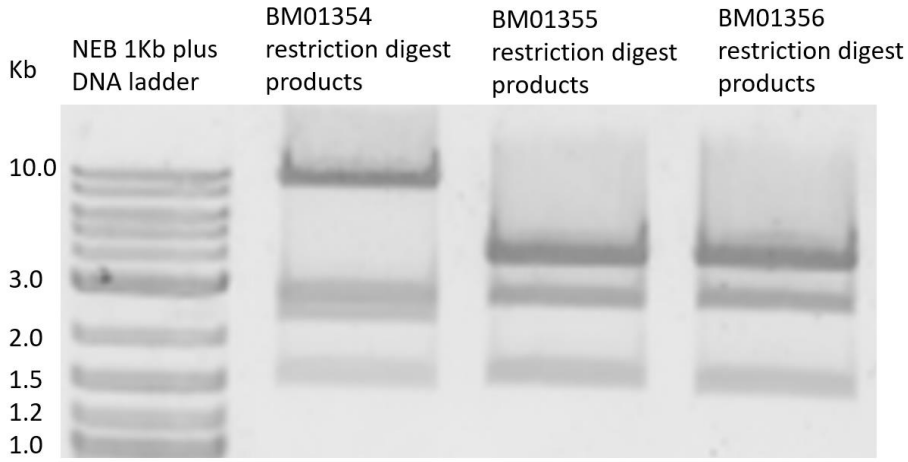

Figure 6.10a) Expected banding pattern of level 2 construct BM01354 when digested with HindIII restriction enzyme. Expected band sizes: 9077, 2774 and 1567 bp. b) Expected banding pattern of level 2 construct BM01355 when digested with HindIII restriction enzyme. Expected band sizes: 4092, 3991, 2774 and 1624 bp. c) Expected banding pattern of level 2 construct BM01356 when digested with HindIII restriction enzyme. Expected band sizes: 4092, 3991, 2774, 1567 bp. d) Agarose gel electrophoresis of products of restriction digest of DNA extracted from *E. coli* transformed with level 2 constructs BM01354, BM01355 and BM01356. Lane 1: NEB 1kb plus DNA ladder. Lane 2: restriction digest products for BM01354. Lane 3: restriction digests for BM01355. Lane 4: restriction digest products for BM01356. Band sizes match expected band sizes in a), b), and c).

For the remaining three level 2 constructs BM01352, BM01353 and BM01357, though multiple positive colony PCR results were found, no restriction digests done gave the expected banding pattern, suggesting that none of the DNA purified from transformed *E. coli* matched the expected level 2 construct. Further *E. coli* transformation and screening will be required to generate these constructs.

6.3 Discussion

In this objective, CBL EF-hand mutants were made, rendering them unable to bind calcium, and Golden Gate level 2 constructs containing CBL-luciferase, promoter-GUS and CIPK-luciferase transcriptional units were assembled. Each construct contained a different CBL-CIPK pair. This was done in preparation for luciferase assays to test the calcium-dependence of interactions between all possible CBL-CIPK pairs.

Although testing of several mutant CBL- wildtype CIPK pair interactions is possible with the materials already made, to allow testing of all mutant CBL – wildtype CIPK pairs, remaining level 2 constructs (BM01352, BM01353 and BM01357) should be generated to continue this objective. Each construct can then be used to transform *Agrobacterium.* Transformed *Agrobacterium* can be used to transiently transform *Nicotiana Benthamiana* leaves so that the genes in the level 2 construct are expressed in that part of the leaf. Successful transformation will be indicated by a blue colour resulting from the constitutive GUS expression. Leaf punches can then be taken and proteins extracted from these. Protein extract can be assayed on a plate reader for bioluminescence which is indicative of CBL-CIPK interaction. All possible CBL-CIPK pairs will be tested as previous work by PhD student Connor Tansley used biomolecular fluorescence complementation (BiFC; Kodama and Hu, 2012) of *M. polymorpha* CBLs and CIPKs in transiently transformed *Nicotiana benthamiana* to show that all 3 MpCBLs interact with both MpCIPKs (Tansley *et al*., 2023).

Overlap extension PCR to introduce EF-hand point mutations worked well. Generation of constructs at all levels took longer than expected, but this was especially apparent at level 2 of cloning. *E. coli* transformation efficiency was low and few colonies grew on selective media. Transformation of larger volumes of *E. coli* cells (100 µl rather than 20 µl per construct) was tried and increased colony number somewhat. In future experiments, transformation by electroporation rather than heat shock in the presence of $CaCl_2$ could be tried as transformation efficiency may increase.

Screening of colonies that did grow by colony PCR frequently gave false positive results, which were discovered only at the restriction digest stage of quality control. At level 2, primers targeting the *M. polymorpha* CIPK genes were used initially to amplify CIPK genes in colony PCR, and this was assumed to represent successful transformation with the entire level 2 construct as planned. When false positive results were discovered, screening was changed to use gene-specific CBL primers. This was more reliable, but false positive colony PCR results were still found. In future level 2 cloning experiments, double-colony PCR screenings should be used, where each colony is screened for the presence of at least two of the genes incorporated in the level 2 construct to reduce likelihood of detecting unsuccessful construct assemblies.

The restriction digest part of the experimental flow has so far proved reliable so is an appropriate quality control method to bring forward as more level 2 cloning is performed.

6.3.1 CBL-CIPK interactions could be calcium dependent or independent

In response to a stimulus, there is an increase in calcium in a plant cell. Calcium ions are decoded by calcium binding proteins such as CBLs which bind calcium via EF-hand domains. CBLs interact with CIPKs which phosphorylate downstream target proteins such as ion channels and transporters to allow plant responses to stimuli (Ma *et al.*, 2020). Though it is commonly assumed that they are, it is not known if CBL-CIPK interactions are calcium dependent. In fact, there are several possible ways that calcium could be involved in CBL-CIPK interactions. It may be that calcium binding to CBLs allows CBL-CIPK interactions and downstream signalling (Figure 6.11a). Alternatively, CBL-CIPK interactions may occur independent of calcium with calcium binding needed for CBL-CIPK complex activity (Figure 6.11b). It is also possible that calcium is bound to CBLs at basal levels and that more calcium binding occurs in response to calcium increases in the cell and this allows CBL-CIPK interaction (Figure 6.11c), or activation of the already formed CBL-CIPK complex (Figure 6.11d). Alternatively, CBL-CIPK complex activity may occur independent of calcium, although this is unlikely as CBLs are well established as calcium-binding proteins.

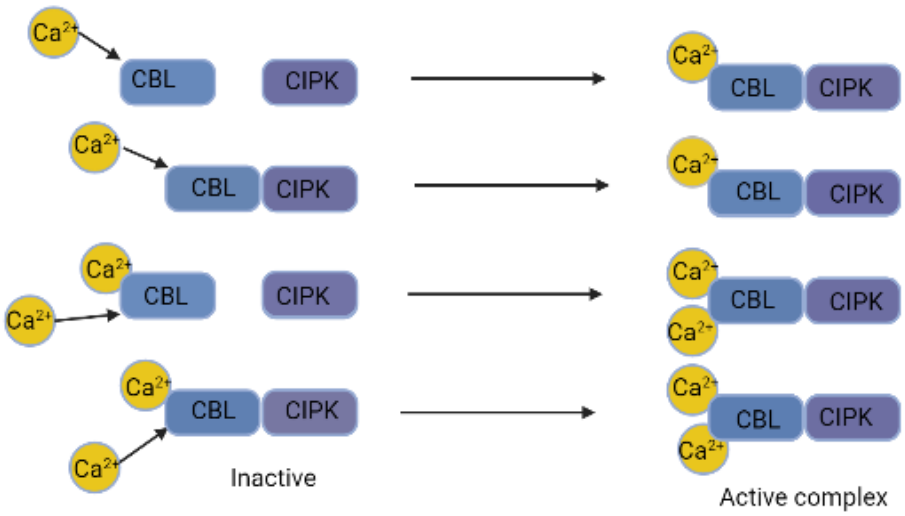

Figure 6.11. Possible ways calcium could be involved in CBL-CIPK interactions and activation. A) Calcium is required for interaction and allows activity B) Calcium is not required for interaction but is required for activation C) Calcium is bound at basal levels but interaction does not occur until more calcium binding occurs. Interaction makes an active complex. D) Calcium is bound at basal levels and allows CBL-CIPK interaction but the complex is inactive until more calcium binds in calcium spiking. Alternatively, CBL-CIPK interaction and activity may be independent of calcium.

If CBL-CIPK interactions are shown to be calcium dependent, this matches the expected outcome and current understanding of the involvement of calcium in CBL-CIPK interactions. However, it may be that some or all CBL-CIPK interactions happen independent of calcium.

If CBL-CIPK interaction is calcium dependent, it is expected that kinase activity of CIPKs in CBL-CIPK interactions are also calcium dependent. Alternatively, if CBL-CIPK interaction is calcium independent, CBL-CIPK pairs may have basal activity which is increased on calcium-binding to EF-hands, or may have activity without calcium that is not affected by addition of calcium ions. The dependence of CIPK activity on calcium could be tested in future experiments by expressing CBL variants in *E. coli* and performing in vitro kinase assays with CIPKs, using western blotting with phospho-specific antibodies. In vitro kinase assays are widely used in investigating kinase activity. For example, a 2018 study by Yadav *et al.* used them to quantify kinase activity of AtCIPK9. We would expect results to show increased phosphorylation by CIPKs partnered with CBLs with active EF-hands because CBL-CIPKs are involved in calcium-dependent signalling. However, if some CBL-CIPK pairs are shown to have notable levels of kinase activity independent of calcium, this would challenge the idea that CIPK activity depends on calcium, and call into question whether all *M. polymorpha* stress response pathways do in fact rely on calcium. Conclusions from this experiment and determination of calcium-dependence of CBL-CIPK interactions will give a clearer picture of how calcium dependence or CBL-CIPK interaction and calcium dependence of CBL-CIPK activity are related.

In the cell there are always basal calcium levels. It is possible that calcium only binds CBLs during calcium increases, but it is also possible that calcium binds to CBLs at these basal levels. Basal calcium levels in *M. polymorpha* are expected to be around ~100nM and increasing to the µM range during calcium elevation, as in *A. thaliana*. This can be tested by microelectrode measurement (Gorman *et al.*, 1984). Whether calcium binds CBLs at basal levels can be investigated by isothermal titration calorimetry (ITC) to find the CBL EF-hand dissociation constants; similar to what was done by Swainsbury *et al.* (2012) to investigate calcium binding of CCaMK in *Medicago truncatula*.

If calcium binds CBLs at basal levels, this means that CBL-CIPK interactions found to be calcium-dependent by earlier experiments may only be dependent on basal calcium levels. Alternatively, CBL-CIPK interaction may only occur when more calcium binds CBLs during calcium increases in the cell (Figure 6.11c). This can be tested by investigating CBL-CIPK interactions at basal calcium levels. This can be done by a luciferase assay and supplementing the leaf protein extract which is imaged for bioluminescence with calcium or EDTA calcium chelator. However, biologically relevant calcium concentrations would be difficult to pinpoint

in an experiment such as this. It may be possible to investigate CBL-CIPK interactions *in planta*. Setting up an experimental system such as this would be extremely useful for investigating of CBL-CIPK interactions under less artificial conditions.

The same set of questions applies to CBL-CIPK activity. If calcium binding to CBLs occurs at basal calcium levels, it may be that CBL-CIPK complexes form at basal calcium levels, but are only activated when more calcium binds during calcium increases in response to stimuli in the cell (Figure 6.11d), or that CBL-CIPK complexes form and are activated even with only basal calcium binding. These questions could be investigated by kinase assays at basal and elevated calcium levels.

It may be that calcium binds specific EF-hands at basal levels, and others during calcium increases and this is what allows CBL-CIPK interaction and activity. This could be tested by generating CBLs mutant in individual EF-hands by overlap extension PCR and using these in calcium binding experiments to identify which EF-hands bind calcium at basal levels and which during calcium increases. Results may vary depending on the calcium signal so different calcium concentrations should be tested.

It is possible that MpCIPKs may have activity independent of their interacting CBL. For example, AtCIPK24 interacts with CAX1: a vacuolar Ca^{2+}/H^{+} antiporter independent of an interacting CBL (Cheng *et al.*, 2004). Whether *M. polymorpha* CIPKs have activity independent of their interacting CBL could be tested by assaying CIPK activity independent of interacting CBLs. If MpCIPKs are shown to have basal activity independent of their interacting CBL, it may be that this activity is insufficient to activate downstream signalling; this can be tested by qRT-PCR to investigate gene expression of target genes in an *M. polymorpha cbl* knockout line. It would be expected that stress response genes would not be upregulated in response to stress at basal CIPK activity levels, but would be when active CBLs are expressed.

An important question is how specificity in downstream signalling can be defined when many stress responses are integrated by calcium. One key mechanism of specificity is the concept of calcium signatures: stimuli initiate calcium increases with specific kinetics which encode information about the stimulus; this information is decoded by specific calcium binding proteins which allow activation of distinct downstream signalling pathways (McAinsh and Pittman, 2009). CBLs are one type of calcium binding protein involved in many stress responses in *M. polymorpha* and other species. Therefore, further levels of specificity are required to determine specific downstream signalling. One mechanism of specificity within CBLs is different CBL-CIPK pairs defining the downstream response (Batistič and Kudla, 2009). It is possible that different calcium binding dynamics resulting from stimulus-specific calcium

signatures result in calcium binding to specific CBL EF-hands, and this may determine which CIPK the CBL interacts with. Individual EF-hand mutant calcium binding can be tested by isothermal titration calorimetry. Which EF-hands must bind calcium to allow CBL interaction with particular CIPKs can be tested by creating mutants in individual EF-hands and different EF-hand combinations, and testing CBL-CIPK interactions by a luciferase assay. Which EF-hands are required to be active for stress tolerance pathway activation can be tested by creating *M. polymorpha* lines with CBLs mutant in individual EF-hands and different EF-hand combinations, and testing their stress tolerance through phenotyping.

M. polymorpha has a network of 3 CBLs and 2 CIPKs, giving a total of 6 possible CBL-CIPK pairs (Edel and Kudla, 2015). However, it must respond specifically to more than 6 stresses, so further levels of specificity are required. It is possible that the same CBL-CIPK pair could activate different downstream signalling pathways depending on the calcium binding kinetics to the CBL in question; this could depend on the calcium signal produced in the plant cell in response to the specific stress the plant is experiencing. Whether different CBL-CIPK pairs can activate different downstream signalling depending on calcium binding could be tested by generating *M. polymorpha* lines expressing specific EF-hand mutant CBLs and investigating the effect on tolerance to several stresses. It may be found that different CBL-CIPK pairs allow different stress responses to occur depending on which CBL EF-hands are capable of binding calcium.

It may also be that EF-hands show cooperativity: that binding of calcium to one EF-hand depends on binding of calcium first to another EF-hand on the protein. This has been shown to be the case in other calcium binding proteins, for example, in calbindin D9k in mammals (Linse and Chazin, 1995). To account for EF-hand cooperativity, multiple combinations of EF-hand mutants should be tested when individual EF-hand mutants are made. To test cooperativity, calcium binding to CBLs can also be investigated directly through experiments such as calcium mobility shift assays or ITC to demonstrate which CBL variants bind calcium. CBLs bound to calcium ions will have altered mobility in SDS-PAGE to CBLs not bound to calcium, so instances in which calcium will only bind a particular EF-hand dependent on if calcium is already bound to another can be identified.

The combination of conclusions from these experiments will unpick the role of calcium in CBL-CIPK interaction and activation, at basal and elevated calcium levels, including which EF-hands are important for calcium binding in which scenarios and how specificity in downstream signalling is allowed. Understanding how calcium is involved in the CBL-CIPK network is useful as it may be used to manipulate CBL-CIPK interactions, when they happen, and if they are

active, and these manipulations can be used to engineer plants which respond more quickly, strongly or constitutively to stresses, improving their tolerance. If, as we hope, dogmas found in *M. polymorpha* are translatable to higher crop plants, this is an avenue towards crop improvement to withstand climate change.

7 Discussion

CBLs and CIPKs allow response to the environment of a cell by regulating ion transport. In *M. polymorpha*, many of the roles of the proteins in its CBL-CIPK network are yet to be established, and the calcium-dependence of the signalling pathways they are involved in is yet to be demonstrated. In this report, we have demonstrated that the salt sensitivity phenotype of *M. polymorpha cipk-b* knockout mutants previously demonstrated is not due to osmotic stress, identified CBL-A as a candidate gene for osmotic stress response signalling in *M. polymorpha*, and materials have been made to allow future investigation of the calcium dependence of CBL-CIPK interactions in *M. polymorpha*.

Objective 1 has demonstrated that CIPK-B is the AtSOS2 homolog. Future work will identify the AtSOS3 homolog in *M. polymorpha* and determine whether multifunctional CBLs and CIPKs exist in *M. polymorpha*. This knowledge can be used to identify candidate genes for crop stress tolerance improvement. Future work from objective 3 will determine if CBL-CIPK interactions are calcium dependent, and will investigate the effect of calcium on CBL-CIPK activity and how specificity in downstream signalling is achieved, for example by calcium binding to specific EF-hands, and whether there's EF-hand cooperativity. This knowledge can be used to manipulate CBL-CIPK interactions to benefit stress tolerance.

Results from this project allow proposition of the following model for how CBLs, CIPKs and calcium are involved in the salt tolerance response in *M. polymorpha*; this model is illustrated in Figure 7.1.

Salt causes a calcium increase in the form of a specific calcium signature. This has been demonstrated in *M. polymorpha* using R-GECO lines of the TAK1 accession of *M. polymorpha* (Miller, 2021; unpublished). The salt-responsive CBL in *M. polymorpha* is likely to be CBL-C. Calcium will bind CBL-C on calcium increase in response to salt stress. Calcium is likely to bind specific EF-hands of CBL-C due to the calcium binding dynamics resulting from the specific calcium signature induced by the salt stimulus. By this method, information encoded in the calcium signature about the nature of the stimulus can be transferred to CBL-C, defining which downstream signalling pathway to induce. Assuming that CBL-CIPK interaction is calcium dependent, Ca^{2+}-CBL-C will then interact with and activate CIPK-B. It may also be that CBL-C and CIPK-B interact independent of calcium and that calcium binding activates the complex, or that calcium binding to CBLs occurs at basal calcium levels but CBL-CIPK interaction and activity depends on further calcium binding during calcium increases in cells. Active CBL-C-CIPK-B will activate the *M. polymorpha* SOS1 homolog to allow salt tolerance by extrusion.

Calcium will also activate transcription factors which are expected to upregulate the *M. polymorpha* SOS2 and SOS3 homologs CIPK-B and CBL-C and long term salt responsive genes. Transcription factors MpBHLH2, MpRR_MYB1, MpABI3A, MpABI5B and MpR2R3-MYB17 have been previously identified as salt-responsive transcription factors in *M. polymorpha*; these were similar to the transcription factor families identified in other species to be involved in salt stress tolerance (Tanaka *et al.*, 2018). It is likely that at least some of these transcription factors are calcium-responsive; this should be tested in future experiments. Target genes of the calcium-responsive transcription factors in *M. polymorpha* can be identified by ChIP-seq to confirm that they upregulate CIPK-B, CBL-C and long term salt responsive genes.

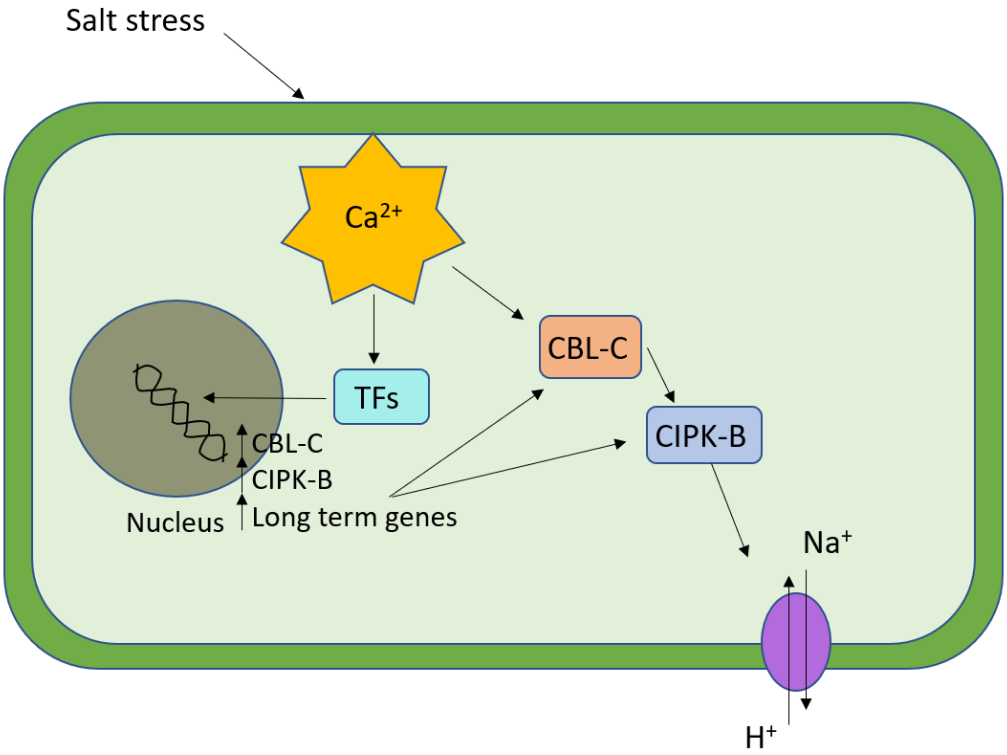

Figure 7.1. Proposed model for how CBLs, CIPKs and calcium are involved in salt tolerance signalling in *M. polymorpha*. Under salt stress, there is a calcium increase in the *M. polymorpha* cell cytosol (Miller, 2021; unpublished). Calcium binding to CBL-C (to be confirmed) specific EF-hands (to be investigated), allows CBL-C-CIPK-B interaction (unless interaction is not calcium-dependent; in which case calcium is likely an activator of the complex). CBL-C-CIPK-B interacts with sodium ion transporters to allow salt tolerance by extrusion. At the same time, transcription factors are activated by calcium and upregulate CBL-C and CIPK-B gene expression, increasing the salt tolerance response by positive feedback, and activating longer term salt responsive genes. When the calcium signal ends, calcium unbinds from CBL-C and CIPK-B activation ends (excepting basal activity levels). Transcription factors are no longer activated so CBL-C and CIPK-B expression returns to basal levels and salt tolerance signalling ceases.

This mechanism of Ca^{2+}-CBL-CIPK interaction can apply in many different stress tolerance pathways which will be investigated in future work. Another stress will produce a distinct calcium signature which may activate another CBL, or cause calcium binding to different EF-hands of the same CBL. The active CBL will pair with a CIPK; this may be defined by which EF-hands on the CBL calcium has bound to. If it is the same CIPK, calcium binding to different CBL EF-hands may determine the downstream target protein that is activated. The calcium signature will activate transcription factors to upregulate the CBLs and CIPKs involved and the long term genes specific to the stress. By this means, multiple stress signalling pathways can be activated independently and specifically based on similar principles of specificity.

Future experiments confirming the identity of the CIPK-B-interacting CBL, investigating potential multifunctionality of CIPK-B and roles of other CBLs and CIPKs in the *M. polymorpha* network, and confirmation of calcium dependence of CBL-CIPK interactions will help refine and increase confidence in the proposed model.

If the SOS pathway is shown to be fully conserved in *M. polymorpha*, this demonstrates remarkable conservation between lineages which diverged more than 450 million years ago, and suggests that application of knowledge of the CBL-CIPK network in *M. polymorpha* to higher crops is likely to be successful. Therefore knowledge of what signalling pathways *M. polymorpha* CBLs and CIPKs are involved in, how their expression changes, and how calcium affects CBL-CIPK interaction can be used for crop improvement.

CBLs and CIPKs from *M. polymorpha* could be expressed in crops to bolster their stress tolerance pathways. For example, CIPK-B could be expressed in crops to improve salt stress tolerance by increasing the available CIPK pool for the salt-responsive CBL to bind to, increasing the number of CBL-CIPK complexes active in the crop, and therefore increasing activation of target salt transporters. Similar experiments have proved successful previously. For example, overexpression of TaCIPK24 in *A. thaliana* improves salt tolerance (Sun *et al.*, 2015). We hope that the same would be true for overexpression of MpCIPK-B in crops.

If multifunctional CBLs or CIPKs are identified in *M. polymorpha*, they could be engineered into crops to confer tolerance to multiple stresses at once. A first step to determining the success of such a strategy would be to test if they work by cross species complementation. For example, MpCIPK-B could be used to transform *A. thaliana* SOS3 knockouts to confirm that the supporting machinery used in the *M. polymorpha* signalling pathway is also present in *A. thaliana*. Experiments such as this would be followed up with similar experiments in crop plants. If MpCIPK-B is compatible with signalling machinery already available in crop plants, it can be expressed in them and effect on stress tolerance assessed by phenotyping experiments.

If genes of interest in *M. polymorpha* cannot function successfully when expressed alone in crop plants, these genes can still be used to engineer new stress tolerance pathways in crops. It may be that other new genes, for example those for ion channel targets, also need to be expressed in crop plants for the CBLs or CIPKs of interest to function. Alternatively, if MpCBLs are being expressed in crops, they may have to be engineered to be responsive to the specific calcium signature generated in response to the stress of interest in the crop species being modified. This could be done for example by creating EF-hand mutants to alter calcium binding capability. Synthetic biology to engineer new signalling pathways in crops is a very active area of science at the moment. For example, Geddes *et al.*, (2019) successfully engineered an inter-species signalling network to allow signalling between rhizosphere bacteria and *Medicago truncatula* or barley, with the aim of improving plant yields due to the growth-promoting action of rhizosphere bacteria. Engineering synthetic stress tolerance pathways is more challenging than simply expressing a new gene but would have worthwhile impacts on stress tolerance and crop yields.

Knowledge of the calcium dependence of CBL-CIPK interactions derived from these experiments may be used to manipulate CBL-CIPK interactions, when they happen, and if they are active. These manipulations can be used to engineer plants which respond more quickly, strongly or constitutively to stresses, improving their tolerance. For example, crop stress tolerance could be improved by engineering CBL mutants which permanently bind calcium, causing calcium-dependent CBL-CIPK interactions to be constitutively on, switching on stress tolerance pathways. This may have detrimental effects on plant productivity as constitutively switching on stress response pathways means a plant must divert resources away from growth and towards stress tolerance, reducing yields, but crops grown on marginal land where they are always under stress conditions will still benefit from this.

Overall, this research addresses fundamental questions about calcium signalling in plants, and there are many avenues through which understanding of the CBL-CIPK network in *M. polymorpha* can be applied in crop improvement to withstand climate change, making this area of science research a valuable one.

Bibliography

Akaboshi, M. *et al.* (2008) 'The crystal structure of plant-specific calcium-binding protein AtCBL2 in complex with the regulatory domain of AtCIPK14', *Journal of molecular biology*, 377(1), pp. 246–257. Available at: https://doi.org/10.1016/J.JMB.2008.01.006.

Batelli, G. *et al.* (2007) 'SOS2 promotes salt tolerance in part by interacting with the vacuolar H+-ATPase and upregulating its transport activity', *Molecular and cellular biology*, 27(22), pp. 7781–7790. Available at: https://doi.org/10.1128/MCB.00430-07.

Batistič, O. *et al.* (2008) 'Dual Fatty Acyl Modification Determines the Localization and Plasma Membrane Targeting of CBL/CIPK Ca2+ Signaling Complexes in Arabidopsis', *The Plant Cell*, 20(5), p. 1346. Available at: https://doi.org/10.1105/TPC.108.058123.

Batistič, O. *et al.* (2012) 'S-acylation-dependent association of the calcium sensor CBL2 with the vacuolar membrane is essential for proper abscisic acid responses', *Cell Research*, 22(7), pp. 1155–1168. Available at: https://doi.org/10.1038/cr.2012.71.

Batistič, O. and Kudla, J. (2009a) 'Plant calcineurin B-like proteins and their interacting protein kinases', *Biochimica et Biophysica Acta (BBA) - Molecular Cell Research*, 1793(6), pp. 985–992. Available at: https://doi.org/10.1016/J.BBAMCR.2008.10.006.

Batistič, O. and Kudla, J. (2009b) 'Plant calcineurin B-like proteins and their interacting protein kinases', *Biochimica et Biophysica Acta (BBA) - Molecular Cell Research*, 1793(6), pp. 985–992. Available at: https://doi.org/10.1016/J.BBAMCR.2008.10.006.

Bowman, J.L. *et al.* (2017) 'Insights into Land Plant Evolution Garnered from the Marchantia polymorpha Genome', *Cell*, 171(2), pp. 287-304.e15. Available at: https://doi.org/10.1016/J.CELL.2017.09.030/ATTACHMENT/98C55E0F-FF7A-4E99-8321-DC1FE520B886/MMC11.XLSX.

Bryksin, A. v. and Matsumura, I. (2010) 'Overlap extension PCR cloning: A simple and reliable way to create recombinant plasmids', *BioTechniques*, 48(6), pp. 463–465. Available at: https://doi.org/10.2144/000113418/ASSET/IMAGES/LARGE/FIGURE2.JPEG.

Chaves-Sanjuan, A. *et al.* (2014) 'Structural basis of the regulatory mechanism of the plant CIPK family of protein kinases controlling ion homeostasis and abiotic stress', *Proceedings of the National Academy of Sciences of the United States of America*, 111(42), pp. E4532–E4541. Available at: https://doi.org/10.1073/PNAS.1407610111.

Cheng, N.H. *et al.* (2004) 'The Protein Kinase SOS2 Activates the Arabidopsis H+/Ca2+ Antiporter CAX1 to Integrate Calcium Transport and Salt Tolerance *', *Journal of Biological Chemistry*, 279(4), pp. 2922–2926. Available at: https://doi.org/10.1074/JBC.M309084200.

Cheong, Y.H. *et al.* (2007) 'Two calcineurin B-like calcium sensors, interacting with protein kinase CIPK23, regulate leaf transpiration and root potassium uptake in Arabidopsis', *The Plant journal : for cell and molecular biology*, 52(2), pp. 223–239. Available at: https://doi.org/10.1111/J.1365-313X.2007.03236.X.

Cui, X.Y. *et al.* (2018) 'Wheat CBL-interacting protein kinase 23 positively regulates drought stress and ABA responses', *BMC Plant Biology*, 18(1). Available at: https://doi.org/10.1186/S12870-018-1306-5.

Daryanto, S., Wang, L. and Jacinthe, P.A. (2016) 'Global Synthesis of Drought Effects on Maize and Wheat Production', *PloS one*, 11(5). Available at: https://doi.org/10.1371/JOURNAL.PONE.0156362.

Day, I.S. *et al.* (2002) 'Analysis of EF-hand-containing proteins in Arabidopsis', *Genome Biology*, 3(1). Available at: https://doi.org/10.1186/GB-2002-3-10-RESEARCH0056.

van Dijk, M. *et al.* (2021) 'A meta-analysis of projected global food demand and population at risk of hunger for the period 2010–2050', *Nature Food 2021 2:7*, 2(7), pp. 494–501. Available at: https://doi.org/10.1038/s43016-021-00322-9.

Dodd, A.N., Kudla, J. and Sanders, D. (2010) 'The language of calcium signaling', *Annual Review of Plant Biology*, 61, pp. 593–620. Available at: https://doi.org/10.1146/annurev-arplant-070109-104628.

Dubeaux, G. *et al.* (2018a) 'Metal Sensing by the IRT1 Transporter-Receptor Orchestrates Its Own Degradation and Plant Metal Nutrition', *Molecular cell*, 69(6), pp. 953-964.e5. Available at: https://doi.org/10.1016/J.MOLCEL.2018.02.009.

Dubeaux, G. *et al.* (2018b) 'Metal Sensing by the IRT1 Transporter-Receptor Orchestrates Its Own Degradation and Plant Metal Nutrition', *Molecular cell*, 69(6), pp. 953-964.e5. Available at: https://doi.org/10.1016/J.MOLCEL.2018.02.009.

Edel, K.H. and Kudla, J. (2015) 'Increasing complexity and versatility: How the calcium signaling toolkit was shaped during plant land colonization', *Cell Calcium*, 57(3), pp. 231–246. Available at: https://doi.org/10.1016/J.CECA.2014.10.013.

Engler, C., Kandzia, R. and Marillonnet, S. (2008) 'A One Pot, One Step, Precision Cloning Method with High Throughput Capability', *PLOS ONE*, 3(11), p. e3647. Available at: https://doi.org/10.1371/JOURNAL.PONE.0003647.

Evans, N.H. *et al.* (2005) 'ROS perception in Arabidopsis thaliana: the ozone-induced calcium response', *The Plant journal : for cell and molecular biology*, 41(4), pp. 615–626. Available at: https://doi.org/10.1111/J.1365-313X.2004.02325.X.

Geddes, B.A. *et al.* (2019) 'Engineering transkingdom signalling in plants to control gene expression in rhizosphere bacteria', *Nature Communications.* 10(1), pp. 1–11. Available at: https://doi.org/10.1038/s41467-019-10882-x.

Gifford, J.L., Walsh, M.P. and Vogel, H.J. (2007) 'Structures and metal-ion-binding properties of the Ca2+-binding helix–loop–helix EF-hand motifs', *Biochemical Journal*, 405(2), pp. 199–221. Available at: https://doi.org/10.1042/BJ20070255.

Global Warming of 1.5 °C — (no date). Available at: https://www.ipcc.ch/sr15/ (Accessed: 8 September 2022).

Gorman, A.L. *et al.* (1984) 'Intracellular calcium measured with calcium-sensitive micro-electrodes and Arsenazo III in voltage-clamped Aplysia neurones.', *The Journal of Physiology*, 353(1), p. 127. Available at: https://doi.org/10.1113/JPHYSIOL.1984.SP015327.

Halfter, U. (2000) 'The Arabidopsis SOS2 protein kinase physically interacts with and is activated by the calcium-binding protein SOS3', *Proceedings of the National Academy of Sciences*, 97(7), pp. 3735–3740. Available at: https://doi.org/10.1073/PNAS.040577697.

Hashimoto, K. *et al.* (2012) 'Phosphorylation of calcineurin B-like (CBL) calcium sensor proteins by their CBL-interacting protein kinases (CIPKs) is required for full activity of CBL-CIPK

complexes toward their target proteins', *Journal of Biological Chemistry*, 287(11), pp. 7956–7968. Available at: https://doi.org/10.1074/JBC.M111.279331/ATTACHMENT/48879D6C-BC7C-49B3-B4EF-7E992D42F882/MMC1.PDF.

He, M., He, C.Q. and Ding, N.Z. (2018) 'Abiotic Stresses: General Defenses of Land Plants and Chances for Engineering Multistress Tolerance', *Frontiers in Plant Science*, 9. Available at: https://doi.org/10.3389/FPLS.2018.01771.

Ho, C.H. *et al.* (2009) 'CHL1 functions as a nitrate sensor in plants', *Cell*, 138(6), pp. 1184–1194. Available at: https://doi.org/10.1016/J.CELL.2009.07.004.

Ishitani, M. *et al.* (2000) 'SOS3 Function in Plant Salt Tolerance Requires N-Myristoylation and Calcium Binding', *The Plant Cell*, 12(9), pp. 1667–1677. Available at: https://doi.org/10.1105/TPC.12.9.1667.

Ishizaki, K. *et al.* (2013) 'Homologous recombination-mediated gene targeting in the liverwort Marchantia polymorpha L.', *Scientific Reports*, 3. Available at: https://doi.org/10.1038/SREP01532.

Ishizaki, K. *et al.* (2016) 'Molecular genetic tools and techniques for marchantia polymorpha research', *Plant and Cell Physiology*, 57(2), pp. 262–270. Available at: https://doi.org/10.1093/pcp/pcv097.

Jalmi, S.K. *et al.* (2018) 'Traversing the links between heavy metal stress and plant signaling', *Frontiers in Plant Science*, 9, p. 12. Available at: https://doi.org/10.3389/FPLS.2018.00012/XML/NLM.

James, R.A. *et al.* (2002) 'Factors affecting CO2 assimilation, leaf injury and growth in salt-stressed durum wheat', *Functional Plant Biology*, 29(12), pp. 1393–1403. Available at: https://doi.org/10.1071/FP02069.

Ji, H. *et al.* (2013) 'The Salt Overly Sensitive (SOS) Pathway: Established and Emerging Roles', *Molecular Plant*, 6(2), pp. 275–286. Available at: https://doi.org/10.1093/MP/SST017.

Kano, M. *et al.* (2011) 'Root plasticity as the key root trait for adaptation to various intensities of drought stress in rice', *Plant and Soil*, 342(1–2), pp. 117–128. Available at: https://doi.org/10.1007/S11104-010-0675-9/TABLES/2.

Kato, N. and Jones, J. (2010) 'The split luciferase complementation assay', *Methods in molecular biology (Clifton, N.J.)*, 655, pp. 359–376. Available at: https://doi.org/10.1007/978-1-60761-765-5_24.

Kim, B.G. *et al.* (2007) 'The calcium sensor CBL10 mediates salt tolerance by regulating ion homeostasis in Arabidopsis', *The Plant journal : for cell and molecular biology*, 52(3), pp. 473–484. Available at: https://doi.org/10.1111/J.1365-313X.2007.03249.X.

Knight, H. (1999) 'Calcium Signaling during Abiotic Stress in Plants', *International Review of Cytology*, 195, pp. 269–324. Available at: https://doi.org/10.1016/S0074-7696(08)62707-2.

Knight, H., Brandt, S. and Knight, M.R. (1998) 'A history of stress alters drought calcium signalling pathways in Arabidopsis', *The Plant journal : for cell and molecular biology*, 16(6), pp. 681–687. Available at: https://doi.org/10.1046/J.1365-313X.1998.00332.X.

Knight, H., Trewavas, A.J. and Knight, M.R. (1996) 'Cold Calcium Signaling in Arabidopsis Involves Two Cellular Pools and a Change in Calcium Signature after Acclimation', *The Plant Cell*, 8(3), p. 489. Available at: https://doi.org/10.2307/3870327.

Knight, M.R. *et al.* (1991) 'Transgenic plant aequorin reports the effects of touch and cold-shock and elicitors on cytoplasmic calcium', *Nature*, 352(6335), pp. 524–526. Available at: https://doi.org/10.1038/352524a0.

Kodama, Y. and Hu, C.D. (2012) 'Bimolecular fluorescence complementation (BiFC): A 5-year update and future perspectives', *BioTechniques*, 53(5), pp. 285–298. Available at: https://doi.org/10.2144/000113943/ASSET/IMAGES/LARGE/FIGURE5.JPEG.

Kolukisaoglu, Ü. *et al.* (2004) 'Calcium Sensors and Their Interacting Protein Kinases: Genomics of the Arabidopsis and Rice CBL-CIPK Signaling Networks', *Plant Physiology*, 134(1), p. 43. Available at: https://doi.org/10.1104/PP.103.033068.

Kreps, J.A. *et al.* (2002) 'Transcriptome Changes for Arabidopsis in Response to Salt, Osmotic, and Cold Stress', *Plant Physiology*, 130(4), p. 2129. Available at: https://doi.org/10.1104/PP.008532.

Krishnamurthy, L. *et al.* (2011) 'Plant Biomass Productivity Under Abiotic Stresses in SAT Agriculture', *Biomass - Detection, Production and Usage* [Preprint]. Available at: https://doi.org/10.5772/17279.

Kubota, A. *et al.* (2013) 'Efficient Agrobacterium-mediated transformation of the liverwort Marchantia polymorpha using regenerating thalli', *Bioscience, Biotechnology and Biochemistry*, 77(1), pp. 167–172. Available at: https://doi.org/10.1271/bbb.120700.

Kudla, J. *et al.* (1999) 'Genes for calcineurin B-like proteins in Arabidopsis are differentially regulated by stress signals', *Proceedings of the National Academy of Sciences of the United States of America*, 96(8), p. 4718. Available at: https://doi.org/10.1073/PNAS.96.8.4718.

Kudla, J. *et al.* (2018) 'Advances and current challenges in calcium signaling', *New Phytologist*, 218(2), pp. 414–431. Available at: https://doi.org/10.1111/nph.14966.

Lara, A. *et al.* (2020) 'Arabidopsis K+ transporter HAK5-mediated high-affinity root K+ uptake is regulated by protein kinases CIPK1 and CIPK9', *Journal of experimental botany*, 71(16), pp. 5053–5060. Available at: https://doi.org/10.1093/JXB/ERAA212.

Lebedenko, E.N. *et al.* (1991) 'Method of artificial DNA splicing by directed ligation (SDL).', *Nucleic Acids Research*, 19(24), p. 6757. Available at: https://doi.org/10.1093/NAR/19.24.6757.

Léran, S. *et al.* (2015) 'Nitrate sensing and uptake in Arabidopsis are enhanced by ABI2, a phosphatase inactivated by the stress hormone abscisic acid', *Science signaling*, 8(375). Available at: https://doi.org/10.1126/SCISIGNAL.AAA4829.

Li, J.F., Li, L. and Sheen, J. (2010) 'Protocol: a rapid and economical procedure for purification of plasmid or plant DNA with diverse applications in plant biology', *Plant methods*, 6(1). Available at: https://doi.org/10.1186/1746-4811-6-1.

Li, L. *et al.* (2006) 'A Ca(2)+ signaling pathway regulates a K(+) channel for low-K response in Arabidopsis', *Proceedings of the National Academy of Sciences of the United States of America*, 103(33), pp. 12625–12630. Available at: https://doi.org/10.1073/PNAS.0605129103.

Linse, S. and Chazin, W.J. (1995) 'Quantitative measurements of the cooperativity in an EF-hand protein with sequential calcium binding', *Protein science : a publication of the Protein Society*, 4(6), pp. 1038–1044. Available at: https://doi.org/10.1002/PRO.5560040602.

Liu, J. *et al.* (2000) 'The Arabidopsis thaliana SOS2 gene encodes a protein kinase that is required for salt tolerance', *Proceedings of the National Academy of Sciences of the United States of America*, 97(7), p. 3730. Available at: https://doi.org/10.1073/PNAS.060034197.

Liu, J. and Zhu, J.K. (1998) 'A calcium sensor homolog required for plant salt tolerance', *Science*, 280(5371), pp. 1943–1945. Available at: https://doi.org/10.1126/SCIENCE.280.5371.1943/ASSET/39B54DA6-5229-4F1C-AED1-62768B9348A9/ASSETS/GRAPHIC/SE2386563003.JPEG.

Liu, K.H. and Tsay, Y.F. (2003) 'Switching between the two action modes of the dual-affinity nitrate transporter CHL1 by phosphorylation', *The EMBO journal*, 22(5), pp. 1005–1013. Available at: https://doi.org/10.1093/EMBOJ/CDG118.

Luan, S. *et al.* (2002) 'Calmodulins and Calcineurin B–like Proteins: Calcium Sensors for Specific Signal Response Coupling in Plants', *The Plant Cell*, 14(Suppl), p. s389. Available at: https://doi.org/10.1105/TPC.001115.

Ma, X. *et al.* (2020) 'The CBL–CIPK Pathway in Plant Response to Stress Signals', *International Journal of Molecular Sciences*, 21(16), pp. 1–27. Available at: https://doi.org/10.3390/IJMS21165668.

Maierhofer, T. *et al.* (2014) 'Site- and kinase-specific phosphorylation-mediated activation of SLAC1, a guard cell anion channel stimulated by abscisic acid', *Science signaling*, 7(342). Available at: https://doi.org/10.1126/SCISIGNAL.2005703.

McAinsh, M.R. and Pittman, J.K. (2009) 'Shaping the calcium signature', *New Phytologist*, 181(2), pp. 275–294. Available at: https://doi.org/10.1111/j.1469-8137.2008.02682.x.

Mehlmer, N. *et al.* (2010) 'The Ca2+-dependent protein kinase CPK3 is required for MAPK-independent salt-stress acclimation in Arabidopsis', *The Plant Journal*, 63(3), pp. 484–498. Available at: https://doi.org/10.1111/J.1365-313X.2010.04257.X.

Nagae, M. *et al.* (2003) 'The crystal structure of the novel calcium-binding protein AtCBL2 from Arabidopsis thaliana', *The Journal of biological chemistry*, 278(43), pp. 42240–42246. Available at: https://doi.org/10.1074/JBC.M303630200.

Ohta, M. *et al.* (2003) 'A novel domain in the protein kinase SOS2 mediates interaction with the protein phosphatase 2C ABI2', *Proceedings of the National Academy of Sciences of the United States of America*, 100(20), pp. 11771–11776. Available at: https://doi.org/10.1073/PNAS.2034853100.

Patron, N.J. *et al.* (2015) 'Standards for plant synthetic biology: a common syntax for exchange of DNA parts', *New Phytologist*, 208(1), pp. 13–19. Available at: https://doi.org/10.1111/NPH.13532.

Permyakov, S.E. *et al.* (2000) 'Effects of mutations in the calcium-binding sites of recoverin on its calcium affinity: evidence for successive filling of the calcium binding sites', *Protein engineering*, 13(11), pp. 783–790. Available at: https://doi.org/10.1093/PROTEIN/13.11.783.

Qiu, Q.S. *et al.* (2002) 'Regulation of SOS1, a plasma membrane Na+/H+ exchanger in Arabidopsis thaliana, by SOS2 and SOS3', *Proceedings of the National Academy of Sciences of the United States of America*, 99(12), p. 8436. Available at: https://doi.org/10.1073/PNAS.122224699.

Quan, R. *et al.* (2007) 'SCABP8/CBL10, a Putative Calcium Sensor, Interacts with the Protein Kinase SOS2 to Protect Arabidopsis Shoots from Salt Stress', *The Plant Cell*, 19(4), pp. 1415–1431. Available at: https://doi.org/10.1105/TPC.106.042291.

Ragel, P. *et al.* (2015) 'The CBL-Interacting Protein Kinase CIPK23 Regulates HAK5-Mediated High-Affinity K+ Uptake in Arabidopsis Roots', *Plant physiology*, 169(4), p. pp.01401.2015. Available at: https://doi.org/10.1104/PP.15.01401.

Ródenas, R. and Vert, G. (2021) 'Regulation of Root Nutrient Transporters by CIPK23: "One Kinase to Rule Them All"', *Plant and Cell Physiology*, 62(4), pp. 553–563. Available at: https://doi.org/10.1093/pcp/pcaa156.

Rolly, N.K. *et al.* (2020) 'Salinity Stress-Mediated Suppression of Expression of Salt Overly Sensitive Signaling Pathway Genes Suggests Negative Regulation by AtbZIP62 Transcription Factor in Arabidopsis thaliana', *International Journal of Molecular Sciences*, 21(5). Available at: https://doi.org/10.3390/IJMS21051726.

Rubinigg, M. *et al.* (2004) 'NaCl salinity affects lateral root development in Plantago maritima', *Functional Plant Biology*, 31(8), pp. 775–780. Available at: https://doi.org/10.1071/FP03222.

Sachdev, S. *et al.* (2021) 'Abiotic Stress and Reactive Oxygen Species: Generation, Signaling, and Defense Mechanisms', *Antioxidants*, 10(2), pp. 1–37. Available at: https://doi.org/10.3390/ANTIOX10020277.

Sánchez-Barrena, M.J., Martínez-Ripoll, M. and Albert, A. (2013) 'Structural Biology of a Major Signaling Network that Regulates Plant Abiotic Stress: The CBL-CIPK Mediated Pathway', *International Journal of Molecular Sciences*, 14(3), p. 5734. Available at: https://doi.org/10.3390/IJMS14035734.

Satir, O. and Berberoglu, S. (2016) 'Crop yield prediction under soil salinity using satellite derived vegetation indices', *Field Crops Research*, 192, pp. 134–143. Available at: https://doi.org/10.1016/J.FCR.2016.04.028.

Schmöckel, S.M. *et al.* (2015) 'Different NaCl-Induced Calcium Signatures in the Arabidopsis thaliana Ecotypes Col-0 and C24', *PLOS ONE*, 10(2), p. e0117564. Available at: https://doi.org/10.1371/JOURNAL.PONE.0117564.

Sharp, R.E. and Davies, W.J. (1989) 'Regulation of growth and development of plants growing with a restricted supply of water', *Plants under Stress*, pp. 71–94. Available at: https://doi.org/10.1017/CBO9780511661587.006.

Shi, J. *et al.* (1999) 'Novel Protein Kinases Associated with Calcineurin B–like Calcium Sensors in Arabidopsis', *The Plant Cell*, 11(12), pp. 2393–2405. Available at: https://doi.org/10.1105/TPC.11.12.2393.

Shimamura, M. (2016) 'Marchantia polymorpha: Taxonomy, phylogeny and morphology of a model system', *Plant and Cell Physiology*, 57(2), pp. 230–256. Available at: https://doi.org/10.1093/pcp/pcv192.

Straub, T., Ludewig, U. and Neuhäuser, B. (2017) 'The Kinase CIPK23 Inhibits Ammonium Transport in Arabidopsis thaliana', *The Plant cell*, 29(2), pp. 409–422. Available at: https://doi.org/10.1105/TPC.16.00806.

Sugano, S.S. *et al.* (2014) 'CRISPR/Cas9-Mediated Targeted Mutagenesis in the Liverwort Marchantia polymorpha L.', *Plant and Cell Physiology*, 55(3), pp. 475–481. Available at: https://doi.org/10.1093/PCP/PCU014.

Sun, J. *et al.* (2014) 'Crystal structure of the plant dual-affinity nitrate transporter NRT1.1', *Nature*, 507(7490), pp. 73–77. Available at: https://doi.org/10.1038/NATURE13074.

Sun, T. *et al.* (2015) 'Identification and comprehensive analyses of the CBL and CIPK gene families in wheat (Triticum aestivum L.)', *BMC Plant Biology*, 15(1). Available at: https://doi.org/10.1186/S12870-015-0657-4.

Swainsbury, D.J.K. *et al.* (2012) 'Calcium ion binding properties of Medicago truncatula calcium/calmodulin- dependent protein kinase', *Biochemistry*, 51(35), pp. 6897–6907. Available at: https://doi.org/10.1021/BI300826M/SUPPL_FILE/BI300826M_SI_001.PDF.

Tan, Q.W. *et al.* (2022) 'Cross-stress gene expression atlas of Marchantia polymorpha reveals the hierarchy and regulatory principles of abiotic stress responses', *bioRxiv*, p. 2021.11.12.468350. Available at: https://doi.org/10.1101/2021.11.12.468350.

Tanaka, H. *et al.* (2018) 'Salinity stress-responsive transcription factors in the liverwort Marchantia polymorpha', *Plant Biotechnology*, 35(3), p. 281. Available at: https://doi.org/10.5511/PLANTBIOTECHNOLOGY.18.0501A.

Tang, R.-J. *et al.* (2015) 'Tonoplast CBL–CIPK calcium signaling network regulates magnesium homeostasis in Arabidopsis', *Proceedings of the National Academy of Sciences*, 112(10), pp. 3134–3139. Available at: https://doi.org/10.1073/PNAS.1420944112.

Tang, R.J. *et al.* (2015) 'Tonoplast CBL-CIPK calcium signaling network regulates magnesium homeostasis in Arabidopsis', *Proceedings of the National Academy of Sciences of the United States of America*, 112(10), pp. 3134–3139. Available at: https://doi.org/10.1073/PNAS.1420944112/SUPPL_FILE/PNAS.201420944SI.PDF.

Tang, R.J., Zhao, F.G., *et al.* (2020) 'A calcium signalling network activates vacuolar K+ remobilization to enable plant adaptation to low-K environments', *Nature.* 6(4), pp. 384–393. Available at: https://doi.org/10.1038/s41477-020-0621-7.

Tang, R.J., Wang, C., *et al.* (2020) 'The CBL–CIPK Calcium Signaling Network: Unified Paradigm from 20 Years of Discoveries', *Trends in Plant Science*. 25(6), pp. 604–617. Available at: https://doi.org/10.1016/j.tplants.2020.01.009.

Tansley, C. (2021). 'Decoding Calcium Signals in the Early Diverging Land Plant, *Marchantia polymorpha'.* PhD thesis. University of East Anglia, Norwich.

Tansley, C. *et al.* (2023) 'CIPK-B is essential for salt stress signalling in Marchantia polymorpha', *New Phytologist* [Preprint]. Available at: https://doi.org/10.1111/NPH.18633.

Tena, G. (2018) 'A window into the past', *Nature Plants*, 4(5), pp. 241–241. Available at: https://doi.org/10.1038/s41477-018-0156-3.

Tian, Q. *et al.* (2016) 'CIPK23 is involved in iron acquisition of Arabidopsis by affecting ferric chelate reductase activity', *Plant science : an international journal of experimental plant biology*, 246, pp. 70–79. Available at: https://doi.org/10.1016/J.PLANTSCI.2016.01.010.

Tian, W. *et al.* (2020) 'Calcium spikes, waves and oscillations in plant development and biotic interactions', *Nature Plants*. Nature Research, pp. 750–759. Available at: https://doi.org/10.1038/s41477-020-0667-6.

Tsuboyama-Tanaka, S. and Kodama, Y. (2015) 'AgarTrap-mediated genetic transformation using intact gemmae/gemmalings of the liverwort Marchantia polymorpha L', *Journal of plant research*, 128(2), pp. 337–344. Available at: https://doi.org/10.1007/S10265-014-0695-2.

Vert, G. *et al.* (2002) 'IRT1, an Arabidopsis transporter essential for iron uptake from the soil and for plant growth', *The Plant cell*, 14(6), pp. 1223–1233. Available at: https://doi.org/10.1105/TPC.001388.

Wang, C., Li, J. and Yuan, M. (2007) 'Salt Tolerance Requires Cortical Microtubule Reorganization in Arabidopsis', *Plant and Cell Physiology*, 48(11), pp. 1534–1547. Available at: https://doi.org/10.1093/PCP/PCM123.

Wang, P. *et al.* (2020) 'Mapping proteome-wide targets of protein kinases in plant stress responses', *Proceedings of the National Academy of Sciences of the United States of America*, 117(6), pp. 3270–3280. Available at: https://doi.org/10.1073/PNAS.1919901117.

Wang, Y., Li, K. and Li, X. (2009) 'Auxin redistribution modulates plastic development of root system architecture under salt stress in Arabidopsis thaliana', *Journal of Plant Physiology*, 166(15), pp. 1637–1645. Available at: https://doi.org/10.1016/J.JPLPH.2009.04.009.

Watts, S. *et al.* (1981) 'Root and Shoot Growth of Plants Treated with Abscisic Acid', *Annals of Botany*, 47(5), pp. 595–602. Available at: https://doi.org/10.1093/OXFORDJOURNALS.AOB.A086056.

Weber, E. *et al.* (2011) 'A Modular Cloning System for Standardized Assembly of Multigene Constructs', *PLOS ONE*, 6(2), p. e16765. Available at: https://doi.org/10.1371/JOURNAL.PONE.0016765.

Xu, J. *et al.* (2006) 'A protein kinase, interacting with two calcineurin B-like proteins, regulates K+ transporter AKT1 in Arabidopsis', *Cell*, 125(7), pp. 1347–1360. Available at: https://doi.org/10.1016/J.CELL.2006.06.011.

Xu, J. *et al.* (2010) 'AtCPK6, a functionally redundant and positive regulator involved in salt/drought stress tolerance in Arabidopsis', *Planta*, 231(6), pp. 1251–1260. Available at: https://doi.org/10.1007/S00425-010-1122-0/FIGURES/6.

Young, J.J. *et al.* (2006) 'CO2 signaling in guard cells: Calcium sensitivity response modulation, a Ca2+-independent phase, and CO2 insensitivity of the gca2 mutant', *Proceedings of the National Academy of Sciences of the United States of America*, 103(19), pp. 7506–7511. Available at: https://doi.org/10.1073/pnas.0602225103.

Yu, L. *et al.* (2010) 'Phosphatidic acid mediates salt stress response by regulation of MPK6 in Arabidopsis thaliana', *New Phytologist*, 188(3), pp. 762–773. Available at: https://doi.org/10.1111/J.1469-8137.2010.03422.X.

Zhang, Y. *et al.* (2011) 'The Role Of Heat Shock Factors In stress-induced Transcription', *Methods in molecular biology (Clifton, N.J.)*, 787, p. 21. Available at: https://doi.org/10.1007/978-1-61779-295-3_2.

Zhao, Y. *et al.* (2011) 'SOS3 mediates lateral root development under low salt stress through regulation of auxin redistribution and maxima in Arabidopsis', *New Phytologist*, 189(4), pp. 1122–1134. Available at: https://doi.org/10.1111/J.1469-8137.2010.03545.X.

Zörb, C., Geilfus, C.M. and Dietz, K.J. (2019) 'Salinity and crop yield', *Plant Biology*, 21, pp. 31–38. Available at: https://doi.org/10.1111/PLB.12884.

Zou, J.J. *et al.* (2010) 'Arabidopsis Calcium-Dependent Protein Kinase CPK10 Functions in Abscisic Acid- and Ca2+-Mediated Stomatal Regulation in Response to Drought Stress', *Plant Physiology*, 154(3), pp. 1232–1243. Available at: https://doi.org/10.1104/PP.110.157545.